An investigation into the flotation response of wollastonite and silicate gangue minerals

Nonkululeko Buthelezi

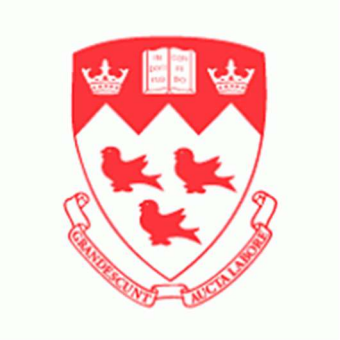

Department of Mining and Materials Engineering
McGill University
Montreal, Canada
January 2020

A thesis submitted to McGill University in partial fulfillment of the requirements of the degree of Master of Science

Abstract

Wollastonite is a calcium silicate mineral which is used in a variety of industries including ceramics, plastics, frictional materials, electrical and thermal insulators, pharmaceutical and paper industries. Flotation of wollastonite ores that contain silicate minerals as gangue, specifically feldspar, diopside and quartz is challenging and seldom discussed in literature.

In this study, microflotation tests, zeta potential measurements, X-ray photoelectron spectroscopy (XPS), Ultraviolet-visible (UV-vis) spectrophotometry and bubble-particle attachment studies were employed to assess the interaction of wollastonite, quartz and diopside with dodecylamine (DDA), sodium oleate (NaOl), tannic acid (TA) and sulphuric acid. Floatability and surface chemistry indicated that dodecylamine was the most effective and selective collector. NaOl was neither effective nor selective in the flotation of diopside, quartz and wollastonite.

TA was employed as a depressant to improve the selectivity between diopside and wollastonite in the presence of DDA. TA was effective in selectively depressing diopside at a low TA concentration, thereby increasing the separation efficiency. An increase in TA concentration resulted in depression of both wollastonite and diopside. Sulphuric acid was tested as a potential depressant of wollastonite in a reverse flotation whereby quartz would be collected as the hydrophobic mineral. Sulphuric acid was effective in depressing wollastonite but was not selective.

TA and DDA were used to assess the flotation behaviour of wollastonite and the associated gangue minerals using batch flotation tests. The purpose was to use a direct flotation to remove diopside as tailings. The tests of DDA alone were in good agreement with microflotation tests although the recoveries of wollastonite were slightly poor than expected. The recovery of wollastonite was closer to that of diopside than that of quartz. It was concluded that wollastonite is less floatable with DDA in batch flotation tests than it was in microflotation tests which is probably related to the solution chemistry and/or the effect of particle shape in a highly turbulent flotation machine. TA demonstrated poor selectivity between diopside and wollastonite which was inconsistent with microflotation tests. Quartz flotation recoveries appeared to not be affected by the presence of TA which implies that quartz can potentially be selectively floated from all the minerals present within the wollastonite ore using TA and DDA.

Résumé

La wollastonite est un silicate de calcium utilisé dans diverses applications industrielles telles que la production des céramiques, des plastiques, d'isolants thermiques, des produits pharmaceutiques et papier. La flottation de minerais de wollastonite contient des minéraux silicatés comme gangue, tel que le feldspath, le diopside et le quartz présentent de nombreuses difficultés et n'est que rarement traitée dans la littérature.

Dans cette étude ont été employés des tests de microflottation, des mesures de potentiel zéta, de la spectrométrie photoélectronique X (SPX), de la spectroscopie ultraviolet-visible (UV-vis) ainsi que des tests d'adhésion bulle-particule, afin d'évaluer les interactions de la wollastonite, du quartz et du diopside avec la dodécylamine (DDA), l'oléate de sodium (NaOl), l'acide tannique (AT) et de l'acide sulfurique. Des analyses de flottabilité et de chimie des surfaces ont révélé que la DDA était le collecteur le plus efficaces et le plus sélectif. Le NaOl s'est avéré être ni sélectif ni efficace pour la flottation de diopside, quartz, et wollastonite.

De l'AT fût employé comme déprimant pour améliorer la sélectivité entre la wollastonite et le diopside, en présence de DDA. Ceci s'est révélé efficace pour déprimer le diopside sélectivement à basse concentration de AT. Une augmentation de la concentration d'AT cause une dépression à la fois de diopside et de wollastonite. Des tests de flottation inversée étaient réalisé en utilisant de l'acide sulfurique comme déprimant potentiel de wollastonite, dans le but d'isoler le quartz dans la phase hydrophobe. Ces essais ont révélé que l'acide sulfurique est déprimant efficace, mais pas sélectif, pour wollastonite.

De l'AT et de la DDA fûrent utilisé dans des tests de flottation par lots pour évaluer le comportement de wollastonite et de ses gangues associées, le but étant d'extraire le diopside comme résidu minier par flottation directe. Les essais réalisés avec de la DDA seulement reproduisirent les résultats des tests de microflottation, mais avec un rendement légèrement plus bas. La quantité de wollastonite récupérée lors de ces tests était plus proche de celle de diopside que de quartz. Il a donc été conclu que la wollastonite est moins flottable en présence de DDA dans des tests par lots que dans des tests de microflottation. Ceci est probablement dû à la

solvatation et/ou aux effets de forme des particules dans un milieu turbulent comme une cellule de flottation. L'AT s'est avérée peu sélectif entre le diopside et la wollastonite, contrairement à ce qui a été observé lors des tests de microflottation. Le rendement de quartz lors de ces tests n'a visiblement pas été affecté par l'addition d'AT, démontrant ainsi que le quartz peut être séparé des autres minéraux présents dans des minerais de wollastonite en utilisant de l'AT et de la DDA.

Acknowledgements

I would like to thank Prof. K.E. Waters for his support and guidance throughout the process of running this project and writing my thesis. I would also like to thank him for giving me this great opportunity.

I was very fortunate to have a research group that was always willing to help. I would like to thank Ronghao Li for helping me with experimental set up. I would also like to appreciate Chris Marion, Dr. Eileen Espiritu, Luis Vinnett and Dr. Ozan Kokkilic for their guidance throughout my research.

I am thankful to Ray Langlois for the training and guidance in the lab. I would also like to thank Dr. Lihong Shang for her help with X-ray diffraction (XRD) and X-ray photoelectron spectroscopy (XPS) analyses. I am also thankful to Aleksandra Djuric for training and support for various analytical instruments.

I would like to express my sincere gratitude to Dr. Tassos Grammatikopoulos for his time invested in running QEMSCAN on my samples and his help with interpretation of the results. In addition, Tassos also took his time to come to McGill to introduce me to the wollastonite project and that is highly appreciated. I would also like to thank Barbara Hanley for her support and guidance during my graduate studies.

I would like to acknowledge the National Sciences and Engineering Research Council of Canada (NSERC) and Canadian Wollastonite for funding this work through the Collaborative Research and Development (CRD) program (CRDPJ 511955-17).

Last but not least, I would like to thank my family for their support throughout the duration of my Masters.

Table of Contents

List of Figures

Chapter 1. Introduction

Wollastonite is an inosilicate mineral with a chemical formula $CaSiO_3$ [1, 2]. The chemical structure of wollastonite is depicted in *Figure 1.1* [1]. Pure wollastonite has a chemical composition of 48.3% CaO and 51.7% SiO_2, but in nature calcium can be substituted by magnesium, iron and manganese [3]. Wollastonite has an acicular crystal habit [1, 2]. Wollastonite is normally found in metamorphic regions, occurring as a product of metamorphism of silica rich limestones [2, 4]. Another model formation of wollastonite is infiltration metasomatism whereby, silica-rich hydrothermal fluids infiltrate limestones and change the original mineralogy [4]. The latter genetic model is normally proposed for formation of high-grade, economic wollastonite deposits [4]. Wollastonite is used in ceramics, plastics, frictional materials, electrical and thermal insulators, and paper industries; it also used in pharmaceuticals due to its bio-activity and bio-compatibility [2, 4, 5, 6]. There is currently an ongoing research on application of wollastonite for entrapment and storage of anthropogenic CO_2 [7].

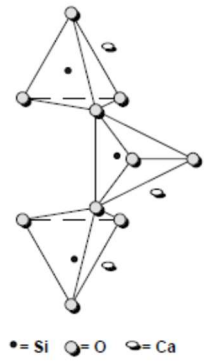

Figure 1.1 Chemical structure of wollastonite [1].

Wollastonite price is reported to be between $210 to $445. Wollastonite prices are higher for fine particle size or high aspect ratio products. Wollastonite market trends are predicted from the industries that consume wollastonite. Ober [8] reported an increase in construction spending in USA, an increase in production of plastics and motor vehicles which suggests an increase in wollastonite demand; which would require an increase in supply as well [8].

The main producers of wollastonite are China, India, USA and Mexico [8]. Canada is a minor producer of wollastonite with Canadian wollastonite being the only mining operation that is

currently exploiting wollastonite [9]. Canadian wollastonite is currently mining the Saint Lawrence wollastonite deposit in Ontario, Canada [9].

The Saint Lawrence wollastonite deposit is a large wollastonite skarn, ~9 Mt at a grade of >40% wollastonite. The wollastonite skarn is associated with the Grenvillian metamorphic region. It is proposed to have formed due to infiltration metasomatism of limestones by magmatose, silica-rich, CO_2-poor hydrothermal fluids. There are two main skarns identified in the region, wollastonite-dominant (>40% wollastonite) and clinopyroxene-dominant (>40% clinopyroxene). The main gangue minerals associated with wollastonite are diopside, feldspar, quartz and minor calcite, pyrrhotite, pyrite, chalcopyrite, titanite and graphite. Wollastonite forms large crystals with lengths ranging between 0.2 cm and 5 cm. A study conducted by Grammatikopoulos, Clark and Vasily [4] shows that wollastonite is well liberated (>80% wollastonite) for particle sizes as coarse as 0.5 mm to 1 mm. Grammatikopoulos, Clark and Vasily [4] reported that post-grinding aspect ratios (length: width ratio) of wollastonite can be >20:1. The high aspect ratios of the Saint Lawrence wollastonite deposit combined with its high purity (<1 wt.% combined content of iron, manganese and aluminium) implies that this deposit has a wide variety of applications in industry [4].

Beneficiation of wollastonite ores that contain silicate minerals as gangue is challenging and seldom discussed in literature. The purpose of the current study is to:

- Assess the interaction of wollastonite and the associated gangue minerals with flotation reagents using various surface chemistry techniques
- Investigate floatability using small scale flotation tests
- Briefly explore the flotation behaviour of wollastonite and the associated gangue minerals in batch flotation tests.

Chapter 2. Literature review

As mentioned in the Introduction (section 1), studies on the beneficiation of wollastonite ores are limited in literature. To gain an insight into various methodologies that could be used to beneficiate wollastonite ores, processing of industrial minerals is reviewed in this section. Furthermore, wollastonite is silicate industrial mineral and the main gangue minerals present within the Saint Lawrence deposit are all silicates [4]. Therefore, the focus of this review will be on processing of silicate industrial minerals, excluding rare earth minerals. Flotation of silicates, focusing mainly on surface chemistry will be discussed in detail to complement the objectives of this study. In addition to surface chemistry, the effect of particle shape of fibres will be briefly discussed to address the physical aspects regarding the floatability of wollastonite.

2.1 Industrial Minerals

Christidis [10] proposed that "*Industrial minerals and rocks are earth materials utilised because of their characteristic physical and/or chemical properties and not because of their metal content and which are not energy sources*" [10]. Most silicate minerals are utilised for their physical and chemical properties and can therefore be classified as industrial minerals [10]. Silicate minerals have a wide variety of applications in ceramics, plastics, paper, frictional materials, thermal and electrical insulator, refractory materials, pharmaceutical industries and more [4, 8].

2.2 Processing of silicate minerals

Economical deposits of silicate minerals are often associated with gangue minerals and thus, beneficiation is required to produce a saleable product [1]. Beneficiation methods that are normally employed by processing plants include magnetic separation, gravity separation, flotation and to a lesser extent, leaching and electrostatic separation [1, 11]. The processing flow sheet normally contains a combination of two or more of these methods [3]. Standards for the grade/quality of the industrial minerals may vary from country to country [12, 13]. Additionally, each silicate mineral

can be used in many industrial applications; as a result, the required quality after processing will also be dictated by the type of industry that will utilise the mineral [1, 4, 8, 14].

2.2.1 Comminution

Comminution is the first step of beneficiation, whereby the particle size of the ore is reduced to liberate valuable minerals from gangue [15]. In a processing plant, comminution is achieved through crushing and grinding [15]. The method and equipment for crushing and grinding should be selected carefully to avoid overgrinding the ore and iron (Fe) contamination from steel rods/balls for certain ore types [12]. Overgrinding and contamination could result in difficulties in downstream processing [12]. Bulut and Yurtsever [12] showed that the Fe contamination from steel grinding media depressed kyanite during flotation, reducing recovery when compared to ceramic grinding media [12]. Comminution of wollastonite ores should be controlled to preserve the high aspect ratio of the final product which demands a higher price [4, 8].

2.2.2 Gravity separation

Gravity separation exploits specific gravity differences to separate minerals based on their relative movement in response to gravitational forces, and other forces such as hydrodynamic forces. Gravity separation machines include jigs, pinched sluices and cones, shaking and pneumatic tables, duplex concentrator, mozley laboratory separator and centrifugal concentrators [15].

High density silicate minerals such as garnet can beneficiated using dry or wet gravitational methods [16]. High density minerals that occur as gangue minerals in certain silicate ores can be removed using gravity separation methods prior or post beneficiation by other methods such as flotation [11, 12, 17]. In some cases, gravity separation methods are effective in the coarse particle size range but the methods lose efficiency for finer particles [13, 14, 17, 18]. Gravity concentration methods such as concentrating tables and heavy liquid are used to beneficiate coarse mica, kyanite and andalusite but these methods are not efficient for finer particle sizes [13, 14, 17, 18].

2.2.3 Magnetic separation

Magnetic separation relies on the differences in the magnetic properties of minerals to separate valuable minerals from gangue [15]. Magnetic separation can be broadly classified into two types: high and low intensity magnetic separators. Low intensity magnetic separators are used to beneficiate ferromagnetic or highly paramagnetic minerals [15]. High intensity magnetic separators are used for paramagnetic minerals with low magnetic susceptibilities, such as diopside [3, 15]. Iron-bearing gangue minerals can be removed from nonmagnetic silicate minerals such as feldspars, andalusite, talc and others, using magnetic separation methods [3, 12, 17, 19]. Some silicate minerals such as micas, garnet and diopside are weakly magnetic and high intensity magnetic separation methods could be used during beneficiation [12, 17, 19, 20].

2.2.4 Flotation

Flotation is usually a necessary step during most silicate separation systems due to either lack of differences in magnetic, density and electrical properties between the gangue and valuable minerals and/or loss of efficiency in gravity beneficiation methods with particle-size [13, 17, 18]. Flotation relies mainly on differences in surface chemistry and the surface chemistry of minerals can be altered using flotation reagents such that flotation can be used to beneficiate a wide variety of ores [15, 21]. Flotation and surface chemistry of silicate minerals will be discussed further in the following sections.

2.3 Flotation fundamentals and silicates flotation

Flotation is a beneficiation method based on the wetting behaviour of minerals [15]. Some minerals are readily wetted by water and they are termed hydrophilic, whereas some minerals repel water and they are termed hydrophobic [15, 21]. The overall flotation process is demonstrated in *Figure 2.1* which shows a schematic diagram of a mechanical flotation cell [15, 21]. During flotation, air is introduced through a shaft and sheared into air bubbles by the impeller which also serves to agitate the pulp and keep particles in suspension [15]. The hydrophobic particles attach to the bubbles and rise to the froth zone [15]. The froth overflows to the launder where hydrophobic

particles are collected as a concentrate [15]. The hydrophilic minerals are collected as tailings from the bottom of the flotation machine [15].

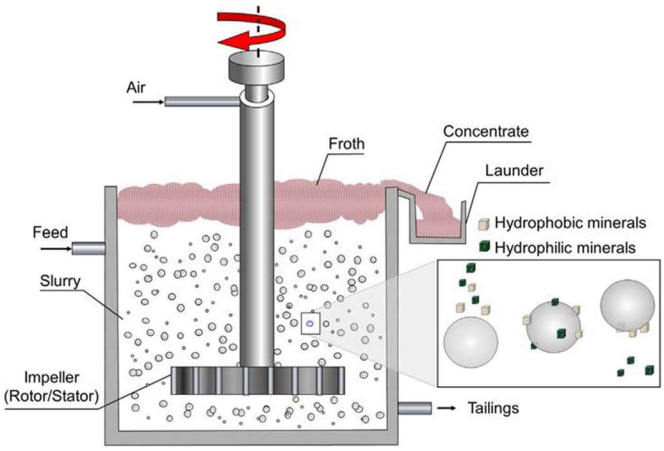

Figure 2.1 Mechanical cell demonstrating the froth flotation process [15].

Hydrophobicity and hydrophilicity are concepts based on surface properties [15]. Non-polar minerals including graphite are hydrophobic, while polar minerals such as oxides and most silicates (except talc) are hydrophilic [15]. The versatility of flotation stems from the fact that the surface chemistry can be altered using collectors and depressants to render valuable minerals hydrophobic and gangue minerals hydrophilic [15, 21]. In reverse flotation, the gangue minerals are rendered hydrophobic and the valuable minerals hydrophilic. In addition to surface chemistry; particle size, liberation and the flotation machine play a vital role in flotation performance [15]. As mentioned earlier, the focus of this review is on the surface chemistry and the other factors will only be discussed briefly [15].

2.3.1 Surface chemistry of silicate minerals

Silicate minerals are generally hydrophilic (talc being an exception) such that hydrophobicity of silicate minerals is often induced using collectors [15, 21]. The wetting behaviour of silicate minerals is related to their chemical structure which will be discussed in the following sections. In addition, other surfactants are used to ensure maximum separation during flotation. These surfactants include depressants, dispersants and activators [15, 21]. Surfactants interact with the

mineral surface through a process called adsorption which can be either chemical or physical [15, 21]. Physical adsorption refers to the adsorption of a surfactant whereby, no chemical bond is formed but the adsorption is through an electrostatic interaction [15, 21]. Chemical adsorption (chemisorption) is an adsorption mechanism whereby a chemical bond is formed between the surfactant and the chemical elements on the mineral surface [15].

The pH of the pulp is an important factor that determines adsorption of surfactants. The pH controls the speciation of metal ions, speciation of certain surfactants and the surface charge of most of the silicate minerals. Therefore, pH is one of the major factors that determines selective flotation. Normally, pH modifiers like sulphuric acid, sodium hydroxide, hydrochloric acid, lime and soda ash are used to adjust the pH [15].

Floatability, collector adsorption and adsorption mechanisms can be studied using various techniques. The studies reviewed here mainly used microflotation tests, zeta potentials measurements, X-ray photoelectron spectroscopy (XPS), Fourier-transform infrared spectroscopy (FTIR), adsorption studies and to a lesser extent contact angle measurements and molecular modelling. These methods are useful in assessing the wetting behaviour of minerals, adsorption of surfactants onto the mineral surface and determining the pH conditions and reagent concentration range that results in selective flotation [21, 22]. In addition, these methods especially zeta potentials measurements, XPS, FTIR and molecular modelling can be used in conjunction with one another to delineate the adsorption mechanisms of surfactants [21, 22].

2.3.1.1 Floatability studies and surface chemistry characterisation techniques

Floatability studies and surface chemistry characterization techniques that are employed by the studies reviewed in this thesis are briefly discussed in this section. The purpose of this section is to give an overall idea of the principles governing these techniques. These techniques include small scale flotation tests, zeta potential measurements and X-ray photoelectron spectroscopy (XPS). Other techniques employed by the reviewed studies on surface chemistry of silicate minerals include adsorption studies, contact angle measurements, Fourier transform infrared spectroscopy

(FTIR) and molecular modelling which are not discussed in this section since they do not form a major component of this thesis. FTIR is discussed further in Appendix E.

(i) Small scale flotation tests

Factors that influence floatability such as surfactants and pH conditions can be assessed using small scale tests [21]. In small scale tests a few grams of pure minerals are used to conduct flotation tests in microflotation cells [21]. An example of these cells is a Hallimond tube depicted in *Figure 2.2*. Air is introduced through a sintered glass frit and sheared into bubbles; floatable minerals are then collected by bubbles [15]. The bubbles burst at the liquid/air interface and drop the mineral particles to the collecting tube [15]. The percentage of the weight collected is taken as an indicator of floatability for the given mineral using a particular reagent scheme and pH conditions [15].

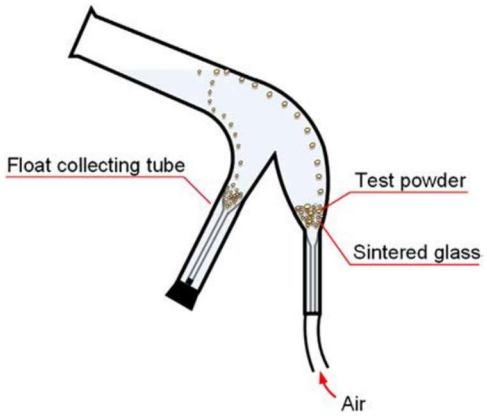

Figure 2.2 Hallimond tube for flotation of single minerals [15].

(ii) Zeta potential measurements

In an aqueous solution, the charge localised at the mineral surface is balanced by solution's counter ions at the liquid/solid interface to attain electroneutrality. The resulting region of electrical heterogeneity at the liquid/solid interface is termed an electrical double layer. The closest distance at which the solution's counter ions in the diffuse layer are encountered from the solid surface is known as a Stern plane. *Figure 2.3* shows that there are two Stern planes, inner Stern plane (β) and outer Stern plane(δ). The outer (δ) and the inner (β) Stern planes are normally treated as the same plane for simplicity. Surface charge measurement techniques usually measure the potential across

the Stern plane. One of the most common and useful technique for quantifying surface charge involves measuring electrokinetic potentials [22].

As the particle moves in a suspension, there will be a relative motion of ions within the electrical double layer. The potential across the slipping plane, where relative movement occurs, is known as the zeta potential. For convenience, the electrical potential across the slipping plane is assumed to be approximately equal to the electrical potential across the Stern plane. As a result, zeta potential measurements are taken across the Stern plane. Zeta potential measurements are determined using a variety of methods, but the most common method is electrophoresis. This method applies an electrical field to the solution, resulting in the movement of the particles under the influence of the electrical field [22].

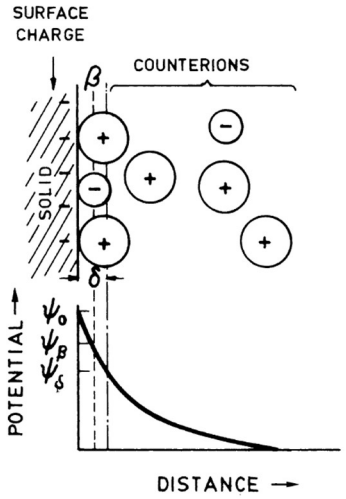

Figure 2.3 Charged mineral surface and solution ions balancing the surface charge. The stern plane is denoted by δ and β. The graph shows the change in potential (Ψ) moving away from the surface [22].

Surfactant adsorption is controlled by the electrical double layer. Physical adsorption of surfactants is determined by the magnitude and sign of the surface charge. The increase of the surface charge will be detrimental to the adsorption of chemically adsorbing surfactants if they have the same charge as the surface. As a result, zeta potential measurements are invaluable in predicting the adsorption of surfactants onto the mineral surface which determines the floatability of minerals [22].

The surface charge of minerals is determined by a variety of factors. Comminution of oxides and silicates normally breaks covalent and ionic bonds [15, 23]. In water, the surface ions will be hydrolysed, and the surface charge will then be controlled by the pH [22-24]. At low pH, the metal hydroxide species at the mineral surface become protonated resulting in a positive charge [22-24]. At high pH, the metal hydroxide species at the mineral surface become deprotonated which results in a negatively charged surface as shown in Equation 1 [22-24]. This is one way to look at the controlling factors of the surface charge, some minerals like muscovite have a permanent charge on certain faces, independent of the pH [18, 22].

$$MOH_{(surf)} = MO^{-}_{(surf)} + H^{+}_{aq}$$
$$MOH_{(surf)} + H^{+}_{aq} = MOH^{+}_{2(surf)} \quad (1)$$

At a certain pH, the mineral surface carries a zero net charge and that pH is termed an isoelectric point (IEP) [22]. The IEP can be used to determine the pH range for selective flotation of the target mineral if the collector is electrostatically adsorbed [15, 22]. Below the IEP, the mineral surface is positively charged and anionic collectors will be able to adsorb to it [12, 13, 17, 21, 24]. Above the IEP, the mineral surface is negatively charged and cationic collectors will be able adsorb to it [12, 13, 17, 21, 24]. Chemically adsorbed surfactants can adsorb to surfaces of the same charge [12, 22, 24]. The surface charge still plays a role in chemical adsorption. An anionic surfactant adsorbing to a negatively charged surface will cease adsorption at high pH where the magnitude of the negative charge on the mineral surface is high [22, 24].

(iii) X-ray photoelectron spectroscopy (XPS)

XPS is a surface analytical technique that uses X-rays to eject core electrons of the atoms on the surface of the sample. The core electrons will only be ejected if the energy of the incident X-rays is sufficient to overcome the binding energy of the core electrons. The binding energy of the core electrons is characteristic for a given element and therefore, the technique is useful for identification of elements on the surface of the sample. Additionally, XPS is sensitive to chemical environments of a given element. The binding energy of core electrons is dependant on the shielding by electrons on the higher energy levels. In a molecule, neighbouring ions may either

withdraw or donate electrons from/to the element of interest. Metal oxides' core electrons will have higher binding energy than that of native metals. The increase in binding energies is due to the fact that oxygen is electron withdrawing and reduces the number of electrons pulled by the nucleus of the metal which results in an increase in the binding energies of core electrons. Thus, XPS is useful for elemental analysis and characterisation of chemical bonding and oxidation state of the elements on the sample surface [25].

XPS is a useful tool to understand flotation by characterising surface chemistry of minerals and assessing adsorption behavior of the surfactants. Adsorption of surfactants may result in the appearance of foreign elements on the mineral surface which can be detected by XPS [18, 26, 27]. Additionally, for chemically adsorbing surfactants, the XPS spectrum may show shifts in the peaks of the binding energies of core electrons due to changes in the chemical environments [18].

2.3.1.2 Collectors

Collectors are surface active reagents which impart or enhance hydrophobicity on the mineral surface [15, 21]. Collectors adsorb to the mineral surface and displace water molecules [15, 21]. Collectors normally contain a charged head group and a hydrophobic hydrocarbon chain [15]. The charged head group interacts with the atoms on the mineral surface through physical and chemical adsorption [15]. However, there are exceptions to this typical collector chemical structure. Kerosene, which is a collector used to enhance the hydrophobicity of naturally hydrophobic materials such as coal and talc does not contain a charged group, and it interacts through hydrophobic interactions with the mineral surface [15]. The collectors that are normally employed for flotation of silicate minerals can be classified as cationic, anionic and mixed collectors (anionic-cationic and cationic-nonionic) [15].

(i) Cationic collectors

Cationic collectors such as long-chain alkyl primary, secondary, tertiary and quaternary ammonium salts are the most commonly used collectors in flotation of silicates [26-29]. Amines

and ammonium salts are predominantly adsorbed to mineral surfaces through an electrostatic interaction and hydrogen bonding [12, 26-30]. Adsorption of amines to mineral surfaces have been studied through adsorption studies, contact angle measurements, zeta potential measurements, FTIR, XPS and molecular modelling [12, 26-30].

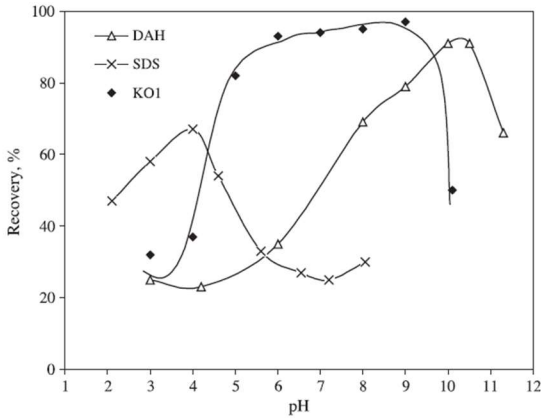

Figure 2.4 Recovery against pH for kyanite microflotation tests. DAH is dodecyl amine hydrochloride, SDS in sodium dodecyl sulfate and KOL is potassium oleate [12].

Adsorption studies are a simple method used to evaluate adsorption of collectors. The mineral of interest is conditioned with a collector, and the concentration of the reagent in the supernatant is determined using methods such as UV/VIS spectrophotometry and Total Organic Carbon (TOC) analyses [29, 31, 32]. The concentration of the amine in the supernatant solution is used to calculate the amount of amine adsorbed to the mineral surface [29, 31, 32]. Adsorption studies performed on muscovite and albite at neutral pH showed that the amine is adsorbed on muscovite and albite surfaces and adsorption increases with an increase in the amine concentration [31, 32]. Adsorption of amines to mineral surfaces has also been studied using contact angle measurements [32, 33]. Contact angle measurements increase with an increase in the concentration of the amine on mineral surfaces, indicating an increase in hydrophobicity [32, 33]

Several studies on amine adsorption on silicate minerals reported that amines and their salts adsorb to the mineral surface when the pH > IEP [12, 17, 18, 21, 24]. This relationship is demonstrated by the increase in floatability when the pH > IEP [12, 17, 18, 21, 24]. The IEP of kyanite is approximately a pH of 5.9, as reported by Bulut and Yurtsever [12]. It is evident from *Figure 2.4*

that, the recovery steeply increases after pH 5.9 which confirms that adsorption of DDA is more effective above the IEP [12].

Additionally, Wang, Sun, Hu and Xu [18] conducted zeta potential measurements on amine treated muscovite. The study showed that, the muscovite surface becomes positive with the addition of an amine, and the surface charge increases steeply after pH 2 (see *Figure 2.5*) [18]. Wang, Sun, Hu and Xu [18] reported that, the IEP of muscovite is at pH 2. The steep increase in the positive charge after the IEP further supports the dependence of amine adsorption on the negative charge of the mineral surface [18]. The correlation of the surface charge and floatability suggests that the collector is physically adsorbed [12, 21, 26, 30]. Zeta potential studies alone are inadequate to conclude on the mechanism of collector adsorption.

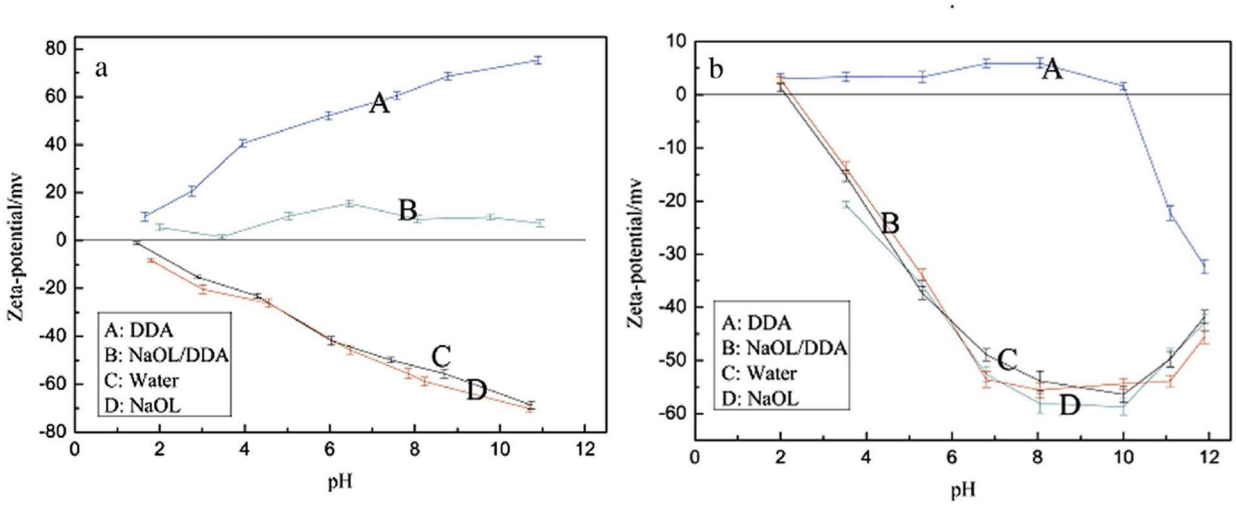

Figure 2.5 Zeta potential measurements of muscovite(left) and quartz(right) (A)treated with DDA, (B) treated with NaOl/DDA, (C) In water and (D) treated with NaOL [18].

Various authors have reported an appearance of amine related absorption peaks on the infrared spectrum of amine treated feldspars, quartz and muscovite [18, 26, 27]. The appearance of these peaks indicate that the amine adsorbed onto the mineral surface [18, 21, 26, 27]. Additionally, the lack of chemical shifts on the infrared spectrum of amine treated mineral surfaces indicates that, it is likely that there are no new bonds formed and the amine is physically adsorbed [18]. In addition to physical adsorption, Vidyadhar et al. [26] suggested that there is also hydrogen bonding between surface silanol groups and an amine [26].

Studies on amine collectors have performed XPS analysis on both pure minerals and amine treated surfaces [18, 26, 27]. Wang et al. [18] demonstrated that adsorption of an amine onto muscovite results in the appearance of nitrogen, an increase in the content of carbon and a decrease in the content of the mineral's elements such as silicon [18]. Vidyadhar [27] presented similar findings on amine treated feldspar and quartz [27]. The lack of chemical shifts on the XPS spectrum of the amine treated surfaces show that the collector adsorption mechanism is predominantly physical [27].

Another method that can be used to asses the adsorption of amines on minerals is molecular modelling. Molecular modelling can determine the value of the interaction energy between the mineral surface and the collector. Chen et al. [30] showed that, the interaction energy between the amine and the sillimanite surface is lower than that with water and therefore, adsorption of an amine is more favourable than adsorption of water molecules. Additionally, Chen et al. [30] showed that, the distance between the sillimanite surface and the amine head group is rather large for a chemical bond (~2,109 Å). Chen et al. [30] concluded that the amine is physically adsorbed to the sillimanite surface [30].

Studies show that maximum floatability using amine collectors occurs around pH 9 [21, 26-28]. Recent adsorption models propose 2D precipitation of molecular amine to occur around this pH [21, 26, 27]. The molecular amine inserted in between ammonium ions screens the electrostatic repulsion between the ammonium ions, resulting in increased adsorption [21, 26, 27]. After pH 10-11, the flotation recovery using amine collectors declines [21, 26-28]. This observation is proposed to be a result of adsorption of amine species in an inverted mode and therefore, rendering the mineral surface hydrophilic [21, 26, 27]. A more recent model proposes 3D precipitation of molecular amine on the mineral surface around pH 10 to 11 [21, 26, 27]. The precipitated amine is oriented disorderly on the mineral surface and therefore, the hydrophobicity decreases [26, 27].

(ii) Anionic collectors

Carboxylic acids are the most commonly used anionic collectors in flotation of silicate minerals, alkyl sulfonates and alkyl sulfates are also used but not as commonly as carboxylic acids. Fatty acids adsorb both physically and chemically to the surfaces of silicate minerals [21, 24]. Alkyl sulfonates and sulfates predominantly adsorb through physical adsorption [12, 17, 21, 34, 35].

Carboxylic acids such ad oleic acid have low solubility at acidic pH because its pKa is at pH 4.95. *Figure 2.6* shows that, the molecular form of oleic acid, which has lower solubility predominates before the pKa [21, 24]. In most cases, oleic acid is used in its salt form to increase its solubility but the species in solution will still depend on the pH. [21, 24].

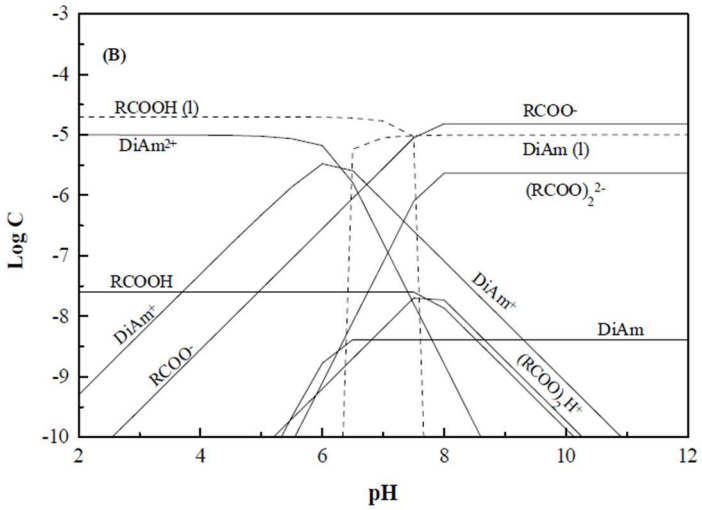

Figure 2.6 Speciation of diamine and oleate [36].

Flotation of kyanite and andalusite using oleic acid and its salts showed that the flotation recovery increased steeply at neutral to basic pH (*Figure 2.4* & Figure 2.7) [12, 17, 24]. Kyanite, sillimanite and andalusite surfaces are negatively charged at neutral to basic pH values, with IEPs between pH 5.4 and pH 6.6 (with the exception of one paper which reported the IEP of sillimanite to be around pH 8 [24]) [12, 17]. It is not plausible for an electrostatic interaction to occur between an anionic collector and negatively charged mineral surfaces [12, 17, 24]. This led to the conclusion that oleic acid is chemically adsorbed to the sillimanite, andalusite and kyanite surfaces [12, 17, 24]. *Figure 2.8* shows that the IEP of sillimanite shifts to lower pH values with oleic acid compared

to the IEP of pure sillimanite [24]. The shift in the IEP confirms that oleic acid is chemically adsorbed [24].

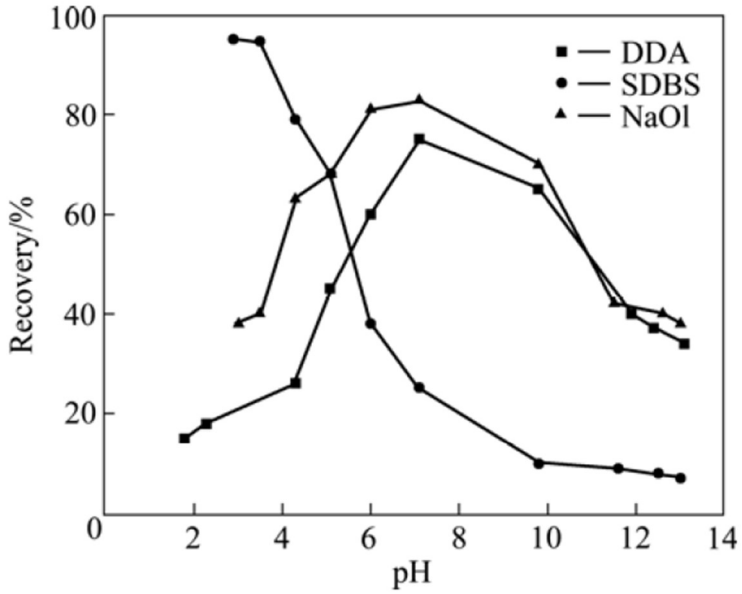

Figure 2.7 Andalusite microflotation results with dodecylamine (DDA), sodium oleate (NaOl) and sodium dodecylbenzene sulfonate (SDS) as collectors [17]

The mechanism of adsorption of oleic acid was further elucidated using FTIR on sillimanite, alumina and precipitated aluminium hydroxide. Adsorption of oleic acid on the sillimanite surface, alumina and aluminium hydroxide, at pH 8 resulted in the appearance of C-H stretch absorption bands. These absorption bands belong to the C-H groups of the hydrocarbon chains and confirms the adsorption of oleic acid onto the mineral surface. In addition, the infrared spectrum of precipitated aluminium hydroxide treated with oleic acid has an infrared absorption band at 1586 cm^{-1} indicating the presence of the carboxylate ion on aluminium hydroxide. Since aluminium is the major element of aluminosilicates, it can be assumed that similar adsorption behaviour occurs on these minerals [24].

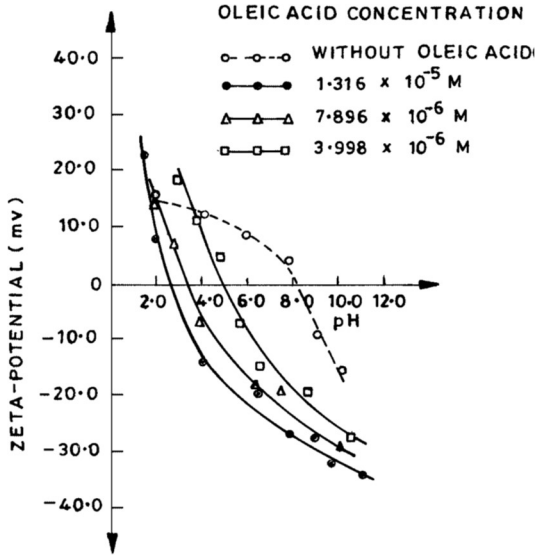

Figure 2.8 Zeta potential measurement on sillimanite treated with different concentrations of oleic acid showing the shift in the IEP with oleic acid adsorption [24].

Kumar et al. [24] proposed that the AlOH species which are predominant at neutral pH are responsible for deprotonating the oleic acid. The oleate species subsequently displace water molecules on the sillimanite surface as they bond to the aluminium [24]. The adsorption of oleic acid is at a maximum at pH 8 where the aluminium species in solution are neutral as shown in the species diagram in *Figure 2.9* [24]. Microflotation tests results (*Figure 2.4*) indicated that flotation recovery of kyanite using potassium oleate declines at high pH values which is attributed to the increase of the negative charge on the mineral surface [12]. As the mineral surface becomes more negative, it repels anionic collectors and hinders chemisorption [22, 24].

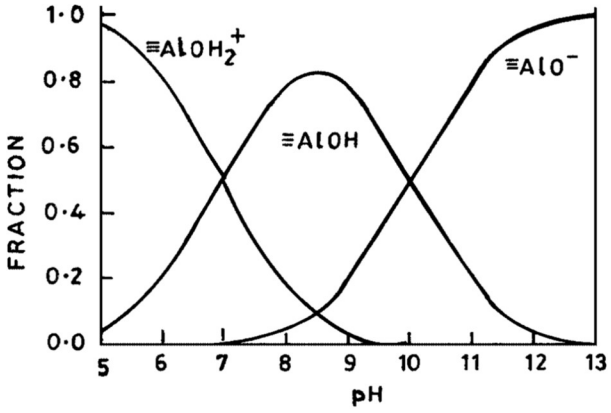

Figure 2.9 Species diagram for aluminium on the sillimanite surface [24].

The studies reviewed in this section demonstrated the evidence for chemical adsorption of oleic acid to aluminosilicates. In addition to chemical adsorption, Rao [21] stated that there is physical co-adsorption of the oleic acid species in either parallel or inverted mode [21]. The parallel mode enhances hydrophobicity whilst the inverted mode reduces hydrophobicity [21].

The second most common anionic collectors used in flotation of silicates are sulfonate collectors [21]. Sulfonic acids and alkyl sulfates are stronger acids than fatty acids and they undergo full dissociation at approximately pH 3 and exist as ions above that pH [21, 35]. Alkyl sulfonates and sulfates are normally adsorbed to mineral surfaces through physical adsorption, but chemical adsorption is possible as well [12, 14, 17, 21, 34, 35]. A study by Zhu et al. [14] reported chemical adsorption in addition to physical adsorption of sodium dodecylbenzene sulfonate onto andalusite [14]. Smaller molecular weight sulfonates normally adsorb electrostatically, whilst larger molecular weight sulfonates can also adsorb chemically [14].

Studies on andalusite and kyanite indicated that the maximum floatability of these aluminosilicates using sulfonates and alkyl sulfates is attained at pH 3-3.5 (*Figure 2.4 & Figure 2.7*) [12, 13, 17]. As mentioned earlier, the IEPs of andalusite and kyanite range from pH 5.2 to pH 6.6, this implies that the maximum floatability is attained below these IEPs, when the mineral surfaces are positive [12, 13, 17]. The floatability of kyanite and andalusite declines as the pH approaches the IEP and beyond the IEP which is due to the surface charge transitioning from positive to neutral and then negative [13, 17]. Anionic collectors cannot physically adsorb to negatively charged surfaces [13, 17, 21, 22]. The correlation between the floatability and the surface charge supports the conclusion that alkyl sulfonate and alkyl sulfate collectors are predominantly physically adsorbed [12, 13, 17].

Physical adsorption of alkyl sulfonates and sulfates allows selective flotation of andalusite and kyanite from other silicate minerals such as quartz and biotite at pH 3-3.5 [13, 17]. Quartz and biotite have IEPs with respective values of 1.8-3.7 and 3.8 [12, 17, 20, 27, 32]. Quartz and biotite are either negative or carry low net charge at pH 3-3.5 [17]. As a result, alkyl sulfonate and sulfate collectors cannot adsorb to quartz and biotite but can adsorb to kyanite and andalusite [12, 17]. Alkyl amine collectors cannot selectively float kyanite and andalusite from biotite and quartz due to maximum floatability of kyanite and andalusite being observed around pH 8-10 [12, 17]. Quartz

and biotite show maximum flotation recovery at similar pH values and thus, separation under these conditions is not possible [12, 17]. This is due to that all these minerals are negatively charged at alkaline pH, thus floatable with amine collectors [12, 13, 17, 20, 27, 32].

(iii) Co-collector

Co-collectors enhance selectivity and have superior collecting abilities compared to individual collectors [18, 26, 27, 36-39]. Co-collectors that are normally used in flotation of silicates can be classified as anionic/cationic and cationic/non-ionic [18, 26, 27, 32, 36]. Studies on co-collectors found that co-collectors can work synergistically to enhance flotation results [18, 26, 27, 36-39].

a) Cationic/anionic collectors

A study on muscovite separation from quartz showed that muscovite can be separated from quartz under acidic conditions as demonstrated in *Figure 2.10*. Wang et al. [18] showed that, the IEP of muscovite is around pH 2 and the IEP of quartz is around pH 2.5. The IEPs given in this study imply that there is a narrow pH window between pH 2 and pH 2.5 whereby muscovite is negatively charged, and quartz has a net charge of zero or is positively charged. This pH window allows selective flotation of muscovite from quartz using cationic collectors (*Figure 2.10*). Flotation in acidic conditions is unfavourable to the environment and corrodes the flotation equipment [18].

When the mixture of sodium oleate (NaOl) and dodecyl amine (DDA) is used, it allows selective flotation of muscovite from quartz at basic conditions [18]. Unlike aluminosilicates (sillimanite, kyanite and andalusite), both muscovite and quartz do not float in the presence of NaOl alone [18, 37]. As seen in *Figure 2.10*, the recovery of muscovite using NaOl/DDA collector remains above 80% for a wide range of pH values and collector concentration, whilst the quartz recovery using NaOl/DDA remains low (<40%) for the entire investigated range of pH and collector concentration [18]. Quartz recovery at alkaline pH, around pH 10 is low (<10 %), and muscovite recovery is high (>90%) [18]. This difference in recovery shows that the separation efficiency using a co-collector system is high at alkaline conditions [18]. The mechanism of the co-collector adsorption was delineated using FTIR, zeta potential measurements and XPS. FTIR and XPS supported the

selective adsorption of NaOl/DDA mixed collector onto muscovite. In addition, XPS indicated that chemisorption is involved in the mixed collector adsorption mechanism [18].

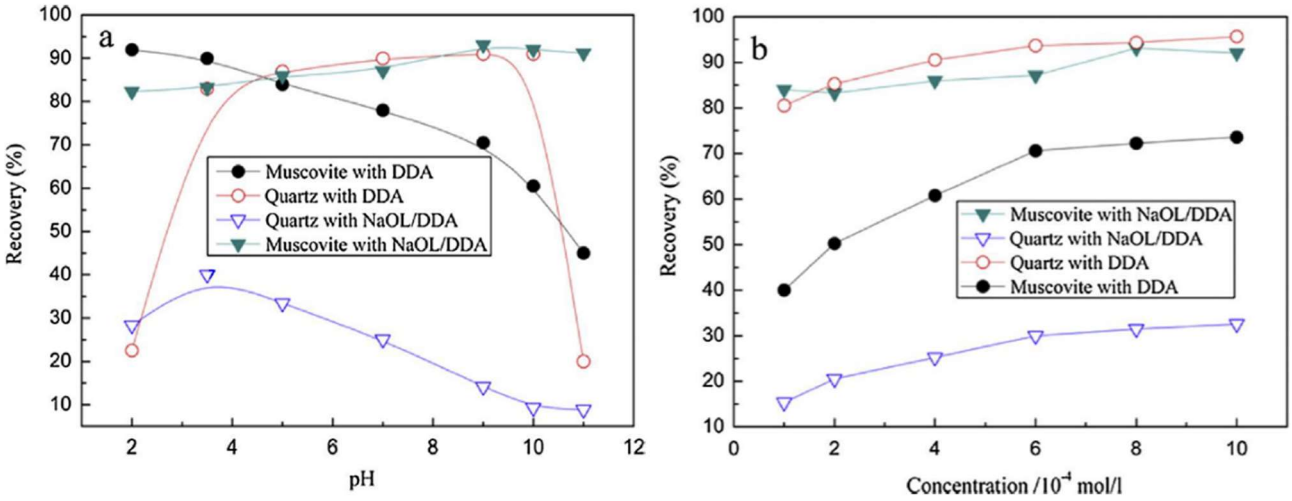

Figure 2.10 Flotation recovery of muscovite and quartz with DDA, NaOl and NaOl/DDA mixture as function of pH (left) and concentration(right) [18].

Vidyadhar [27] performed a similar study to separate feldspar and quartz [27]. The mixed collector systems that were employed are diamine/sulfonate and diamine/dioleate collectors [27, 36]. Vidyadhar [27] reported quartz's IEP to be around pH 2 and the feldspar to have an IEP at a slightly lower pH than 2 [27] . There is a narrow pH range in acidic conditions where quartz and feldspar can be separated using a cationic collector [27]. As the pH increases, the selectivity between quartz and feldspars is lost [27]. Vidyadhar [27], reported that quartz and feldspar can be separated using an amine at pH 2 if the collector concentration is kept low [27]. As the concentration increases, both quartz and feldspar are floated equally [27]. Although separation is possible at pH 2, the recovery of feldspar is low [27]. The recovery and grade of the feldspar concentrate can be improved by employing hydrofluoric acid as an activator for feldspar and a depressant for quartz [19, 20, 31]. Hydrofluoric acid is harmful to the environment and as a result, studies have investigated the possibility of using co-collectors to enhance the grade and recovery of feldspars [19].

Feldspar and quartz do not float in the presence of oleic acid and sulfonate, having a similar flotation behaviour to muscovite [27]. Application of mixed collectors, diamine/sulfonate and

diamine dioleate collectors at low pH values (pH~2) result in selective flotation of feldspar from quartz [27, 37]. Unlike the muscovite-quartz system, the selectivity is lost at high pH values for feldspar and quartz [18, 27]. The information which is currently available in literature shows that feldspars can only be separated from quartz at acidic conditions [19, 20, 26, 27, 31, 36, 37].

The diamine/sulfonate collector will adsorb to the negatively charged surfaces through the positive diamine, and sulfonate will co-adsorb through electrostatic interactions with the diamine head groups and tail-tail hydrophobic interactions [27, 37]. Similarly, the diamine/dioleate collector will adsorb to the negatively charged surfaces through the diamine [27]. Although the head groups of the diamine and oleic acid will be detached due to the neutral state of oleic acid, oleic acid can interact with the diamine through tail to tail hydrophobic interaction [27].

The observed selectivity between feldspar and quartz using the diamine/sulfonate collector is attributed to the surface charge of the two minerals. At pH 2, feldspars are negatively charged whilst quartz carries near zero surface charge [27, 37]. At this pH, diamine adsorbs on feldspar but not on quartz [27]. As a result, the addition of sulfonate will enhance the flotation of feldspar, but it will have no influence on quartz since sulfonate cannot be adsorbed alone by either quartz or feldspar [27, 37]. The diamine/dioleate collector also adsorbs to feldspars but not quartz for a similar reason as diamine/sulfonate co-collector [27].

b) Cationic/nonionic collectors

Cationic/nonionic collectors are used to enhance flotation behaviour of silicate minerals. Jiang et al. [32] conducted a study on flotation of muscovite using a mixture of cetyltrimethylammonium chloride (CTAC) which is a quaternary amine and octanol (OCT). Contact angle measurements, surface tension measurements, microflotation tests and adsorption studies were used to study the adsorption behaviour of the mixed collector [32].

Microflotation studies showed that CTAC/OCT collector has a higher recovery than CTAC or alcohol alone for the entire pH and concentration range investigated. Muscovite floats with CTAC

but not with the alcohol, which shows that CTAC is the main collector and the alcohol supports CTAC [32].

Adsorption studies show that OCT has very low adsorption when used alone and the adsorption increases sharply when mixed with CTAC [32]. CTAC adsorbs to the muscovite surface even when added alone but the adsorption is enhanced in the presence of octanol [32]. The enhancement shows the synergistic behaviour of CTAC and OCT which leads to high adsorption at lower bulk concentration of the collector [32]. This synergistic behaviour leads to increased floatability and lowers the collector dosage which reduces production costs [32, 37]. Similar findings were reported by Wang et al. [39] on muscovite flotation using DDA/OCT collector mixture [39].

The mechanism proposed for the synergistic collector adsorption is that the alcohol interacts with CTAC through hydrogen bonding and tail to tail interactions. The CTAC/OCT complex is adsorbed to the surface through an electrostatic interaction and the adsorption density is enhanced by tail-tail hydrophobic interaction [32].

When studying feldspars, similar adsorption mechanism was proposed by Vidyadhar et al. [26] on flotation using amine/alcohol mixed collectors [26]. FTIR, XPS, zeta potentials and microflotation tests were used to study the flotation behaviour, adsorption and the adsorption mechanism of the mixed collector [26]. The study proposed formation of an amine-water-alcohol complex [26]. The complex is depicted in *Figure 2.11* whereby, both the amine and alcohol interact through hydrogen bonding with the water molecule inserted in-between the two collectors [26]. The complex is adsorbed through electrostatic interaction to the mineral surface and the collector packing density is enhanced by tail-tail hydrophobic interactions [26, 38].

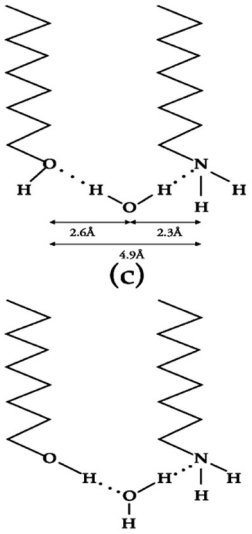

Figure 2.11 Proposed amine/alcohol complex [26].

2.3.1.3 Activators and Depressants

Activators and depressants are used extensively in silicate flotation to improve selectivity. An activator modifies the surface chemistry of the mineral to enhance collector adsorption. A depressant modifies the surface chemistry of the mineral to render the mineral hydrophilic and/or inhibit collector adsorption [15].

i) Inorganic depressants

Inorganic depressants and activators that have been tested or currently employed on silicate bearing ores include HF, HBR, Na_2SiO_3 and Na_2CO_3. These depressants have their shortcomings including issues with environmental considerations or lack of selectivity and these will be discussed briefly in this section.

Hydrofluoric acid (HF) is used during selective flotation of feldspar from quartz as a depressant and an activator [19, 20, 31, 40]. Díaz et al. [19] conducted batch flotation tests at acidic conditions, using an amine as a collector [19]. The results demonstrated that the grade of the feldspar concentrate is enhanced in the presence of HF [19].

A study by Chaib [20] demonstrated that it is possible to activate feldspars and depress quartz using hydrobromic acid (HBR). The study was conducted using batch flotation tests and it was demonstrated that the grade and recovery of feldspar in the concentrate were higher with HBR as a modifier than with HF. HBR is more environmentally friendly and thus a more favourable reagent compared to HF [20].

Lastly, Na_2SiO_3 and Na_2CO_3 are normally employed as depressants for silicate minerals [41]. These depressants normally prove to be inefficient during separation of silicate minerals because they depress all silicates [12, 17]. Bulut and Yurtsever [12] used Na_2SiO_3 and Na_2CO_3 during beneficiation of kyanite from quartz bearing ore [12]. It was demonstrated that, the flotation results were poor in the presence of these depressants when sodium oleate was used as a collector [12].

ii) Organic depressants

Organic compounds such as starch, dextrin, carboxymethyl cellulose (CMC), humic acid and sodium hexametaphosphate have been reported as effective depressants for oxide minerals, calcite, barite, fluorite, talc and quartz [15, 17, 21, 42, 43, 44].

Starch and dextrin are both polysaccharides which have been tested on iron oxides reverse flotation [42]. Veloso et al. [42] showed that both starch and dextrin are effective in selectively depressing iron oxide and not silicates like diopside, quartz and epidote [42]. In contrast, starch was used to depress quartz, biotite and garnet during andalusite flotation [17]. The results showed that starch was effective in depressing silicate gangue minerals including quartz [17]. The discrepancy between the two studies could be due to the differences in pH conditions and reagent schemes.

CMC has been used to depress iron oxides, talc and quartz [21, 42, 43]. Studies applying CMC as a depressant reported that CMC is more effective in the presence of metal ions [21, 42, 43]. Burdukova Van Leerdam et al. [43] reported enhanced adsorption of CMC on talc in the presence of calcium ions, similar to findings reported by Rao [21, 43]. Rao [21] also reported enhanced adsorption of CMC on quartz surface in the presence of lead ions [21].

Humic acid was used during reverse flotation of iron oxides to render iron oxides hydrophilic whilst diopside, chamosite and epidote remain unaffected. The adsorption of humic acid on silicate minerals was dependent on pH. At low pH values, humic acid adsorbed to the silicate minerals, rendering them hydrophilic and thus contaminating the concentrate grade of iron ores. At high pH values, humic acid does not adsorb to silicate minerals which results in maximum separation efficiency around a pH of 10 [42].

The last organic depressant that will be discussed in this review is sodium hexametaphosphate (SHMP). SHMP was used during selective flotation of talc using a sodium oleate/kerosene collector. Sodium hexametaphosphate decreased the calcium content in the talc concentrate but not the aluminium content. Thus, SHMP could be an excellent depressant for calcium bearing minerals but not for Al-bearing minerals. This selective depression was attributed to SHMP being excellent at sequestering calcium and forming stable complexes, but it does not sequester aluminium [11].

Some studies have also reported that SHMP complexes well with magnesium ions [45, 46]. SHMP has been used to depress and disperse serpentine subgroup minerals to selectively float valuable minerals such as pyrite and ascharite [45, 46]. Serpentine is magnesium bearing and dispersion or depression occurs through dissolution of magnesium ions from the mineral surface and chemical adsorption of SHMP [45, 46]. Surprisingly, SHMP was used to selectively depress gangue minerals and allow selective flotation of talc and ascharite. Both talc and ascharite are Mg^{2+} bearing and should ideally be depressed as well. The study on ascharite reported that ascharite is in fact depressed by SHMP but the effects are less pronounced compared to serpentine [45].

iii) Solution ions

Ions present in process water can accidentally activate or depress silicate minerals [14, 30]. Additional ions in process water are unavoidable during flotation [14, 30]. Chen et al. [30] studied the depression of sillimanite by calcium ions (Ca^{2+}) during flotation using dodecylamine as a collector [30]. Microflotation tests showed that the recovery of sillimanite at neutral pH decreases with an increase in Ca^{2+} concentration [30]. Zeta potential measurements shown in *Figure 2.12*

indicated that the IEP of sillimanite is 5.4, and shifts to 6.9 in the presence of Ca^{2+} ions [30]. This shift indicates that adsorption of Ca^{2+} ions results in a positive charge on the surface of sillimanite which has adverse effects on adsorption of cationic collectors [30]. Furthermore, the shift in the IEP suggests a chemical adsorption mechanism of Ca^{2+} ions onto the sillimanite surface [30].

The adsorption of Ca^{2+} ions competes with RNH_3^+ ions which are adsorbed to the sillimanite surface through an electrostatic interaction [30]. Molecular modelling confirmed that Ca^{2+} ions render the sillimanite surface positive and weakens the interaction of sillimanite and RNH_3^+ which is only adsorbed after the adsorption of Ca^{2+} ions [30]. Scott and Smith [47] studied the effect of calcium ions on quartz with an amine as a collector and showed that the presence of calcium ions in solution depresses quartz and decreases its floatability [47].

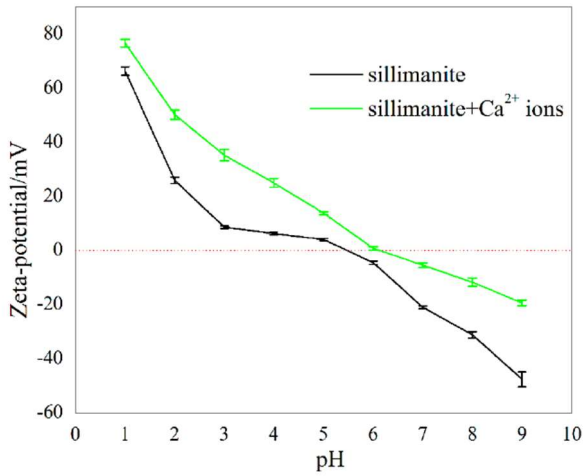

Figure 2.12 Zeta potential measurements on sillimanite surface with and without calcium ions [30].

The depression or activation effect of the solution ions is also dependant on the choice of the collector for flotation [30]. For anionic collectors, calcium ions serve as activators by rendering the surface positive and increasing its affinity for anionic collectors [30]. Another example of solution ions that can accidentally activate or depress silicates are Fe^{2+}/Fe^{3+} ions [12]. Iron (Fe) is one of the main components of steel, thus iron contamination during beneficiation can be from steel grinding media and other steel-based flotation equipment [12]. A study by Bulut and

Yurtsever [12] showed that using steel ball grinding method is detrimental to flotation selectivity in comparison to using ceramic balls and that was due to Fe contamination [12]. Zhu et al. [14] reported that the presence of iron can activate quartz during selective flotation of andalusite using a sulfonate collector, thereby decreasing the concentrate grade [14]. El-Salmawy et al. [48] reported that alkaline earth metals such as Ca^{2+}, Ba^{2+}, Sr^{2+} can activate quartz, allowing flotation using sulfonate collectors [48].

2.3.1.4 Frothers

The main function of frothers during flotation is to preserve bubbles by increasing the stability of the bubbles through decreasing the local surface tension at the air/water interface. Preservation of bubbles leads to increased surface area of bubbles which, in turn, enhances flotation. Frothers consist of a hydrophobic tail and a hydrophilic head. Frothers attach to the bubbles with the hydrophobic tail pointing towards the bubble and the hydrophobic head pointing towards the water. The most commonly used frothers are alcohols such as Methyl isobutyl Carbinol (MIBC) and polygycols [15].

The similarities in the chemical structures of frothers and collectors result in collecting abilities in frothers and frothing abilities in collectors [15]. As stated earlier, the most commonly used collectors in flotation of silicates are amines, fatty acids and sulfates/sulfonates. All these collectors have some level of frothing abilities [12, 15, 19]. As a result, most microflotation testwork is usually conducted in the absence of frothers. In some cases, frothers are also not used in batch flotation tests [19]. A study by Díaz et al. [19] on the batch flotation tests of feldspar using an amine collector indicated that, using pine oil as a frother resulted in a froth that was too consistent and it was detrimental to the flotation efficiency [19]. Batch flotation tests of kyanite ore performed by Bulut and Yurtsever [12] employed a combination of sulfonate collectors [12]. The sulfonate collectors exhibited frothing characteristics and there was no need for frother addition [12].

2.3.2 Liberation and Batch flotation tests

2.3.2.1 Liberation

Liberation is one of the factors that affect the flotation behavior of minerals. Good liberation will result in a better separation than poor liberation, if all the other flotation parameters are kept constant. Liberation is assessed using automated mineralogy. The instruments used include QEMSCAN (Quantitative Evaluation of Minerals by Scanning Electron Microscopy), MLA (Mineral Liberation Analyser) and TIMA (Tescan Integrated Mineral Analyser). All these instruments are based on electron microscopy. The chemical spectra are collected in selected intervals in a 2D field of view. The image obtained is colour coded and can be used for modal mineralogy and texture. The data could be used to deduce grain size which can in turn be used to deduce liberation. Particles can be classified according to the area percentage of the mineral of interest. The classification categories include free (≥95% of the total particle area), liberated (≥80%) and non-liberated (<80%). This information can be used to deduce the appropriate feed particle size distribution whereby high flotation efficiency can be achieved with the right flotation conditions [15].

2.3.2.2 Batch flotation tests

Batch flotation tests are usually performed with 500g to 2kg of ore. The tests are normally performed using a single stage and do not properly mimic the commercial plants which usually have cleaners and recycling of material. Normally, batch flotation tests in laboratories are performed using a mechanical cell. Figure 2.13 shows a batch flotation test performed in a laboratory using a Denver cell. The air is introduced through an impeller and controlled using a valve. Bubbles are produced through the shearing action of the impeller. The impeller also serves the purpose of agitating the pulp and keeping the particles in suspension. Unlike microflotation tests, batch flotation tests are performed using tap water. The pulp normally requires conditioning with reagents prior to the introduction of the air [15].

Figure 2.13 Batch flotation tests using a Denver Cell [15]

Although laboratory tests are normally conducted using mechanical cells, for certain ores, it is more suitable to use a reactor/separator set up such as a Jameson cell. The difference between these cells and a mechanical cell is that the mixing zone is separate from the zone where the bubbles rise to the froth. This cell set up provides a bigger quiescent zone, higher gas hold-up in the reactor and higher energy that goes directly to bubble-particle collision compared to mechanical cells [15].

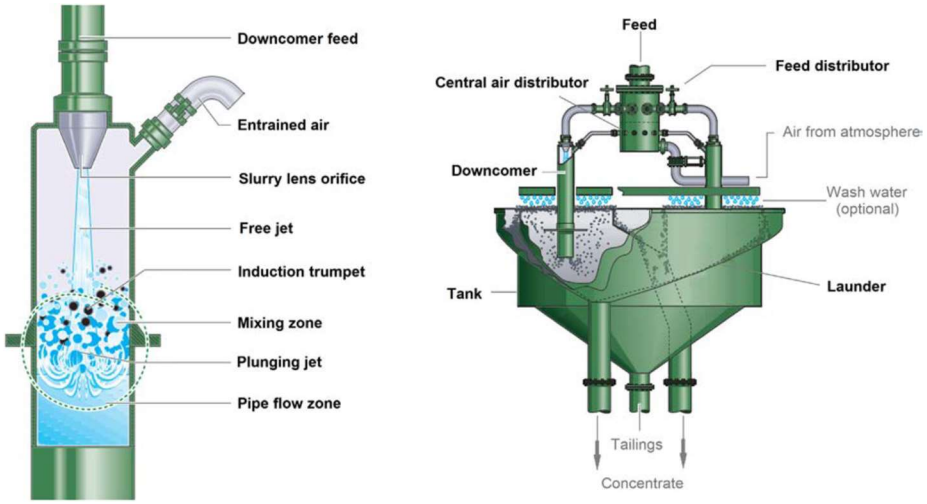

Figure 2.14 Jameson cell [15]

2.5 Processing of wollastonite ores

Wollastonite is processed through gravity separation, hand cobbing, magnetic separation and flotation [3, 6]. Currently, the most commonly applied beneficiation methods are magnetic separation, flotation and to a lesser extent, gravitational methods [3, 6]. The beneficiation method is selected based on the gangue minerals present within the ore [3].

Wollastonite deposits that contain mainly garnet as a gangue mineral can be beneficiated using high intensity magnetic separation [3]. A study on a wollastonite rich skarn composed mainly of garnet, feldspar, quartz, dolomite and calcite used magnetic separation to remove garnet, followed by flotation to remove carbonates [6]. No attempts were made to float quartz and feldspar which accounted for approximately 10 wt.% of the ore [6]. In diopside-bearing wollastonite deposits, diopside may also be beneficiated through wet, high intensity magnetic separation (WHIMS) [3]. In most operations, diopside usually requires a further beneficiation step of flotation [3].

There are insufficient differences in the magnetic, specific gravity and electrical properties between wollastonite and most of the silicate gangue minerals apart from garnet and diopside, which indicates that their removal can only be achieved using flotation [49]. Wollastonite exhibits similar flotation characteristics to many silicate gangue minerals, as such selective flotation is difficult [3]. Furthermore, wollastonite has an acicular crystal habit and for aspect ratios >8, the shape of wollastonite's needles is non-ideal for adhering to bubbles [1, 2, 3]. For these reasons, wollastonite ores are normally beneficiated through a reverse flotation and depressants are used to render wollastonite hydrophilic [3].

In calcite bearing ores, calcite is normally floated first using long-chain carboxylic acids. Feldspars and quartz are normally floated using long-chain alkyl amines. Garnet and diopside are floated using sulphate soap collectors, in some cases lead nitrate activator is used for pyroxenes flotation [3].

Normally wollastonite floats to a certain extent and therefore depressants are needed to minimize the floatability. Depressants that have been tested on wollastonite's reverse flotation are acetic acid, oxalic acid, lactic acid, citric acid and EDTA [3, 50]. A study conducted by Bulatovic [3]

reported that the most promising results were achieved with acetic acid which reduced the recovery of wollastonite from about 70% to <10% in the gangue concentrate as shown in *Figure 2.15* [3].

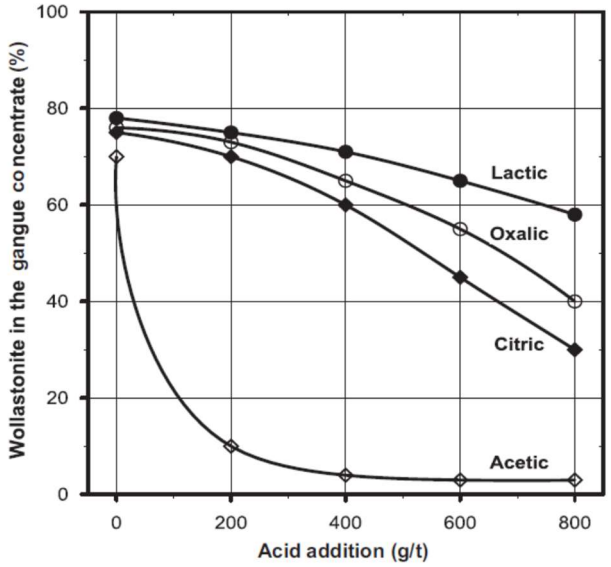

Figure 2.15 Wollastonite depression using different carboxylic acids [3].

Belardi et al. [50] reported successful depression of wollastonite from feldspar using EDTA as a depressant and an amine as a collector at pH 3-5 [50]. EDTA has been reported as either a modifier or a depressant in calcite bearing ores and iron oxide reverse flotation [51, 52, 53]. EDTA is a chelating agent with a high affinity for ions like calcium, iron and manganese and as a result it is used to clean mineral surfaces to avoid accidental depression of minerals in the presence of depressants like SHMP and starch [51, 52, 53]. It has also been reported that, at high EDTA concentrations, EDTA starts behaving like a depressant [51, 52, 53]

2.4.1 Surface chemistry of wollastonite and selected gangue minerals

The surface chemistry of wollastonite and the associated silicate gangue minerals is briefly discussed in this section. The surface chemistry of quartz and feldspars was discussed thoroughly in section 2.3.1 and therefore, only diopside will be discussed in this section.

i) Dissolution studies

Wollastonite is a chain silicate mineral and is naturally hydrophilic [1]. Wollastonite contains about 48 % calcium, which is an alkaline metal and renders wollastonite partially soluble [3, 49]. The release of calcium ions into solution is evidenced by an increase in pH when a calcium bearing mineral is suspended in an aqueous solution [49]. Dissolution studies reported that, at acidic pH, wollastonite undergoes incongruent dissolution whereby calcium ions are preferentially lost into solution and silica is retained on the mineral surface [49, 54] .

Wollastonite loses up to ~90 atoms nm^{-2} at a pH of ~7.5 whilst diopside only loses less than 35 atoms nm^{-2} at acidic pH (pH of ~2) which implies that wollastonite's dissolution rate is much faster than that of diopside (Figure 2.16) [54]. Studies report that, wollastonite dissolves faster than most alkaline metal bearing silicates [49].

Prabhakar et al. [49] reported dissolution of wollastonite at pH 8. The study indicated that, after conditioning wollastonite for 5 mins in an aqueous solution, ~51-66 % of Ca is released into solution compared to only ~19% of silicon. Wollastonite's surface becomes silica rich due to this incongruent dissolution and that will have a major effect on the floatability of wollastonite [49].

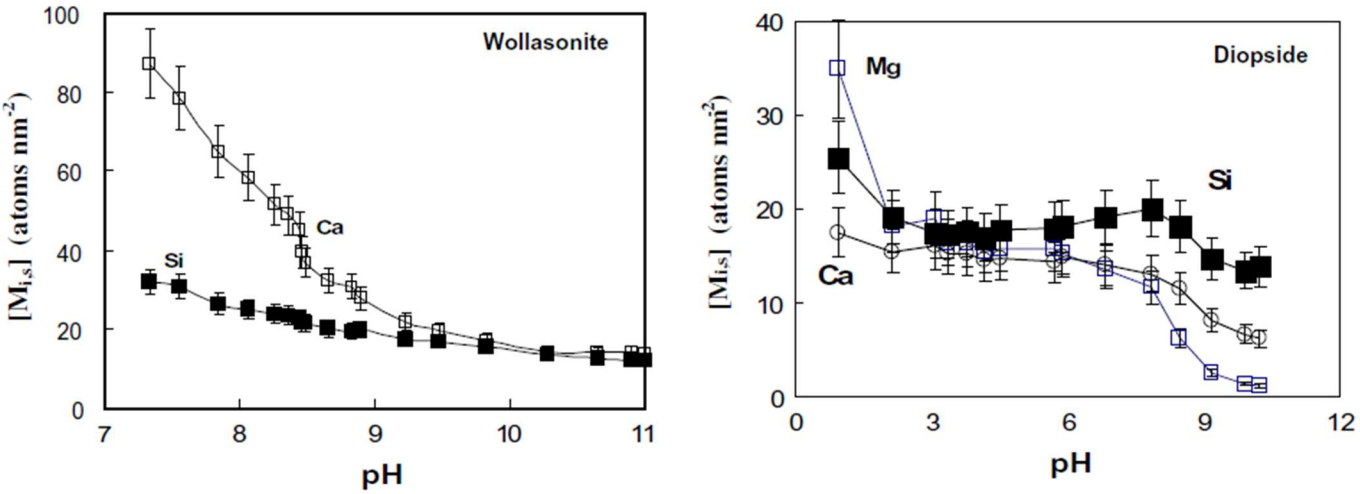

Figure 2.16 Metal loss from the mineral surface in an aqueous solution as function of pH for wollastonite (left) and diopside (right) [54] .

ii) Floatability and collector adsorption

The floatability of wollastonite was studied using microflotation tests and a diamine collector was employed to impart hydrophobicity onto wollastonite [49]. The flotation recovery of wollastonite using a diamine collector at neutral pH, increases with diamine concentration in a similar manner to quartz flotation response to an increase in DDA concentration (Figure 2.17) [49]. The similarities in the flotation response of wollastonite and quartz may be due to the preferential dissolution of calcium which leaves the surface of wollastonite silica rich [49]. The maximum flotation recovery of wollastonite using a diamine collector is obtained at a pH range between 7 and 8.5 (Figure 2.18) [49]. At low pH wollastonite is only slightly negatively charged. Since the diamine adsorbs electrostatically, collector adsorption is low at acidic pH and flotation recovery is also low [49]. At alkaline pH, flotation recovery declines due to lesser ionic amine species in solution and possibly, the presence of calcium hydroxy species [47, 49]

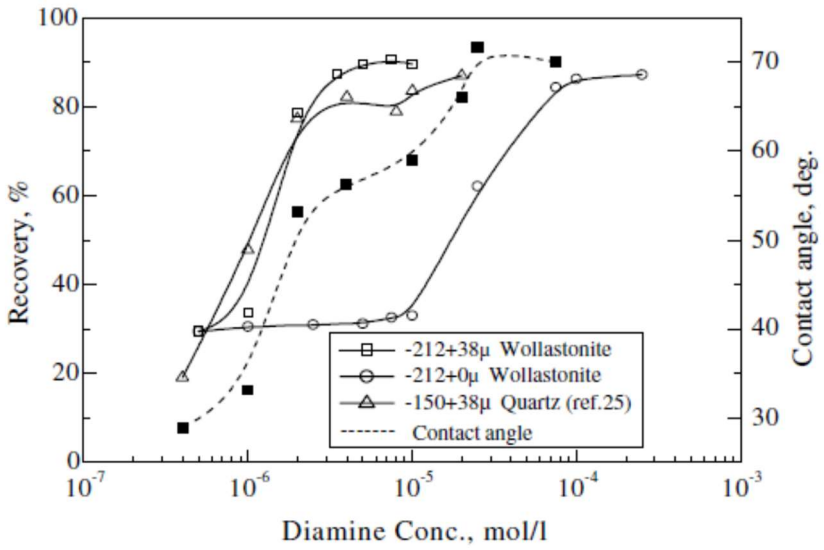

Figure 2.17. Flotation recovery of wollastonite as a function of diamine concentration [49].

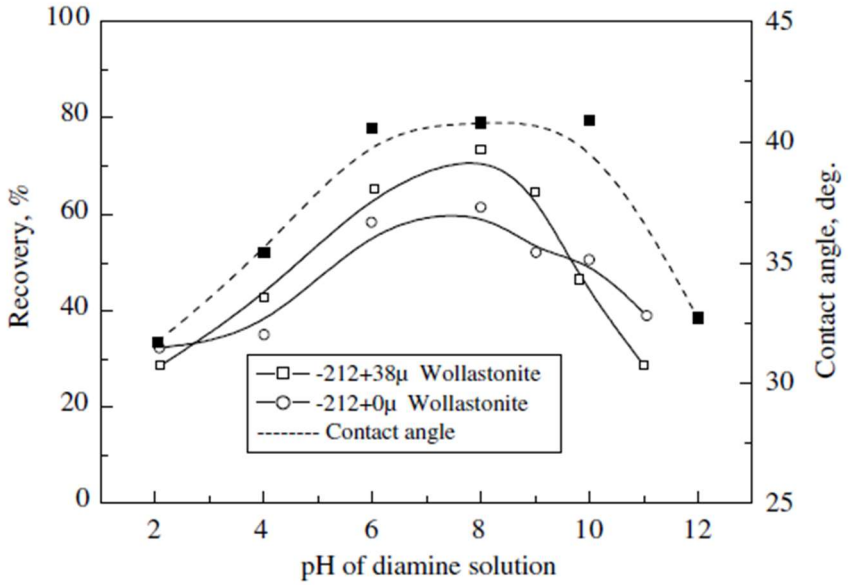

Figure 2.18. Flotation recovery of wollastonite as a function of pH [49].

Adsorption of the diamine collector was further investigated using FTIR [49]. Wollastonite treated with diamine at natural pH showed an increase in the intensity of the alkyl chains infrared absorption bands with increasing diamine concentration [49]. The increase in the intensity of the peaks indicates an increase in collector adsorption onto the wollastonite surface and thus, floatability as well [49].

Flotation recovery was also correlated with contact angle measurements to further investigate collector adsorption. Contact angle measurements indicated a good correlation with flotation recovery as a function of both pH and concentration. This correlation indicates that increased diamine adsorption results in an increase in hydrophobicity which in turn results in an increase in the contact angle and floatability of wollastonite. Contact angle measurements were also used to evaluate surface free energy. The total free energy of wollastonite decreases with an increase in concentration of the diamine collector, which indicates that the wollastonite/diamine aggregate has high stability [49].

A study on flotation behavior of wollastonite using dodecylamine hydrochloride (DDA. HCl) demonstrated similar behavior as in the presence of diamine (Figure 2.19) [55]. Wollastonite recovery was low at acidic pH, and the recovery increased to greater than 80% at pH 7 to 10 and then started to decrease after pH 10 (Figure 2.19) [55]. Diopside exhibited similar flotation

behavior as wollastonite but, a higher concentration of DDA.HCl was required to float diopside as shown by the recovery against concentration curves in Figure 2.19 [55]. This flotation behavior implies that wollastonite can be selectively floated using DDA.HCl if the concentration of DDA is kept low [55]. The selectivity using physically adsorbing collectors is usually low.

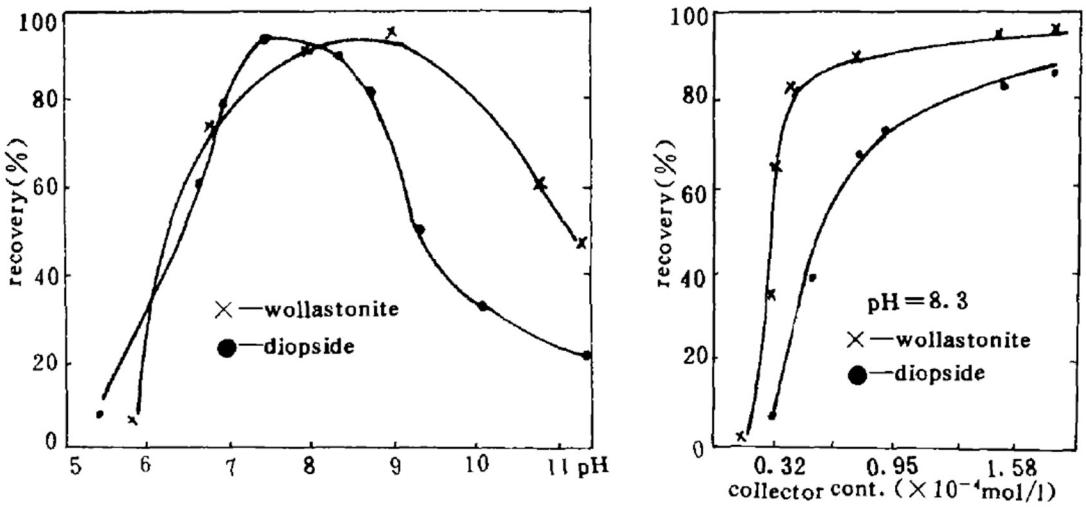

Figure 2.19 Microflotation tests of wollastonite and diopside. Recovery against pH at 2.37 x 10^{-4}mol/L DDA. HCL (left). Recovery vs concentration at pH 8.3 (right) [55].

Jizu et al. [55] investigated the use of tannic acid to improve the separation efficiency through a selective depression of diopside. Tannic acid (TA) selectively depressed diopside at pH 7.8 to 8.8 (Figure 2.20) [55]. Figure 2.20 shows that, the selectivity of tannic acid is lost at higher tannic acid dosages [55]. Tannic acid was reported to adsorb chemically to the Mg^{2+} and Ca^{2+} species on the diopside surface, which was confirmed by XPS and UV-Vis spectrometry [55]. Tannic acid adsorbs similarly to wollastonite through Ca^{2+} species but, since wollastonite is more soluble than diopside, most of the calcium species are dissolved into solution leaving wollastonite devoid of metal sites [55]. As a result, tannic acid has more affinity for the diopside surface than wollastonite [55]. Tannic acid adsorption through metal ions was also reported in flourite flotation [56]. It was proposed that TA adsorbs mainly through the caboxylate and alcohol functional groups, possibly forming chelates [56].

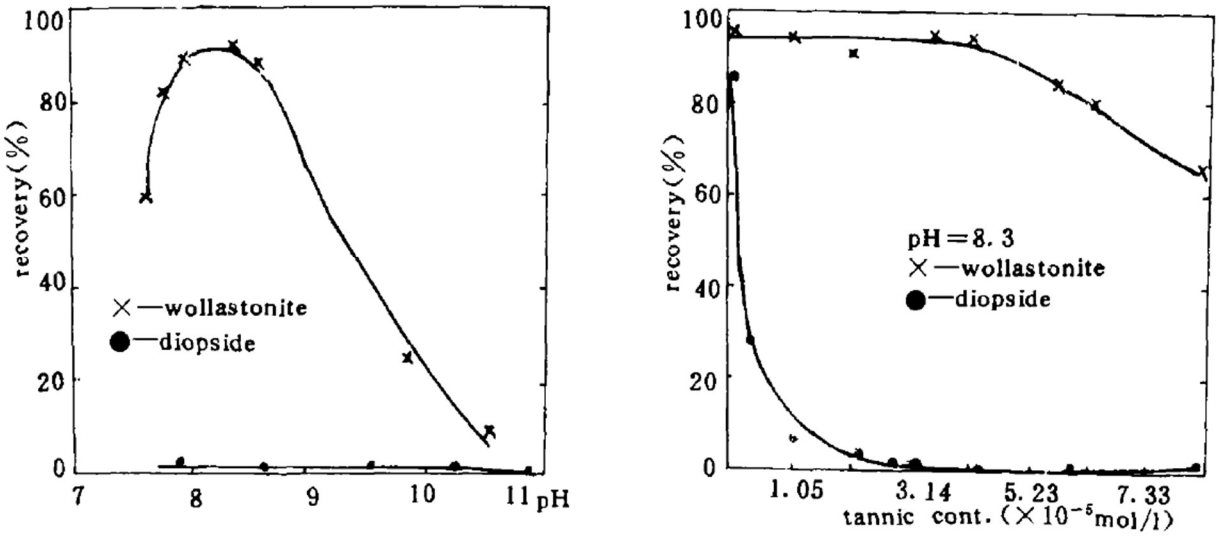

Figure 2.20 Flotation behavior of diopside and wollastonite with tannic acid as a depressant. Recovery against pH at 1.58 x10^{-4}mol/L DDA. HCl and 3.14x 10^{-5}mol/L tannic acid (left). Recovery against tannic acid concentration at pH 8.3 and 1.58 x 10^{-4}mol/L DDA.HCl (right) [55].

Adsorption of flotation reagents is influenced by the species on the mineral surface and surface charge. Zeta potential measurements determined the isoelectric (IEP) of wollastonite and diopside to be at pH 2.6 and pH 2.78-4.4, respectively [49, 42]. The IEP of quartz and feldspar were reported to occur around pH 2 [20, 27].The IEPs of wollastonite and its gangue minerals implies that most of the minerals present within the Saint Lawrence deposit can be floated at alkaline pH using cationic collectors [49]. Various studies have reported flotation of quartz and feldspar using cationic collectors at alkaline pH [18-21, 26, 27, 29].

2.4.2 The effect of particle shape on floatability of wollastonite

Wollastonite has an acicular crystal habit and results in needle-like shaped particles upon comminution [4]. Bulatovic [3] reported that wollastonite's particle shape results in poor flotation recovery especially for aspect ratios > 8. There are currently no studies that look at the effect of particle shape of wollastonite in detail. To address the issue of particle shape, a study by Lecrivain

et al. [57] which looks at particle-bubble interaction for glass fibres will be discussed briefly in this section [57].

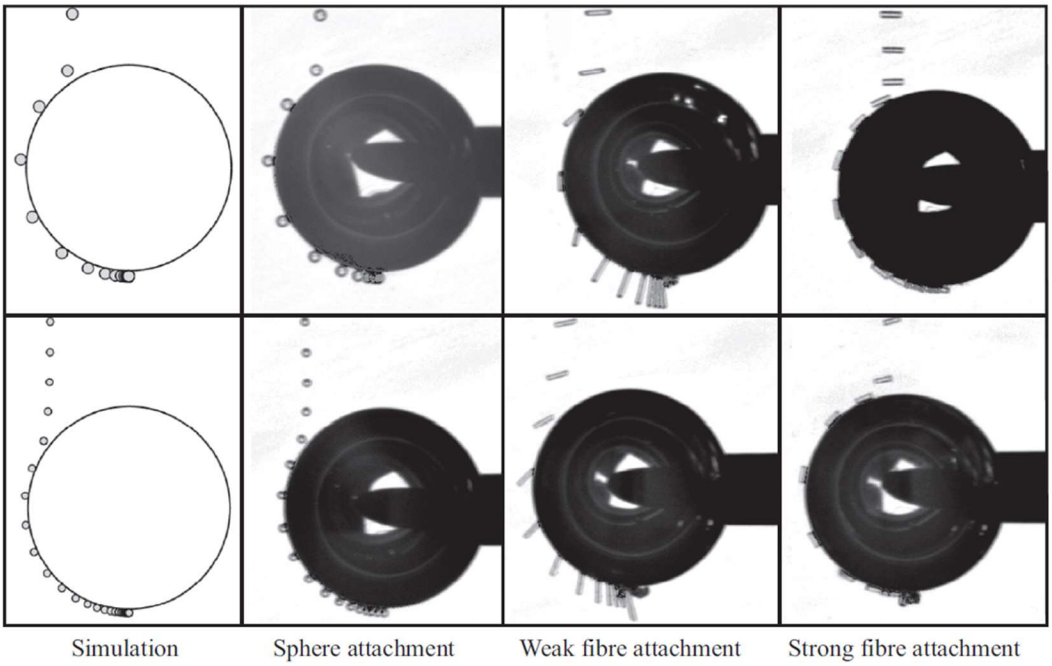

Figure 2.21 Particle-bubble interaction as particle slides along a stationary bubble. Spherical interaction (simulation and experimental) (left). Elongated particles, weak and strong interaction (right). [57]

The elongated particle behavior was compared to that of spherical particles. Their findings demonstrated two modes of fibre attachment, a weak and a strong fibre attachment (Figure 2.21). A weak fibre attachment occurs when a particle reorientates to a radial alignment to the air/water interface as it slides along the bubble (Figure 2.21). A weak attachment is also associated with collision angles >30º. A strong attachment occurs when the particle attaches to the bubble with its major axis parallel to the air water/air interface, the contact area is bigger and therefore, the attachment is stronger. The strong attachment for prolate particles is stronger than that of spherical particles of the same volume due to larger particle interface area (*Figure 2.21*). Lecrivain et al. [57] reported that, the strong attachment forms as a result of collision angles < 30 º. It must be noted that this study was conducted with fibres of aspect ratios up to 8, the aspect ratios of wollastonite by far exceeds that and the findings from this study might not fully explain wollastonite behaviour [57].

To summarise, the flotation work performed on wollastonite ores is limited and the details on surface chemistry of wollastonite and respective gangue minerals requires further investigation. In addition, there are no detailed studies on physical aspects such as the effect of grinding methods on aspect ratios and how the aspect ratio impacts flotation recovery. The purpose of the current study is to investigate the flotation behaviour of wollastonite and associated gangue minerals.

Chapter 3. Methodology

3.1 Materials

3.1.1 Minerals

Pure (>95%) wollastonite, quartz and diopside were used for microflotation tests, zeta potential measurements, adsorption density studies and X-ray photoelectron spectroscopy (XPS). Wollastonite in the particle size range of -212 µm was obtained from Canadian wollastonite, Ontario. The particle size distribution of wollastonite was determined using sieve analysis and >80 % of the material was below 106 µm. Wollastonite was wet screened at 212 µm, 150 µm, 106 µm, 75 µm, 54 µm and 38 µm to avoid particle aggregation. Pure quartz was obtained from Unimin Canada Ltd and pulverised using LM2-P pulverizing mill (Labtechnics, Australia). Diopside was obtained from Ward's Scientific (Canada) ground down to a top size of 600 µm and then handpicked from feldspars and micas. The remaining micas were then removed using dense medium separation (DMS) to obtain pure diopside. Lithium metatungstate with a specific gravity of 2.95 was used as a dense medium and diopside was collected as a sink fraction since it has a slightly higher density than the micas. The separation was conducted under the influence of gravity, no centrifuge was required. X-ray diffraction (XRD) using Bruker D8 Discovery X-ray diffractometer (Copper Kα source) was used to test the purity of each mineral used for microflotation tests, zeta potential measurements, adsorption density studies, X-ray photoelectron spectroscopy (XPS) and particle-bubble attachment studies.

The ore was obtained from Canadian Wollastonite already pulverised to the k80 of 188 µm (particle size distribution was determined using sieve analysis). The feed was characterised using Quantitative Evaluation of Minerals by Scanning Electron Microscopy (QEMSCAN) and X-ray fluorescence (XRF). QEMSCAN analyses were conducted at SGS Canada (Lakefield, Ontario). QEMSCAN analyses were carried out on polished sections, further details on the equipment and analyses are described by Jordens et al. [58]. XRF was conducted in Université Laval. The samples were pulverised using a Pulverissette 6 planetary monomill (Fritsch, Germany). The fused sample beads were prepared using a X-300 fusion fluxer made by Katanax Inc. (Quebec

City, Canada). The samples were analysed on an Epsilon 1 instrument using an Epsilon 3 Software produced by Malvern PANalytical.

3.1.2 Reagents

Table 3.1 List of Reagents

Reagent type	Reagent name
Collector	Sodium dodecylamine (DDA), sodium oleate (NaOl)
Depressant	Tannic acid (TA), sulphuric acid (H_2SO_4)
Frother	Isobutyl methyl carbinol (MIBC)
pH modifier	Hydrochloric acid (HCl), sodium hydroxide (NaOH)
Dense medium	Lithium metatungstate

Sodium dodecylamine (DDA) obtained from Sigma Aldrich (USA) was dissolved in a 1:1 mass ratio with acetic acid purchased form Sigma Aldrich (USA). Analytical grade tannic acid (95%) was obtained from Fisher Scientific (USA). Fresh solutions of Tannic acid (TA) were prepared for each condition due to tannic acid degradation. Sodium oleate (NaOl) (≥82%) was obtained from Sigma Aldrich. Lithium metatungstate was purchased from LMT liquid, LLC. Hydrochloric acid (HCl) and sodium hydroxide (NaOH) purchased from Fisher scientific (USA) were used as pH modifiers. The structure of tannic acid and sodium oleate is shown in Figure 3.1. Isobutyl methyl carbinol (MIBC) (98%) was purchased from sigma Aldrich. ACS grade sulfuric acid was purchased from Fisher scientific (Canada). The purpose of each reagent is specified in Table 3.1.

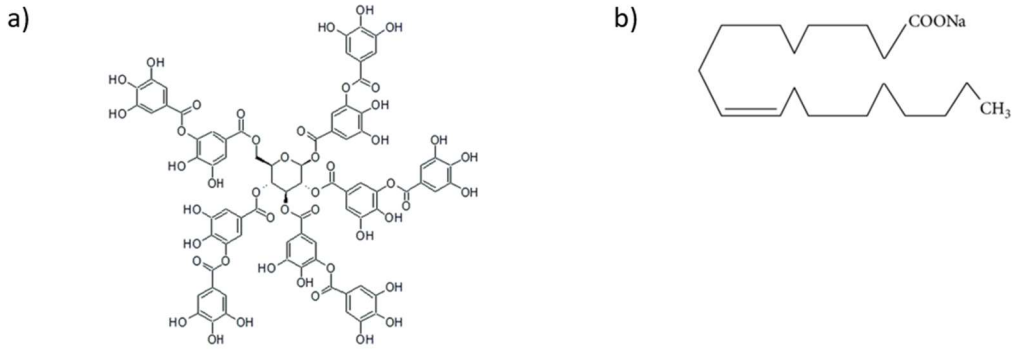

Figure 3.1 Tannic acid structure (a) and sodium oleate structure (b). [59, 60]

3.2 Microflotation tests

Microflotation tests were performed using a 170 ml Hallimond tube (Figure 3.2) on 1 g of pure wollastonite, diopside or quartz. The particle size range of -106 µm to +38 µm was used for microflotation tests since wollastonite is fully liberated below 106 µm. The lower size limit was chosen as 38 µm to avoid entrainment and slow flotation kinetics related to fine particles [15] . The specific surface area of diopside, wollastonite and quartz samples were 0.1798 m^2/g, 0.1174 m^2/g and 0.0715 m^2/g, respectively. One gram of a pure mineral was conditioned for 5 minutes in a 30 ml solution of deionized water and a collector. The mixture was then transferred to the Hallimond tube and then a 140 ml of pH adjusted deionized water was added. In the case of a collector and depressant, the depressant was added first, and conditioning was carried out for 3 min before the addition of a collector. The slurry containing both the collector and the depressant was then conditioned for another 5 min. The conditioning time was chosen as greater than 3 minutes for all reagents based on literature and to ensure reagent adsorption. The flotation time was 1 min for all tests which is normally an adequate amount of time required to float 1g of sample (based on literature). Additionally, it was observed that the flotation of floatable particles was complete before the end of 1 minute although it might be useful to increase the flotation time and compare the recoveries. The air was introduced at a rate of 34 ml/min.

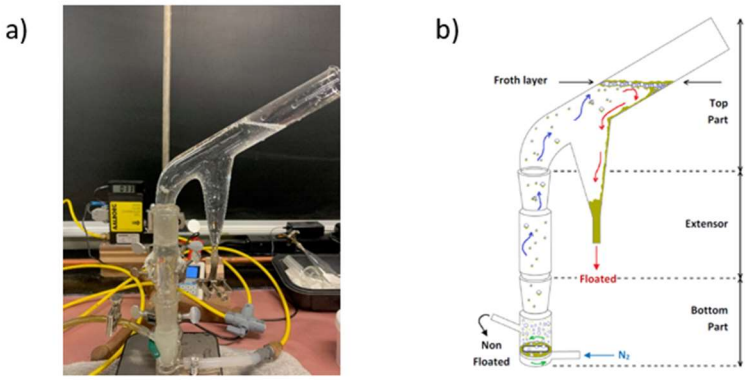

Figure 3.2 Laboratory set up of a Hallimond tube (a) and a schematic diagram of a Hallimond tube (b) [61]

3.3 Zeta potential Measurements

Zeta potential tests were performed on pure mineral particles pulverised using a Pulverissette 6 planetary monomill (Fritsch, Germany) to ≲10 μm. The d50 of quartz, wollastonite and diopside were 1.75 μm, 5.14 μm and 10.4 μm, respectively. The particle size for zeta potential measurements using electrophoretic mobility should be ultrafine [62]. Particle size distribution was analysed using Horiba Laser Scattering Particle Size Distribution Analyzer LA-920 (ATS Scientific Inc., Canada). The specific area of diopside, wollastonite and quartz samples were 3.42 m^2/g, 4.64 m^2/g and 6.7932 m^2/g, respectively. The surface area was analysed using a Brunauer–Emmett–Teller (N2-BET) technique using a TriStar Surface Area and Porosity Analyzer (Micromeritics, USA). Zeta potential measurements were taken using a NanoBrook 90Plus Zeta Particle Size Analyzer (Brookhaven Instruments, USA). A 200 ml suspension containing 0.08 grams of a pure mineral (0.04 wt. % solids) and an electrolyte solution of 1 x 10^{-2} M NaCl (indifferent background electrolyte) was prepared. The mineral suspension was dispersed for 30 seconds using UP400S Ultrasonic processor (Hielscher, USA) to ensure complete dispersion. Pure minerals were conditioned for 1 hr in an electrolyte solution to reach equilibrium. Fresh solutions were prepared at each pH. For reagent addition, the solution was conditioned for an extra 15 mins in the presence of the reagent prior to taking the first measurement. The dosages for TA and DDA in g/m^2 are given in Table 3.2 which are an equivalent of a 100g/t TA and DDA microflotation dosages for each mineral.

Table 3.2 Zeta potential measurements dosages. The dosages are an equivalent of 100g/t microflotation dosage for each mineral

Mineral	DDA dosage (g/m^2)	TA dosage (g/m^2)
Quartz	1.39 x 10^{-3}	1.39 x 10^{-3}
Diopside	5.56 x10^{-4}	5.56 x10^{-4}
Wollastonite	8.52 x 10^{-4}	8.52 x 10^{-4}

3.4 X-ray Photoelectron spectroscopy (XPS)

XPS analyses were performed on both the pure samples and samples treated with reagents. The conditions for reagent addition were similar those used for microflotation tests with an exception of tannic acid. The samples were washed thoroughly with de-ionised water and air dried. The samples were then degassed for 3 hours under room temperature in a vacuum oven. The analyses were performed using Thermo Scientific K-Alpha Monochromatic X-ray Photoelectron Spectrometer (Thermo Fisher Scientific Inc., USA), ultrahigh vacuum chamber (10-9 Torr) and micro focused monochromator. The respective pass energy values for elemental survey scans and high-resolution scans were 1 and 0.1 eV. The spot size was 400 μm. The electron gun was employed to avoid surface charging. Data analysis was performed using Thermo Avantage 4.60 (Thermo Fisher Scientific Inc., USA) software. The C1s peak at 284.8 cm^{-1} was used for charge correction.

3.5 Adsorption density measurements

Diopside, quartz and wollastonite were conditioned with TA at three concentrations, 5ppm, 8 ppm and 10 ppm. The concentration values were chosen to cover the microflotation concentration range. The mineral samples used were in a -54/+38 μm particle size range due to sample availability. The specific area of diopside, wollastonite and quartz samples were 0.2088 m^2/g, 0.2705 m^2/g and 0.1205 m^2/g, respectively. The conditions for TA addition were similar to those used in microflotation. 0.5 grams of a pure mineral was conditioned in 12.5 ml solution containing de-ionized water and TA. The particles were filtered using a 0.45 μm pore size syringe filter. The concentration of the supernatant was measured using UV-vis spectrophotometry (Lambda 20, PerkinElmer instruments) and the amount adsorbed was calculated from the supernatant concentration using the following equation:

$$Adsorption\ density = \frac{(Cf - Ci)\,V}{Mineral\ surface\ area} \tag{3.1}$$

Where, Cf is the final TA concentration in the supernatant in ppm, Ci is the initial TA concentration in ppm and V is the total volume in litres. The principles governing UV-vis spectrophotometry are described in Appendix B.

3.6 Aspect ratio measurements

Aspect ratios of wollastonite particles were measured using Olympus BX51 (Olympus, Canada) reflected/transmitted light microscopy. Measurements were taken manually from photomicrographs. Image analysis software could not define the particle boundaries due to overlaps and fractures within the particle. More than 150 particles were measured to ensure statistical significance.

3.7 Particle-bubble attachment studies

Visualisation of particle-bubble attachment was achieved using a method introduced by Uddin et al. [63]. A stationary bubble is introduced using a capillary (4 mm inner diameter) (Figure 3.3). 1 g of a pure mineral is conditioned using a 30 ml solution of de-ionised water and the collector. 30 ml was chosen to maximise the particle density in order to increase the probability of collisions between wollastonite particles and a stationary bubble. The mineral suspension is then agitated for 1 min and then the particles are left to settle before the picture is taken. The picture was taken using a digital camera Canon EOS500D digital camera equipped with an EF 100 mm f/2.8 USM Macro lens.

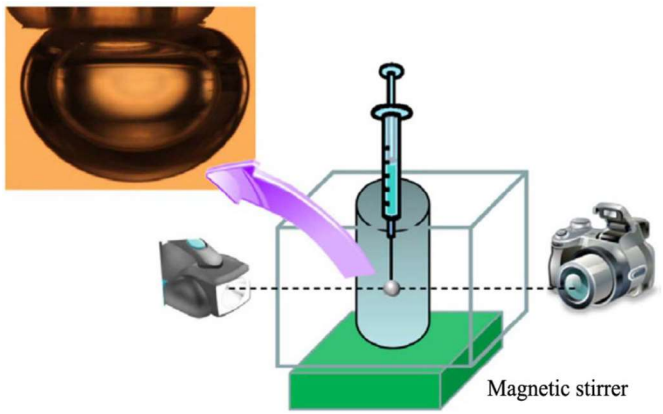

Figure 3.3 Experimental set up for the bubble-particle attachment photos [63]

3.8 Speciation diagrams

Speciation diagrams of ions in solution and reagents were modelled by HySS2009 software (Protonic software) and data from literature and experimental conditions.

3.9 Batch flotation tests

Batch tests were conducted using a 1.5 L Denver cell. The slurry contained 24% (by mass) solids. The pH, impeller speed and the air flow rate were kept constant at 8.5, 1200 rpm and 2.8 L/min, respectively. The air rate was chosen empirically and based on the flotation cell size. DDA and Tannic acid were employed as a collector and a depressant, respectively. The tests were conducted using tap water. Methyl isobutyl carbinol (MIBC) was used as a frother and HCl and NaOH were used as pH modifiers. The slurry of the ore and tap water was adjusted to the pH of 8.5 (the pH was chosen based on microflotation tests results). Tannic acid was added, and conditioning was carried out for 3 minutes. DDA was then added and the slurry was conditioned for another 5 minutes. The conditioning time was chosen based on the microflotation test results. MIBC (18 ppm which was chosen using the rougher stage plant data [15] and empirically) was added and the slurry was conditioned for another 1 minute. A total of four concentrates were collected for each test at 0.5, 1, 3 and 7 minutes. The flotation tests were carried out for 7 minutes as it was observed in the preliminary tests that the kinetics were fast such that the flotation of floatable particles was complete before the end of 7 minutes. The pulp level and the pH were kept constant during the entire experiment. A minimum of three replicas were ran for each condition. The concentrates and tails were then composited and characterised using XRF (Epsilon 1).

Chapter 4. Results and Discussion

4.1 Single mineral tests

4.1.1. Mineral characterization

4.1.1.1 Sample purity

Mineral characterization using XRD shows that all the major peaks of the pure mineral samples match well with the major peaks from the reference spectra obtained from the International centre for diffraction data (*Figure 4.1*) . This correlation shows that the mineral samples are relatively pure. Further details on XRD can be found in Appendix A.

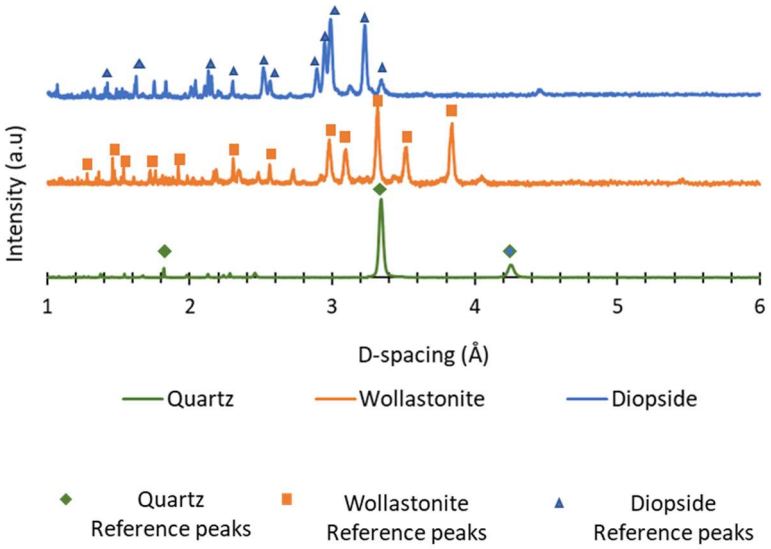

Figure 4.1 XRD patterns for quartz, diopside and quartz

4.1.1.1 Aspect ratio measurements

The particle distribution of the wollastonite sample shows that wollastonite aspect ratios (L/W) are high, ~78 % of the data lies above an aspect ratio of 10 (Figure 4.2).

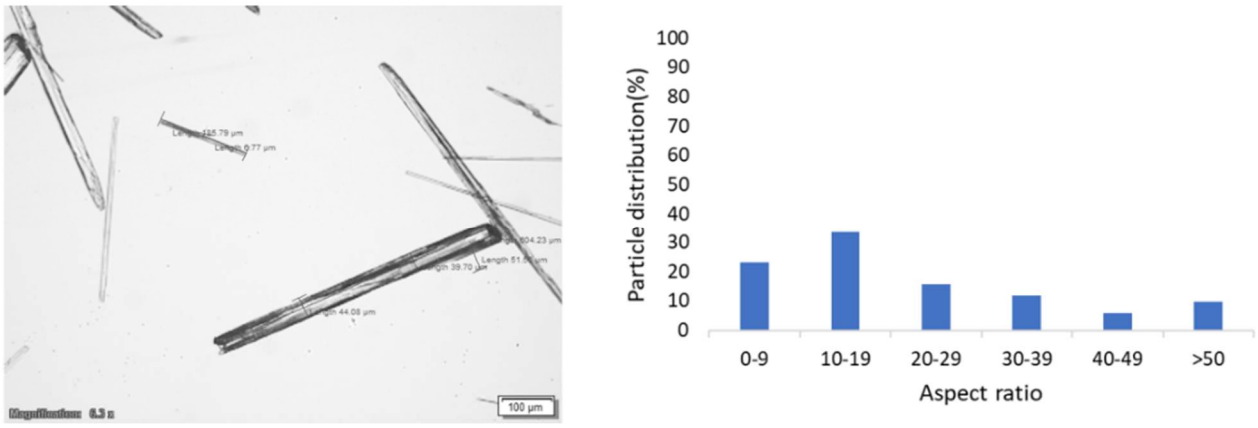

Figure 4.2 Aspect ratio measurements on the wollastonite sample

4.1.2 Small-scale flotation tests and surface chemistry

The following section discusses floatability and surface chemistry of wollastonite, quartz and diopside with various reagents.

4.1.2.1 Zeta Potential measurements

a) Pure minerals

Zeta potential data shows that the isoelectric point (IEP) for each mineral is below pH 3, which is consistent with previously published values [20, 27] (*Figure 4.3* a). This suggests that all these minerals are floatable with physically adsorbing cationic collectors such as dodecylamine (DDA) and possibly floatable with anionic chemically adsorbing collectors such as sodium oleate (NaOl) depending on surface ions [12, 21, 26, 27, 32, 42, 49] .

b) Dodecylamine (DDA)

Zeta potential measurements were performed on minerals in the presence of DDA as a collector. The results indicated a shift to positive values for quartz and wollastonite suggesting the presence of positively charged species on the mineral surfaces. The shift was pronounced at higher pH

values compared to lower pH, suggesting that the adsorption is stronger when the mineral surfaces are strongly negatively charged. This trend was well observed for quartz compared to wollastonite whereby the shift became significant again after pH 5. The lack of any appreciable shift on the diopside surface from pH 3-8 suggests that, amine species are not adsorbed onto diopside at the DDA concentration investigated in this study. At pH 9, there is a slight shift observed showing that there is some DDA adsorption on diopside. The shift could be related to an increase in molecular amine, which has been reported to increase DDA adsorption through minimising head to head repulsion of ammonium ions [21, 26, 27, 28]. The overall lower amine adsorption onto diopside might be related to that, diopside is less negatively charged compared to both quartz and diopside. Since the amine is predominantly a physically adsorbing collector, it will have less affinity for a less negatively charged mineral surface. It should be noted that the dosage per surface area is slightly lower for diopside than that of wollastonite and that might account for the lack of a positive shift. XPS will assist in further evaluation of collector adsorption.

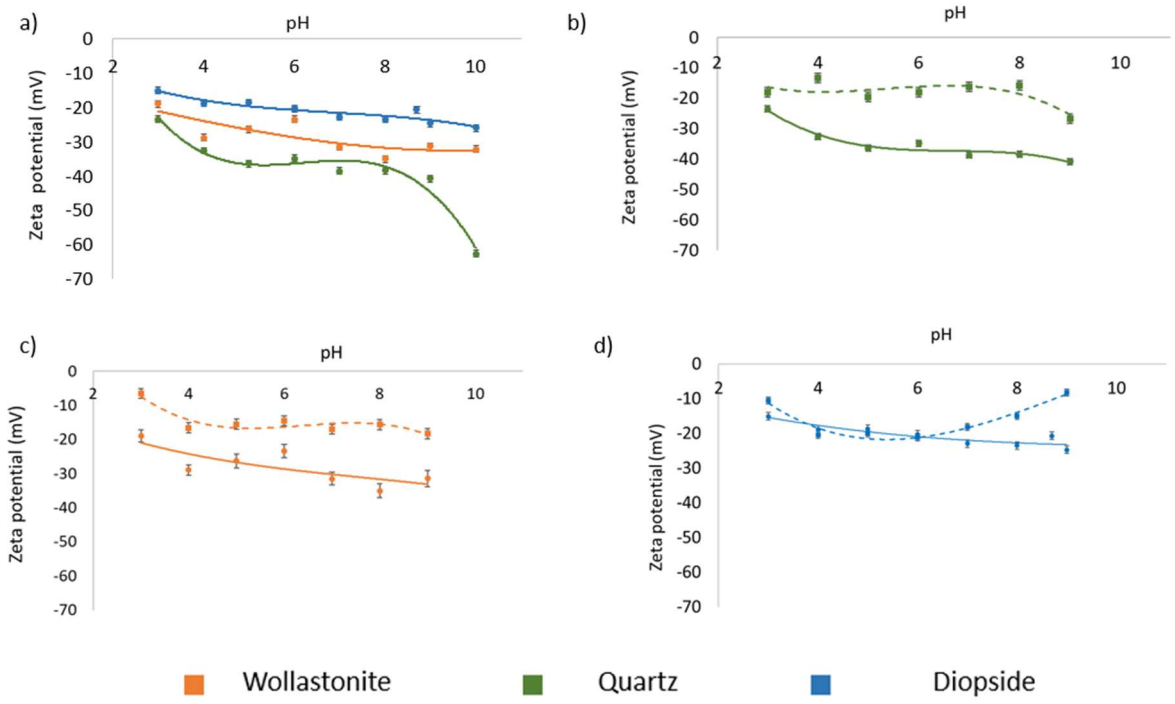

Figure 4.3 Zeta potential measurements plots showing untreated minerals(a) and DDA treated minerals surfaces (dashed lines) compared to untreated mineral surfaces (solid lines) for quartz (b) wollastonite(c) and diopside (d). Error bars represent 95% confidence intervals. Trendlines are added as visual aids only

c) Sodium Oleate (NaOl)

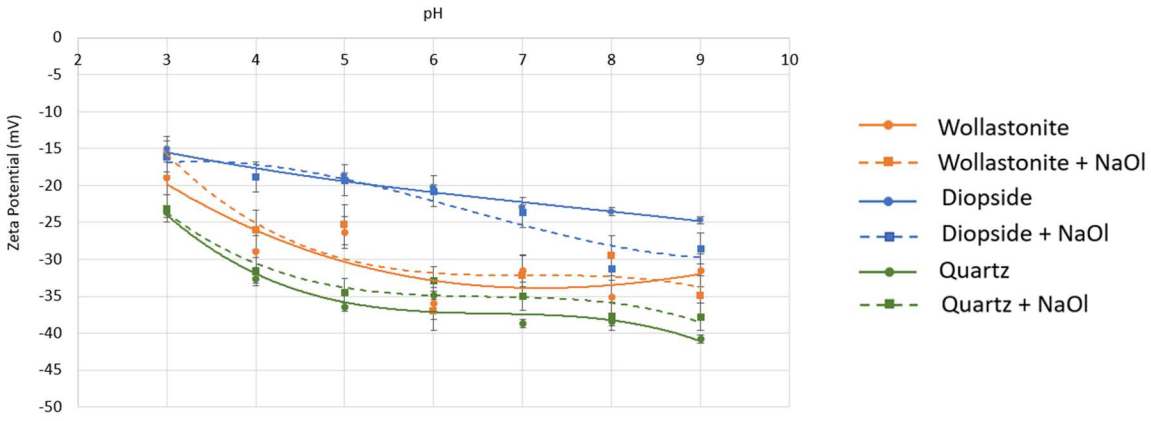

Figure 4.4 Zeta potential measurements on wollastonite, quartz and diopside treated with Sodium oleate. Solid lines represent pure (untreated) minerals, whilst dashed lines represent minerals treated with DDA. Error bars represent 95% confidence intervals. Trendlines are added as visual aids only

Zeta potential measurements were also performed on mineral surfaces treated with NaOl. Zeta potential measurements indicate that there are no major shifts in zeta potential values after treatment with sodium oleate. The results indicate a lack of adsorption of NaOl on all the mineral surfaces. Quartz, wollastonite and diopside are negatively charged from pH 3-9 and it would be expected that anionic physically adsorbing collectors would not be able to adsorb. Sodium oleate has been reported as a chemically adsorbing collector by various studies [12, 24]. Sodium oleate adsorbs through forming bonds with ions such as Ca^{2+}, Mg^{2+} and Al^{3+} [24, 64]. Ideally, wollastonite and diopside should be floatable with sodium oleate. The reasons for the lack of adsorption will be discussed further under Section 4.1.2.5 (speciation section).

d) Tannic acid

Zeta potential measurements were performed on TA treated wollastonite, diopside and quartz (*Figure 4.5*). The wollastonite zeta potential did not change (within experimental error) with

addition of TA. Diopside demonstrated a slight shift to more negative values from pH 6 to 8 with addition of TA. Quartz demonstrated a slight shift to less negative values with addition of TA although the statistical significance of this shift is minor compared to the shift observed on diopside.

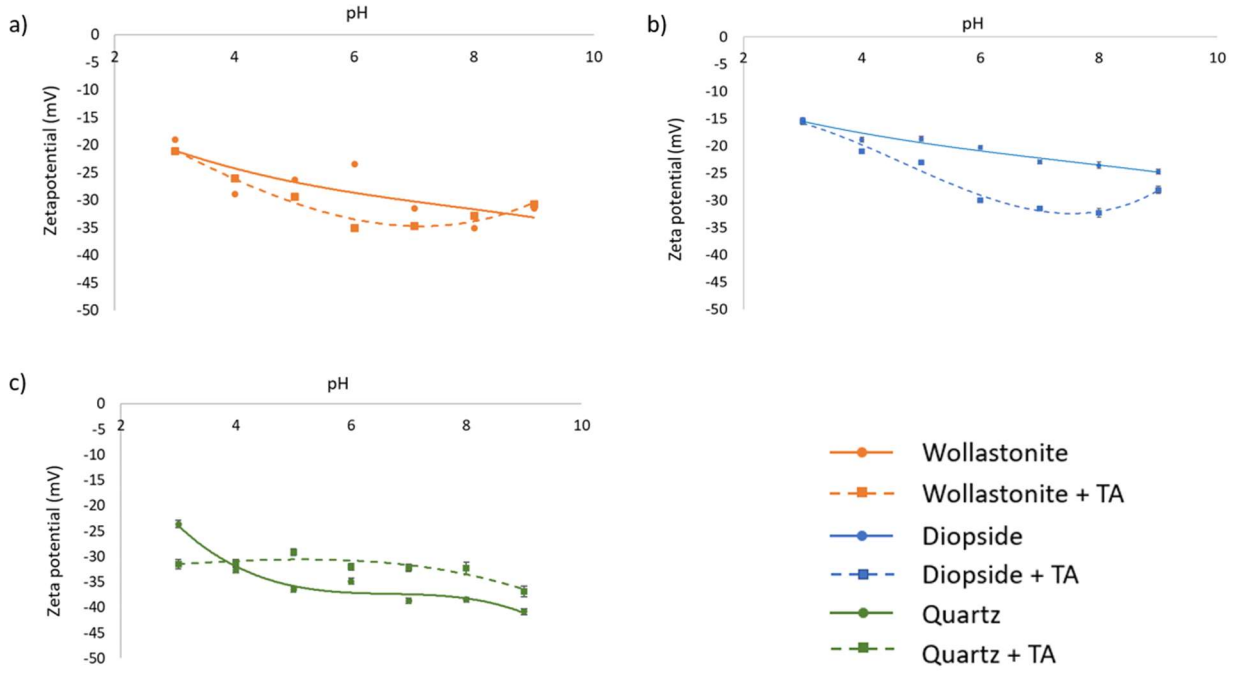

Figure 4.5 Zeta potential measurements of untreated (solid lines) and TA treated (dashed lines) wollastonite (a), diopside (b) and quartz (c) surfaces. The error bars indicate 95% confidence intervals. Trendlines are added as visual aids only

The shift on the diopside surface might indicate a change in the surface charge introduced by the addition of TA. Since TA is anionic, the shift should be towards more negative values. The shift is more significant in the pH range of 6 to 8 (~Δ10mV) which will be discussed further in the speciation section. The diopside surface is negatively charged in the pH range 6-8 which implies that electrostatic adsorption of anionic surfactants is not possible; therefore, it is likely that the mechanism of adsorption is chemical. The quartz shift is not consistent with adsorption of TA since it is towards less negative values. The shift appears to be minor to signify any major change which suggests that it might be related to a slight change in the experimental conditions or the machine.

4.1.2.2 X-ray photoelectron spectroscopy (XPS)

a) Dodecylamine (DDA)

XPS analyses were performed on diopside and wollastonite treated with 1.80 x 10^{-5} mol/L DDA at pH 7 to assess the collector adsorption and selectivity observed in zeta potential measurements. DDA introduced nitrogen onto the wollastonite surface but not onto the diopside surface (*Figure 4.6* & *Figure 4.7*). The appearance of nitrogen indicates the presence of an amine on the surface of wollastonite. The lack of nitrogen on DDA treated diopside surface indicates the lack of adsorption of DDA at a low DDA concentration. Overall, XPS confirmed adsorption of DDA onto wollastonite and a lack of adsorption on diopside.

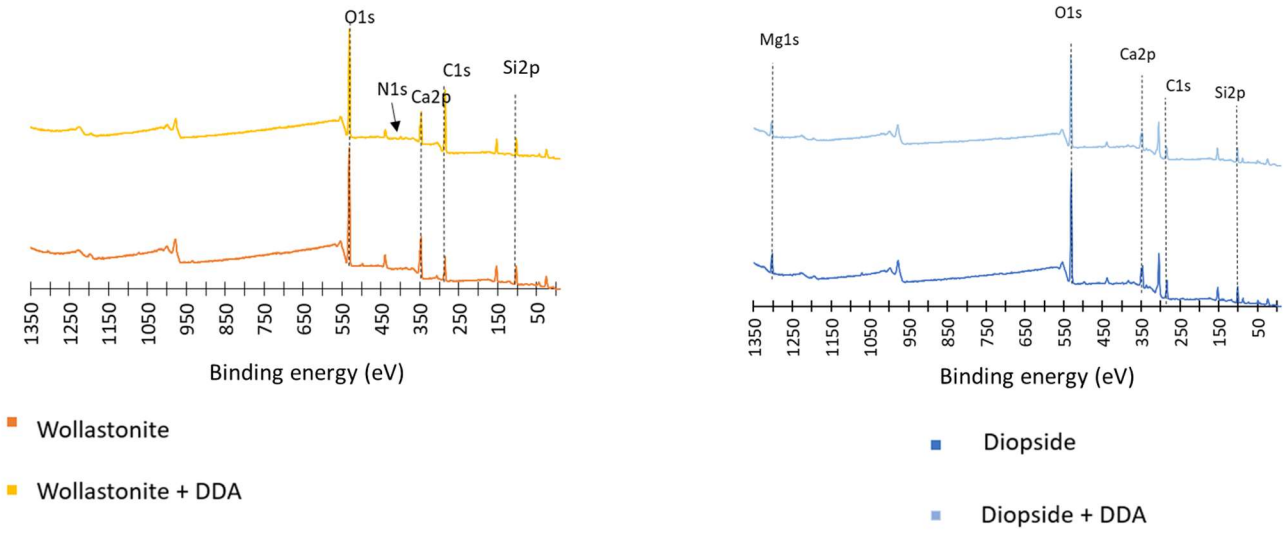

Figure 4.6 XPS analysis on wollastonite surface, untreated and treated with 1.8 x 10^{-5}M DDA (left). XPS analysis on diopside surface, untreated and treated with 1.8 x 10^{-5} M DDA (Right).

The wollastonite XPS results were further used to assess the mechanism of adsorption. No shifts were observed on wollastonite's surface elements. This indicates that the chemical environments of the wollastonite species did not change after addition of DDA. It can be concluded that the interaction of wollastonite and DDA is predominantly electrostatic, confirming that DDA is physically adsorbed to the mineral surface.

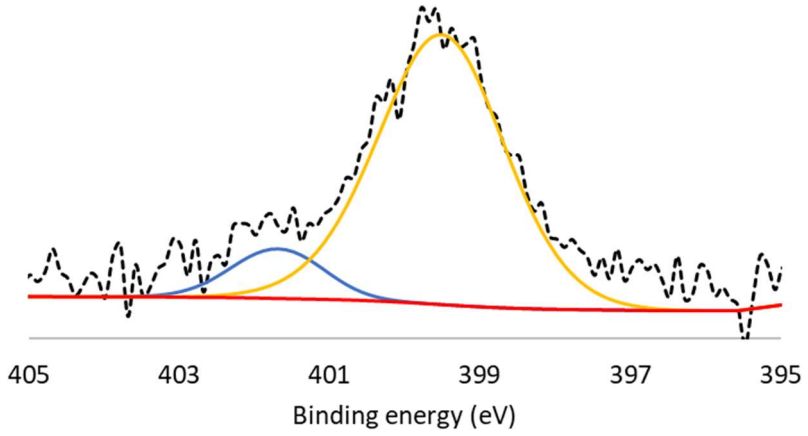

Figure 4.7 N1s XPS spectrum of wollastonite treated with DDA. The dashed lines represent the data and the solid lines represents the fit

a) Tannic acid (TA)

XPS was performed on mineral surfaces treated with 1.06 x 10^{-5} mol/L TA. Diopside XPS spectrum shows that the C1s peak of TA treated diopside is complex and cannot be simply fitted by C1s (284.79 cm^{-1}), C1s (285.8 cm^{-1}) and C1s (288.28 cm^{-1}) (*Figure 4.8*). There are additional peaks at C1s peaks at 286.86 cm^{-1} probably indicating the ester functional group and a peak at 289.28 cm^{-1} indicating a carboxylic acid functional group. These additional peaks might indicate the functional groups of TA. Ca2p doublet shifted to $Ca2p_{3/2}$(347.61 cm^{-1}) and $Ca2p_{1/2}$(351. 08 cm^{-1}) from $Ca2p_{3/2}$ (347.30 cm^{-1}) and $Ca2p_{1/2}$ (350.75 cm^{-1}), respectively after treatment with TA (*Figure 4.8*). Magnesium major peaks did not shift within analytical error (*Figure 4.8*).

The shift in Ca2p indicates that the chemical environment of calcium might have changed with addition of TA. The shift in Ca2p peak not only represents the adsorption of TA but also shows a chemical bond formed between the carboxylate or hydroxyl oxygen and calcium. The formation of a bond between calcium and oxygen will result in an increase in the binding energy of the core electrons which is what is observed in this case. The lack of shifts in magnesium photoelectrons might suggest that TA might have a higher affinity for Ca^{2+} compared to Mg^{2+}. A chemical shift in MgKLL auger peak was observed and this might indicate some adsorption of TA through

magnesium. Since, no shifts were observed on the photoelectrons, this might be an indication that the adsorption I s weak on magnesium compared to calcium.

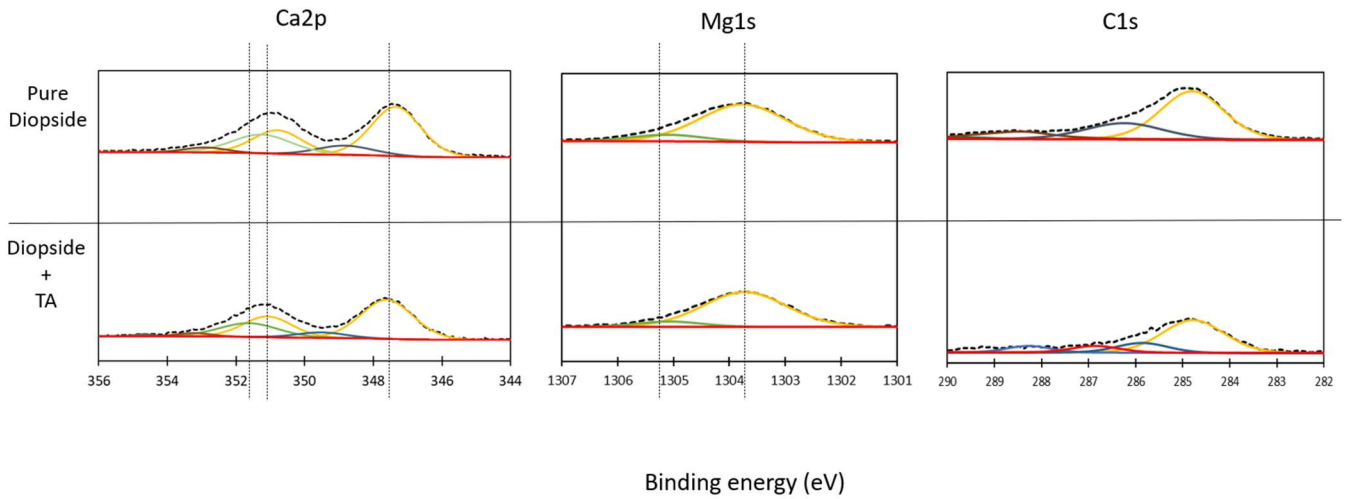

Figure 4.8. Diopside untreated (top) and treated (bottom) with Tannic acid at pH 8.5. The dashed lines represent the data and the solid lines represent the fit.

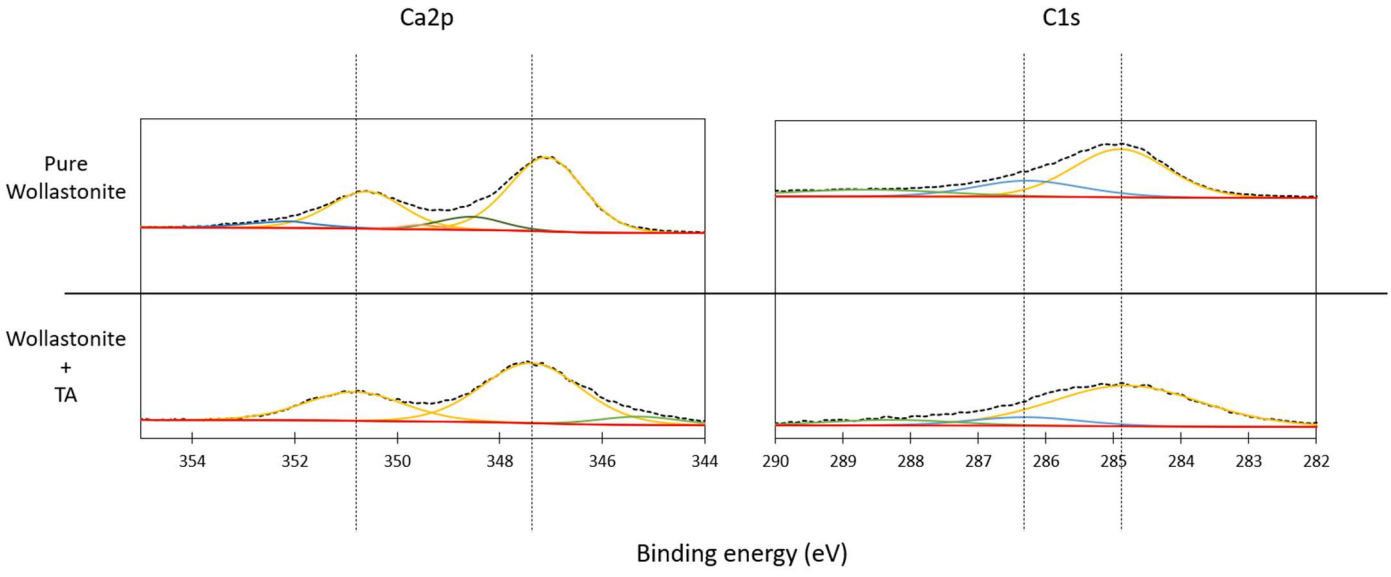

Figure 4.9. Wollastonite treated with tannic acid at pH 8.5. Dashed lines represent the data and the solid lines represent the fit

The XPS spectrum of wollastonite treated with TA showed no change in C1s. Calcium peaks shifted slightly from 347.18 cm^{-1} to 347.39 cm^{-1} for $Ca2p_{3/2}$ and 350.69 cm^{-1} to 350.84 cm^{-1} for $Ca2p_{1/2}$ (*Figure 4.9*). There is also an appearance of a new peak at a low binding energy (345.28 cm^{-1}). The slight shift on wollastonite's calcium species show that there might be a change in the chemical environment of calcium but not to the same extent as diopside. The XPS results support that TA has lower affinity for wollastonite compared to diopside.

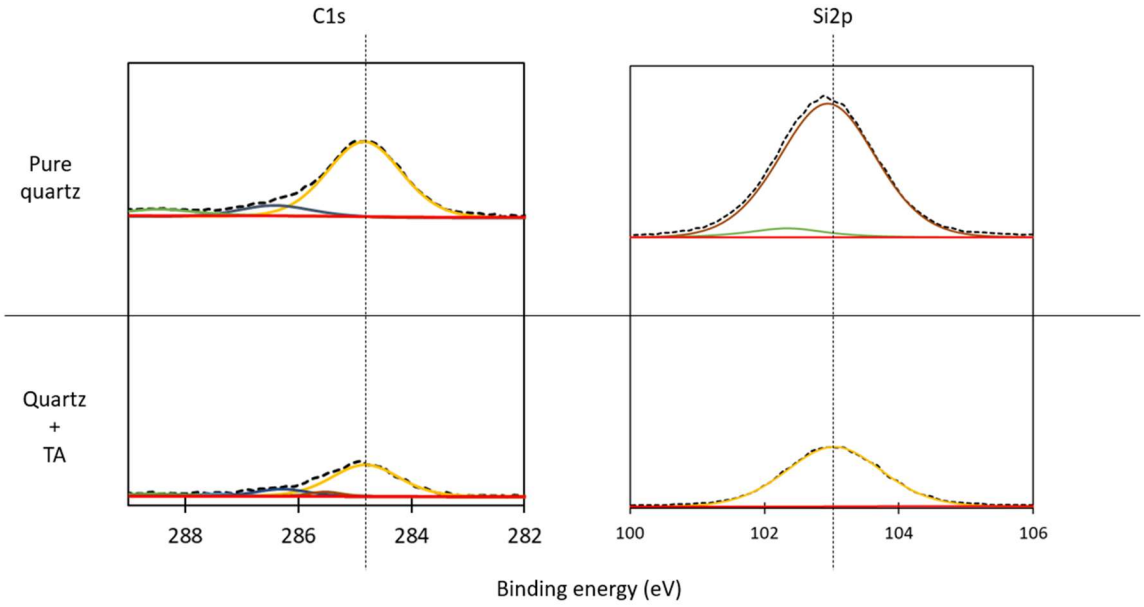

Figure 4.10 Quartz treated with tannic acid at pH 8.5. The dashed lines represent the data and the solid lines represent the fit

The XPS spectrum of quartz treated with TA did not show any change in the binding energies of C1s. The main Si2p peak shifted from 102.275 cm^{-1} to 103.03 cm^{-1} after treatment with TA (*Figure 4.10*). Tannic acid treated quartz XPS spectra shows a decrease in the broadness of both Si2p and C1s which probably indicates a change in experimental conditions. Tannic acid was proposed to bond through metal ions [55, 56]. Quartz contains no metal ions except for silicon which is a metalloid with a pure quartz silicon major peak being around 103.7 cm^{-1} [65]. The appearance of the major peak at slightly lower binding energy might suggest the presence of other metals on the mineral surface as impurities. The shift to binding energies closer to that of pure quartz after addition of TA might indicate the cleaning effect of TA, sequestering the metals in solution and

on the quartz surface which is a similar effect to EDTA in sulphide processing [66]. It must be noted that complexing agents can only sequester weakly attached metal hydroxide species [66]. It is doubtful that the weakly attached metal hydroxide species can cause a shift of ~0.75 eV which might imply that the shift in Si2p peak might be caused by other factors. If the shift is due to impurities, the impurities might also result in TA adsorption but the adsorption is probably minor and cannot be detected through XPS. The impurities, mainly iron (Fe) may have been introduced during the grinding stage [12].

Additionally, it must be noted that the significance of chemical shifts could be questionable and verifying adsorption and adsorption mechanisms using other methods is necessary. Conclusions on TA adsorption behaviour drawn from XPS data are well correlated with zeta potential measurements. Adsorption density studies in the following section will further investigate the adsorption mechanisms of TA.

4.1.2.3 Adsorption density measurements

Adsorption density measurements were only us ed to assess the adsorption behaviour of TA since the other reagents do not exhibit ultraviolet-visible absorption peaks.

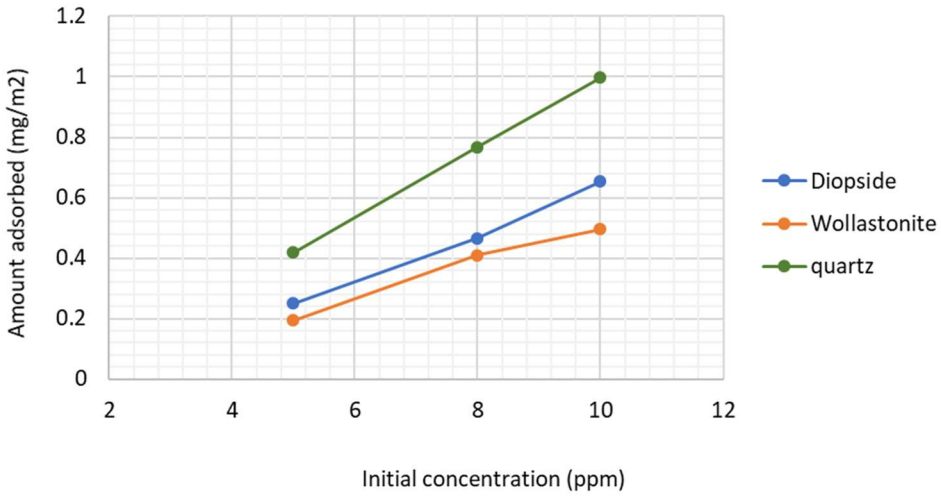

Figure 4.11 Adsorption density plots of quartz, wollastonite and diopside treated with TA at pH 8.5.

The adsorption behaviour of TA was investigated through analysing the supernatant concentration using ultraviolet-visible absorption spectroscopy (UV-vis spectroscopy) after conditioning the minerals with TA. The adsorption density was calculated as the mass of TA per square metre. The UV-vis spectrum of TA at pH 8.5 indicated that TA contains two absorption bands at 212 nm and 314 nm. The absorption band at 212 nm was chosen for adsorption density calculations.

Adsorption density measurements show that TA adsorbed onto all mineral surfaces and the amount adsorbed increases with an increase in the TA initial concentration. The adsorption density results also demonstrated that the amount of TA adsorbed on diopside is greater than the amount adsorbed on wollastonite at every TA concentration (*Figure 4.11*). The findings are consistent with zeta potential measurements and XPS which confirms preferential adsorption on diopside in comparison to wollastonite. The preferential adsorption seems to be more pronounced at 10 ppm.

Quartz appears to have the highest adsorption density compared to both diopside and wollastonite. This is unexpected and inconsistent with zeta potential measurements which indicated no major shift on quartz's surface charge with addition of TA. It would be expected that TA will not be able to adsorb to quartz since quartz contains no metal ions to bond with TA. The only explanation would be that TA is adsorbing through iron (Fe) acquired from the grinding stage since steel-based equipment was used to pulverise quartz.

4.1.2.4 Microflotation tests

The information from surface chemistry was used to define conditions suitable for microflotation tests.

a) Dodecylamine (DDA)

Quartz and wollastonite demonstrate high flotation recoveries from pH 5 to pH 9 for both 1.80 x 10^{-5} mol/L and 1.26 x 10^{-4} mol/L (Figure 4.2). Diopside demonstrates low flotation recoveries from pH 5 to pH 10 with 1.80 x10^{-5} mol/L DDA and the flotation recoveries improve at 1.26 x10^{-4} mol/L DDA (Figure 4.12). The recoveries generally drop at pH 10 due to the increase in molecular amine

species close to the amine pKaH [21, 26, 27] . Diopside flotation recovery is lower than that of quartz and wollastonite at all pH and DDA concentrations. These findings are consistent with both XPS and zeta potential measurements results which indicated lower affinity of DDA for the diopside surface. The overall DDA results of this study are consistent with the findings by Jizu et al. [55].

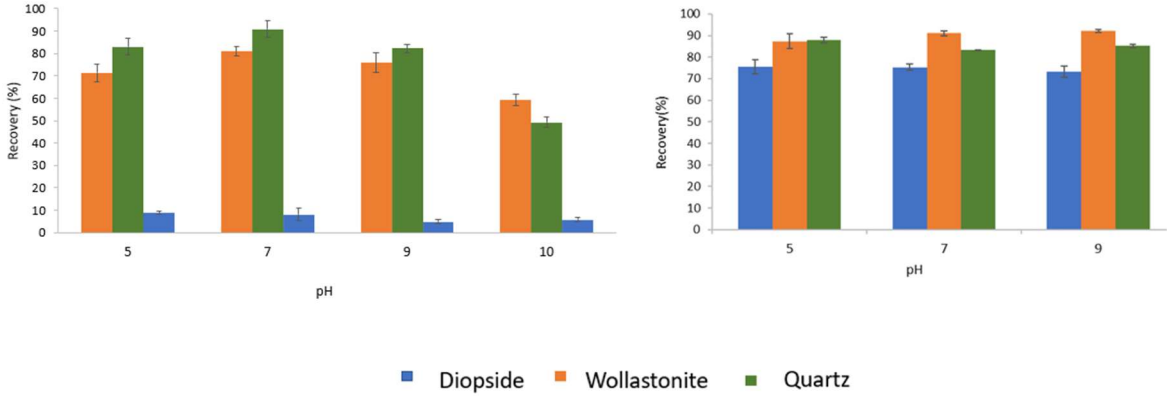

Figure 4.12. Quartz, diopside and wollastonite treated with DDA at $1.80x10^{-5}$ mol/L(left) and 1.26×10^{-4}mol/L(right). Error bars represent 95% confidence intervals

b) Sodium Oleate (NaOl)

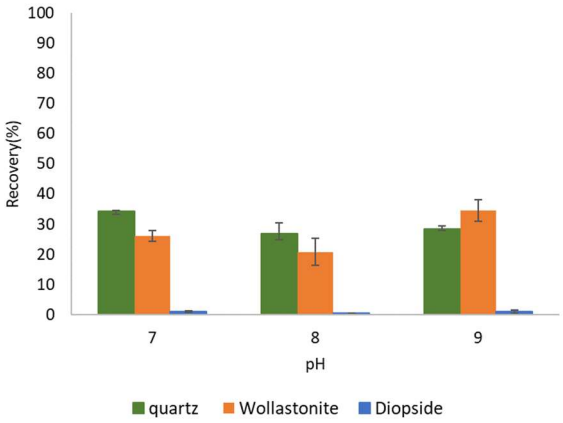

Figure 4.13. Microflotation results of quartz, wollastonite and diopside treated with sodium oleate

Microflotation results using sodium oleate at pH 7 to 9 with 5.47 x 10^{-5} mol/L NaOl yielded low recoveries for all the minerals and diopside had the lowest recoveries (*Figure 4.13*). These results show that NaOl is neither effective nor selective in floating quartz, wollastonite and diopside. The findings are consistent with zeta potential measurements as no major change was observed on the surface charge of all the minerals after addition of NaOl.

c) Tannic acid (TA)

Microflotation tests were conducted on quartz, diopside and wollastonite using tannic acid (TA) and DDA (*Figure 4.14*). The pH range 8.5 to 9 was chosen both empirically and based on literature. DDA concentration was chosen based on the concentration whereby all minerals are floatable.

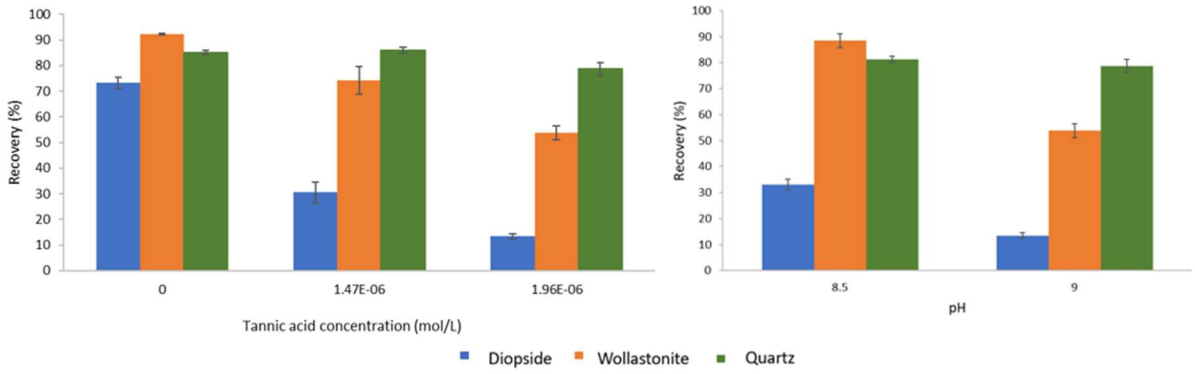

Figure 4.14. Microflotation tests on quartz, diopside and wollastonite with TA and 1.26 x 10^{-4}mol/L DDA at pH 9(left). Microflotation tests on quartz, diopside and wollastonite with 1.96 x 10^{-6} TA and 1.26 x 10^{-4}mol/L DDA (right). The error bars represent 95% confidence intervals.

The TA microflotation results show that diopside recovery decreases from 73% to 30%, wollastonite decreases from 92% to 74% and quartz recovery remains the same at pH 9 using 1.47 x 10^{-6} mol/L TA (*Figure 4.14*). Increasing the TA concentration to 1.96 x 10^{-6} mol/L results in a decrease in diopside recovery to 13% and wollastonite to 50%. TA depressant strength decreases on both wollastonite and diopside at pH 8.5 using 1.96 x 10^{-6} mol/L TA. The decrease in the depressant strength is pronounced on wollastonite than on diopside, increasing the difference in

recoveries from ~37% at pH 9 to ~55% at pH 8.5. Microflotation results demonstrated the possibility of increasing the selectivity between diopside and wollastonite at high DDA concentration. Furthermore, since quartz does not seem to be affected by TA, there might be a possibility of a selectivity between quartz and wollastonite with an increase in TA concentration. This was not investigated further due to sample availability.

The TA microflotation results are consistent with zeta potential measurements, adsorption density studies and XPS for diopside and wollastonite. Quartz exhibits some inconsistencies, specifically between microflotation tests and adsorption density studies. Adsorption density studies indicated that quartz has the highest TA adsorption density at every TA initial concentration. In contrast, microflotation tests demonstrated that, quartz recovery is not affected by the addition of TA. It was suggested that TA might be adsorbing through iron (Fe) acquired from the grinding stage since steel-based equipment was used to pulverise quartz. It would be expected that the Fe coating on quartz particles would also affect the microflotation results. This was not observed on microflotation results and the reasons for this are not clear, but it could be proposed that the effect is related to particle size. The particle size range used for microflotation tests is -106/+38 μm, whilst the particle size range used for the adsorption density study is -54/+38 μm. It might be possible that the finer particles have higher Fe content on the surface in comparison to the slightly coarser fraction. A similar effect was reported in sulphide flotation whereby inadvertent depression of galena and chalcopyrite was more pronounced for the fine particles in comparison to intermediate particles. This effect was attributed to greater oxidation of fine particles during the grinding stage and higher adsorption of Fe species on the mineral surfaces [67]. The quartz surface would not undergo oxidation, therefore the reasons for higher adsorption of Fe species onto finer quartz would have to be investigated further.

d) Sulphuric acid

Sulphuric acid was tested as a depressant to improve selectivity between quartz and wollastonite. Sulphuric acid was only investigated using microflotation tests due to the lack of selectivity in the results obtained and the difficulty in controlling dosage as sulphuric acid is a pH modifier and not a conventional depressant.

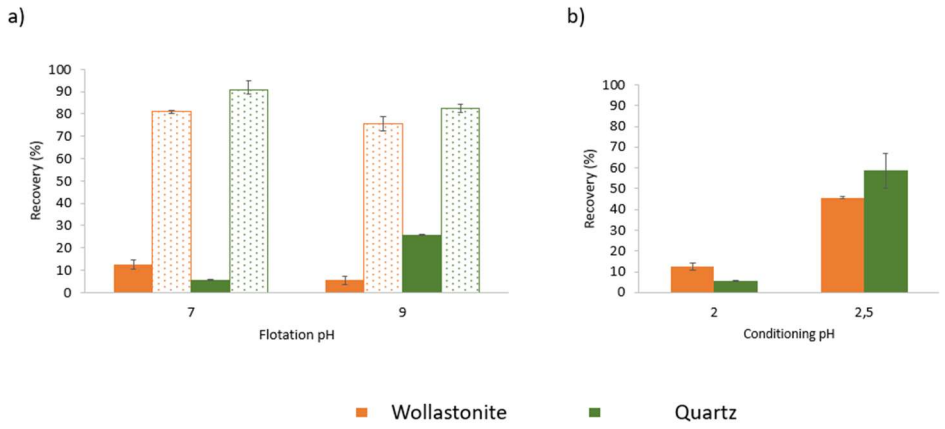

Figure 4.15 Sulphuric acid microflotation results. Solid filled bars represent samples treated with sulphuric acid whilst dot-filled bars represent samples treated with DDA only. a) DDA/sulphuric acid mixture of 1.8 x 10^{-5}mol/L DDA/2.55x10^{-4} mol/L sulphuric acid at conditioning pH of 2 (right). b) DDA/sulphuric acid mixture of 1.8 x 10^{-5}mol/L DDA/2.55x10^{-4} mol/L at flotation pH of 7

Sulphuric acid decreased the flotation recoveries for both quartz and wollastonite to less than 15% for the flotation pH of 7 and conditioning pH of 2 (*Figure 4.15* a). At pH 9, wollastonite recovery remained low whilst quartz slightly increased to 25.83 ± 4.74 % (*Figure 4.15* a). Increasing the conditioning pH led to an increase in recoveries of both quartz and wollastonite to above 40% (*Figure 4.15* b). In summary, sulphuric acid was an effective depressant but it is not selective. It was also observed that sulphuric acid is only effective if the conditioning pH is low.

4.1.2.5 Speciation

a) Sodium Oleate (NaOl)

Speciation diagrams for sodium oleate, Ca^{2+} and Mg^{2+} were modelled using the data from Shibata & Fuerstenau [68] and Chen & Tao [69]. The models were used to further explain flotation behavior and adsorption behaviour of NaOl treated wollastonite and diopside.

$$COOH_{(l)} \leftrightarrow COOH_{(aq)} \qquad S = 2.51\,x10^{-8} \qquad (4.1)$$

$$COOH \leftrightarrow COO^- + H^+ \qquad K_a = 10^{-4.95} \tag{4.2}$$

$$2COO^- \leftrightarrow COO_2^{2-} \qquad K_D = 10^4 \tag{4.3}$$

$$COOH_{(aq)} + COO^- \leftrightarrow (RCOO)_2H^- \qquad K_{AD} = 10^{4.95} \tag{4.4}$$

$$Ca^{2+} + OH^- \leftrightarrow CaOH^+ \qquad K_1 = 10^{1.3} \tag{4.5}$$

$$CaOH^+ + OH^- \leftrightarrow CaOH \qquad K_2 = 10^{-1.3} \tag{4.6}$$

$$Mg^{2+} + OH^- \leftrightarrow MgOH^+ \qquad K_1 = 10^{2.57} \tag{4.7}$$

$$MgOH^+ + OH^- \leftrightarrow MgOH \qquad K_2 = 10^{5.81} \tag{4.8}$$

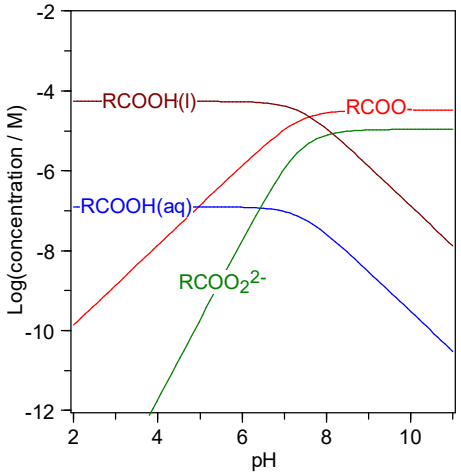

Figure 4.16. NaOl speciation diagram [68].

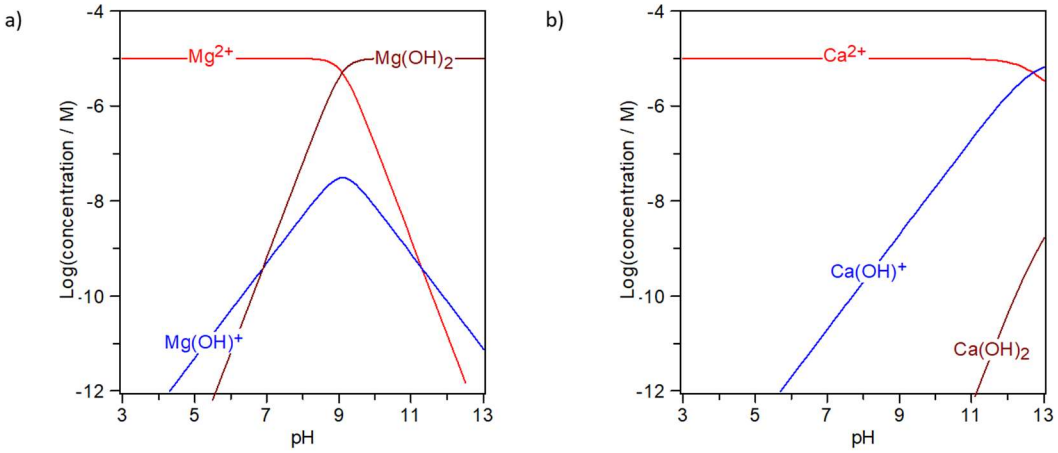

Figure 4.17 Calcium and Magnesium speciation in an aqueous solution of 1 x 10^{-5} M for each species

NaOl pKa is at pH 4.95 which implies that the concentration of deprotonated species increases above this pH (*Figure 4.16*). The deprotonated species are responsible for forming bonds with the cations which implies that chemical adsorption should be favourable above the pKa. Kumar et al. [24] reported NaOl to preferably form bonds with metal hydroxide species. The Mg and Ca speciation diagrams demonstrate an increase in metal hydroxide species in solution above pH 4.2 and 5.7, respectively (Figure 4.17). A similar speciation would be expected on the mineral surfaces which is probably the reason behind the increase of a negative charge with increasing pH. Speciation suggests that the pH range chosen for microflotation is the most favourable pH range for floatability of wollastonite and diopside with NaOl but neither of the minerals were floatable. In the case of wollastonite, the behaviour can be explained by high dissolution rate and preferential loss of calcium ions into solution reported by Prabhakar et al. [49] which leaves the surface of wollastonite devoid of metal species, therefore hindering sodium oleate adsorption. The reason behind the lack of NaOl adsorption on diopside is not clear. It could be suggested that increasing the dosage might eventually float diopside.

b) Tannic acid (TA)

Tannic acid, Ca^{2+} and Mg^{2+} speciation were modelled using the data from Chen & Tao [69] and Ghigo et al. [59]. The TA speciation diagram shows that neutral TA dominates at low pH until the pH of ~7.8 where the charged species begin to dominate (*Figure 4.18*). Neutral TA decreases as the pH increases. The dominance of charged TA at higher pH is well correlated with higher depressant strength demonstrated by microflotation tests at high pH as there would be more charged species available for complexing metal ions.

$$TA \leftrightarrow TA^{-} + H^{+} \qquad pK_{a1} = 6.34 \pm 0.01 \tag{4.9}$$

$$TA^{-} \leftrightarrow TA^{2-} + H^{+} \qquad pK_{a2} = 7.39 \pm 0.01 \tag{4.10}$$

$$TA^{2-} \leftrightarrow TA^{3-} + H^{+} \qquad pK_{a3} = 8.59 \pm 0.01 \tag{4.11}$$

$$TA \leftrightarrow TA^{3-} + 3H^{+} \qquad -log\beta = 22.32 \pm 0.01 \tag{4.12}$$

Zeta potential measurements indicated a more pronounced shift at pH 6 to pH 8 which is probably related to the pKas. The first pKa of TA is at pH 6.3 (equation 4.9), which means that TA starts

having a higher proportion of negatively charged species available for chemical adsorption after pH 6.3. The increase in the shift from pH 6 is well correlated with the availability of charged TA species resulting in an increase in TA adsorption. A less pronounced shift at pH 9 could potentially be explained by a higher negative charge on the diopside surface at high pH. This high negative charge could possibly hinder adsorption of an anionic surfactant through an electrostatic repulsion. These findings are inconsistent with microflotation since the depressant strength is high at pH 9. The reason for a less pronounced shift at pH 9 is unclear.

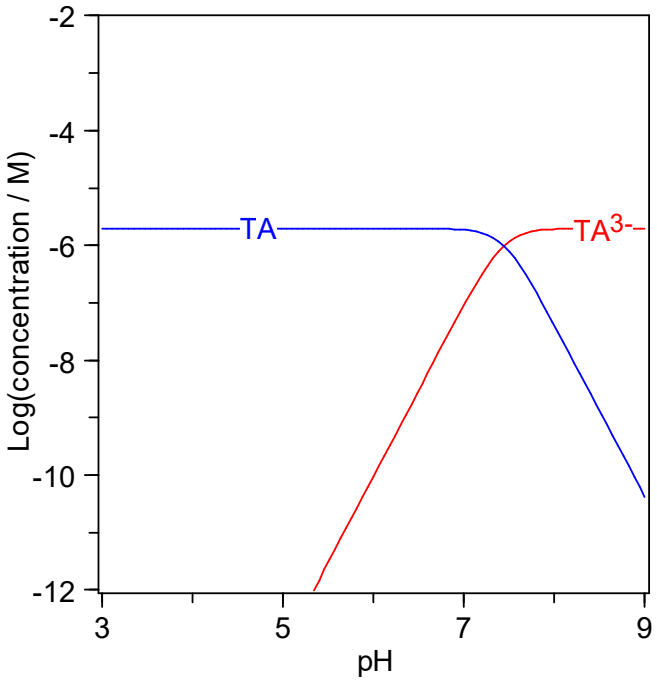

Figure 4.18 Tannic acid speciation at 1.96 x 10^{-6} M TA in an aqueous solution.

TA is proposed to form chemical bonds predominantly with metal hydroxide species [56]. Calcium and magnesium speciation diagrams show an increase in the metal hydroxide species with pH (*Figure 4.17*). The high availability of metal hydroxide species at pH 8.5 to 9 suggests that TA is probably bonding through these species both in solution and on mineral surfaces (*Figure 4.17*). TA can either form one bond with the metal or probably chelate like other multidentate ligands such as EDTA (*Figure 4.19*). Chemical adsorption through metal hydroxide species has also been proposed for adsorption of sodium oleate onto aluminosilicates [24]. The species diagrams do not

really explain higher affinity of TA to calcium compared to magnesium (as indicated by XPS) since magnesium has a higher content of metal hydroxide species at pH 8.5-9.

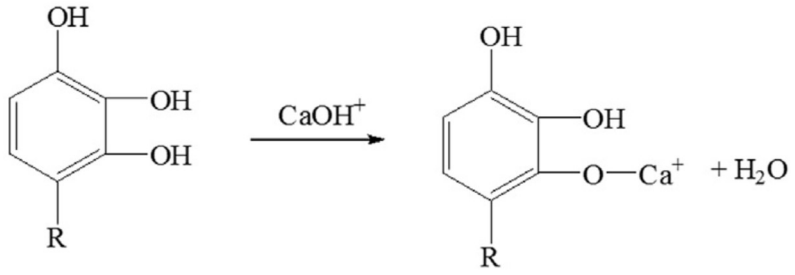

Figure 4.19. Proposed model for tannic acid adsorption [56]

4.1.2.6 Particle-bubble attachment studies

DDA treated particles were used to assess the effect of particle shape. DDA was chosen due to that it was the most effective collector. It was stated in the introduction that poor wollastonite floatability is due its particle shape which is elongated. Microflotation recoveries showed that wollastonite can have recoveries > 80%. Assessment of aspect ratios of the samples used for microflotation tests demonstrated that most of the particles have high aspect ratios (>8) (Figure 4.2). In literature, it was reported that wollastonite particles with aspect ratios (>8) have a difficulty in attaching to bubbles and therefore hindering flotation. This particle shape effect was not observed on the microflotation tests perfomed in this study.

Bubble-particle attachment studies were performed on amine treated quartz and wollastonite. Quartz particles typically have low aspect ratios whereas wollastonite particles have high aspect ratios (fibres) therefore, quartz serves as a good comparison to assess the effect of particle shape. The experiments demonstrated equivalent attachment of quartz and wollastonite particles onto the bubbles (*Figure 4.20*). Wollastonite particles adsorb parallel to the surface which either indicates the preferred mode of attachment or the most stable mode of attachment of wollastonite particles. No studies in mineral processing have evaluated the effect of particle aspect ratio in flotation.

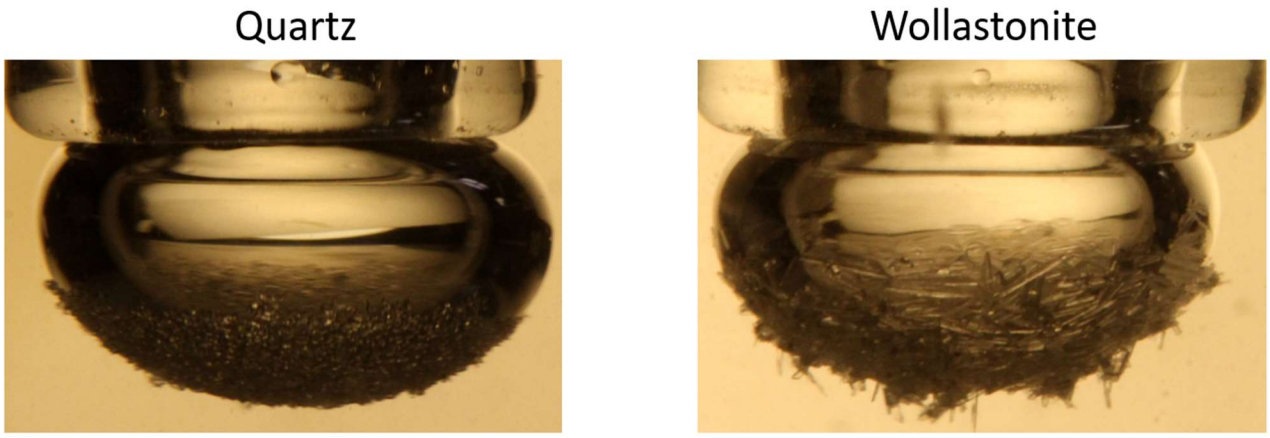

Figure 4.20. Bubble-particle interaction of quartz(left) and wollastonite (right) treated with 1.80 x 10^{-5} mol/L

To address the issue of particle shape, a study by Lecrivain et al. [57] which looks at particle-bubble interaction for glass fibres will be used to discuss the observations of wollastonite attachment to bubbles. Lecrivain et al. [57] concluded that the fibres have two modes of attachment. A weak fibre attachment occurs when a particle reorientates to a radial alignment to the air/water interface as it slides along the bubble (*Figure 4.21*) [57]. A strong attachment occurs when the particle attaches to the bubble with its major axis parallel to the water/air interface, the contact area is bigger and therefore, the attachment is stronger [57].

From the attachment mechanism stated above, it could be concluded that the wollastonite particles (*Figure 4.21*) were observed predominantly in an orientation parallel to bubbles due to this being the most stable configuration. This implies that for successful wollastonite flotation, the probability of a collision between wollastonite particles and the bubbles must be increased to allow particles to attach to the bubbles in a stable manner. The probability of particle-bubble collisions can be increased by increasing the bubble surface area, through frother control or increasing the impeller speed, keeping it at optimum speed to avoid destabilising the system. This would have to be balanced with ensuring that the shearing in the cell does not remove the weakly attached particles. Another approach could be using a reactor/separator flotation cell or a hydrofloat where bubbles could rise to the froth zone in a quiescent zone that minimizes detachment of the particles.

A reactor/separator could ensure that even the weak fibre attachments are not destabilized. Designing an experiment that assesses particle detachment might shed light towards understanding the stability of the bubble-particle aggregates.

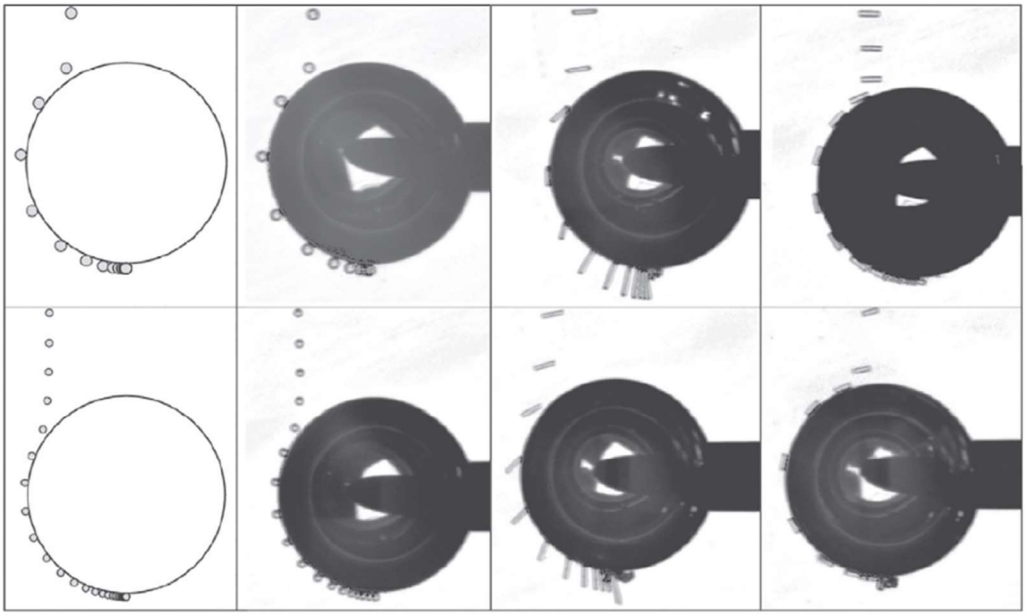

Figure 4.21 Attachment of fibre particles onto stationary bubble compared with the attachment of spherical particles [57]

4.2 Wollastonite ore flotation

4.2.1 Ore characterisation

The feed was characterised using QEMSCAN and X-ray Fluorescence (XRF) techniques. The following section will discuss the QEMSCAN results, specifically size by size mineralogy and liberation of wollastonite.

4.2.1.1 Quantitative Evaluation of Minerals by Scanning Electron Microscopy (QEMSCAN)

.

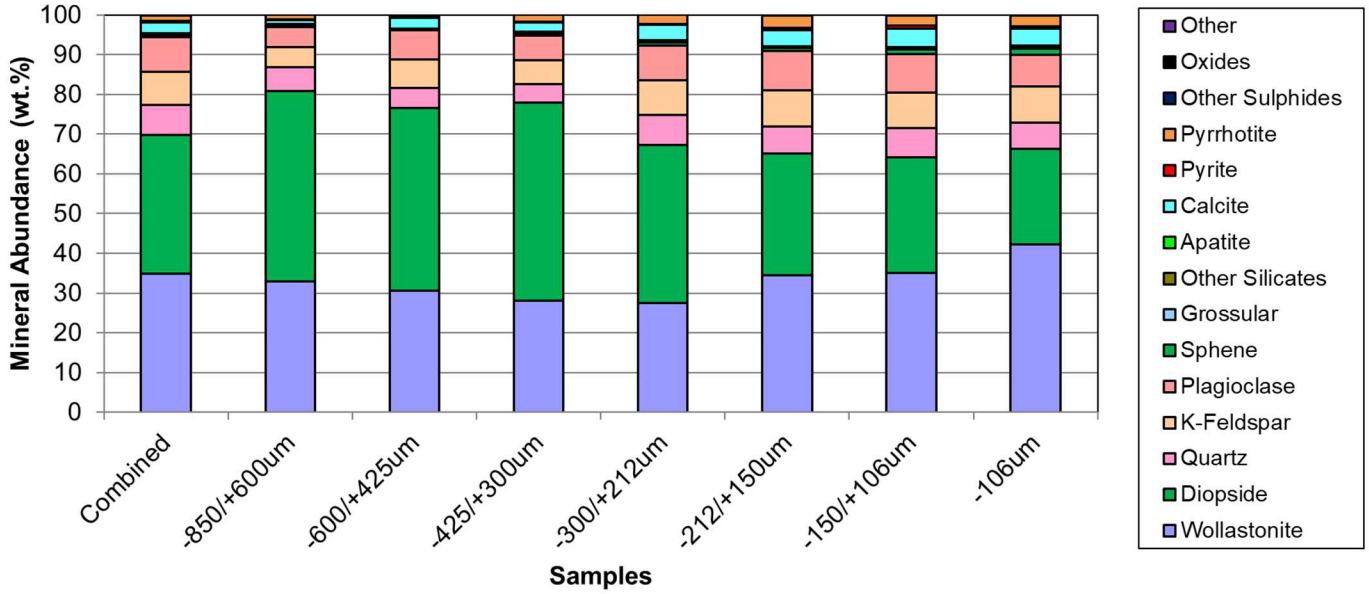

Figure 4.22 Size by size mineralogy

The QEMSCAN results show that the main gangue mineral present within the wollastonite ore is diopside followed by K-feldspar, quartz, plagioclase and some calcite (*Figure 4.22*). All the other gangue minerals such as sulphides form a minor component of the ore. Wollastonite and diopside (major gangue mineral) are almost the same proportion for the combined size fractions, 34.9 % and 34.8 %, respectively (Figure 4.22). For the size fraction -106 µm, wollastonite is enriched in comparison to diopside, with respective modal percentages of 42.2% and 24.1%. The enrichment of wollastonite in the lower size fractions might be related to that wollastonite is softer in comparison to diopside and most of the other major gangue minerals including quartz and

feldspars. This implies that, wollastonite ores could potentially be preconcentrated using controlled grinding and particle size classification and perhaps the fine and coarse size fractions could be further processed separately.

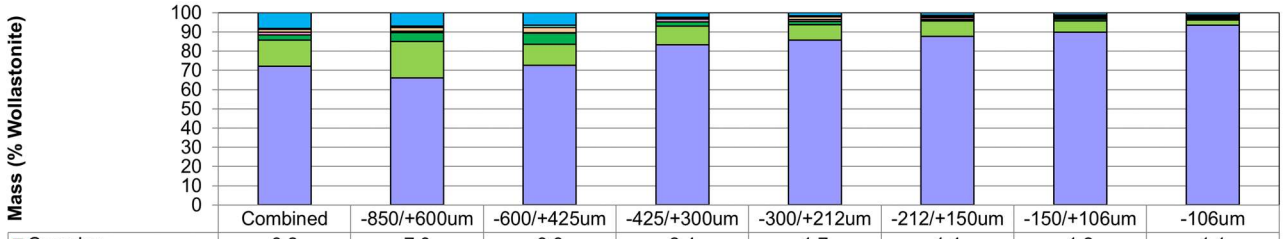

	Combined	-850/+600um	-600/+425um	-425/+300um	-300/+212um	-212/+150um	-150/+106um	-106um
Complex	8.2	7.0	6.6	2.4	1.7	1.4	1.2	1.1
Wo:Other	0.0	0.0	0.0	0.0	0.0	0.0	0.0	0.0
Wo:Oxides	0.0	0.0	0.0	0.0	0.0	0.0	0.0	0.0
Wo:Fe Sulphides	0.0	0.0	0.0	0.0	0.0	0.1	0.1	0.0
Wo:Calcite	0.4	0.0	1.0	0.1	0.4	0.2	0.7	0.8
Wo:Other Silicates	0.1	0.6	0.0	0.1	0.0	0.0	0.1	0.1
Wo:Feldspars	1.5	1.9	2.9	0.8	1.5	0.9	0.7	0.5
Wo:Quartz	1.4	0.7	0.2	1.4	0.9	0.9	0.8	0.6
Wo:Diopside	2.7	4.8	5.7	2.2	1.7	0.7	0.8	0.6
Liberated Wollastonite	13.5	18.8	11.0	9.7	8.1	8.0	5.9	2.7
Free Wollastonite	72.2	66.1	72.7	83.4	85.6	87.6	89.9	93.5

Figure 4.23 Wollastonite mineral associations

Another important piece of information obtained from QEMSCAN data is liberation. The QEMSCAN data shows that wollastonite is well liberated below 600 µm and the liberation increases with the decreasing particle size (Figure 4.23). Good liberation of wollastonite at coarse size fractions implies that, wollastonite can be floated coarse. Any challenges in flotation of coarse wollastonite will likely be related to flotation physics such as particle weight and its effect on bubble-particle stability rather than liberation.

4.2.1.2 X-ray fluorescence (XRF) analyses

XRF was used to characterise the flotation feed with the K80 of 188 µm. The results indicated that the feed consists of 41.8 % wollastonite and 27.9 % diopside. The discrepancy between XRF and QEMSCAN might be explained by that, the pulverised ore that was sent to McGill university might have been from a different zone from the ore analysed using QEMSCAN. The discrepancy might also arise from the accuracy of each analysis technique and sample preparation methods. Most XRF equipment have limitations with detecting elements with low atomic numbers (Z<11), it then

follows that the accuracy will increase with the atomic number. Sodium was not detected for the wollastonite ore although the ore contained plagioclase which contains sodium.

4.2.2 Batch flotation tests

Wollastonite, diopside, quartz, plagioclase and K-feldspar recoveries were calculated from the assays. The other minerals were not assessed due to that they form a minor component of the ore. The batch flotation tests evaluated 5 conditions which are given in *Table 4.1*.

Test 1 (35g/t DDA and no TA) yielded 64.8 % diopside recovery, 74.7 % wollastonite recovery, 100 % quartz recovery, 90.1 % K-feldspar recovery and 86.2 % plagioclase recovery (*Figure 4.24*). Diopside recovery was lower than that of other minerals which is consistent with microflotation tests. The recovery of feldspars with DDA was high which is consistent with the previous studies [19, 21, 26, 36].

Table 4.1 Batch flotation tests conditions

Test	DDA dosage (g/t)	TA dosage (g/t)	MIBC dosage (ppm)	pH
1	35	0	18	8.5
2	35	75	18	8.5
3	35	100	18	8.5
4	35	150	18	8.5
5	45	100	18	8.5

Wollastonite recovery was relatively low compared to that of quartz, whereas microflotation tests indicated that the two were very close to one another. The low recovery of wollastonite resulted in poor separation efficiency (SE= $R_{Wollastonite}$- $R_{Diopside}$) between diopside and wollastonite. Poor separation efficiency is also reflected by the lack of improvement of the grade of wollastonite in the concentrate (40.8 % wollastonite) which is close to the feed grade (Figure 4.25). Ideally, the

recovery of wollastonite should be close to that of quartz (as demonstrated by microflotation tests) which would have resulted in a slightly higher separation efficiency. The discrepancy between the expected wollastonite flotation behaviour and the observed flotation behaviour might be attributed to: a) Solution chemistry in batch flotation tests is hindering collector adsorption onto wollastonite and b) the particle shape of wollastonite is hindering the floatability of wollastonite.

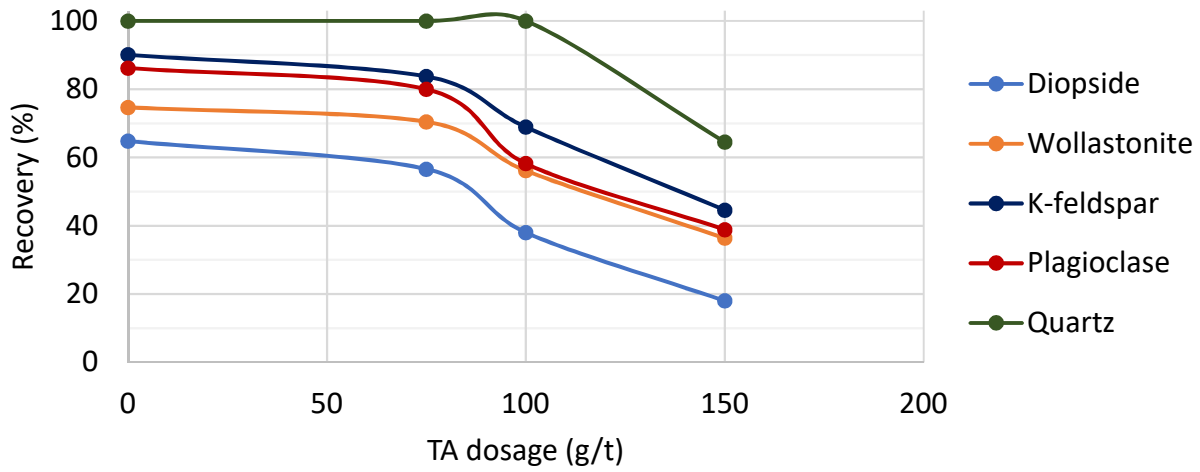

Figure 4.24 Recovery vs TA dosage for wollastonite, diopside, quartz, plagioclase and K-feldspar with 35 g/t DDA as a collector.

Assessing whether the observed wollastonite flotation behaviour is due to collector adsorption can be achieved by analysing the surface chemistry of wollastonite in the tailings. If the collector adsorption is not the issue, then the problem might be related to the particle shape such that changing cell parameters such as the impeller speed or using a reactor separator cell might be necessary to achieve a direct flotation of wollastonite. In section 4.1.2.6, it was shown that wollastonite particles with high aspect ratios can attach to bubbles. Literature reported poor flotation recoveries for high aspect ratio wollastonite particles. As a result, it was suggested that in a highly turbulent flotation machine, the stability of the particle-bubble aggregates might be lowered resulting in poor flotation recoveries. A mechanical cell was used for the batch flotation tests. Mechanical cells predominantly have a highly turbulent, mixing zone and a small quiescent zone which might be responsible for destabilizing the wollastonite particle-bubble aggregates leading to relatively lower flotation recoveries.

Tannic acid was added to lower the recovery of diopside without affecting the recovery of wollastonite and quartz and thereby improving selectivity at 35 g/t DDA. The results indicated that adding 75 g/t TA decreased the recovery of diopside to 56.6 % whilst the recovery of wollastonite decreased slightly to 70.5 % (*Figure 4.24*). K-feldspar and plagioclase recoveries also decreased to 83.7 % and 79.6 %, respectively. Quartz recovery remained constant at 100 %. Increasing the TA dosage to 100 g/t led to a further decrease in diopside recovery to 38 % whilst the recovery of wollastonite decreased to 56.1 %. K-feldspar and plagioclase recoveries decreased to 68.9 % and 58.2 %, respectively with 100 g/t TA. Quartz recovery remained constant with 100 g/t TA. A further increase in the TA dosage resulted in a decrease in recoveries for all the minerals analysed. Wollastonite recovery decreased to 36.35 %, diopside decreased to 17.8 %, quartz decreased to 64.5 %, K-feldspar decreased to 44.6 % and plagioclase decreased to 38.9 %.

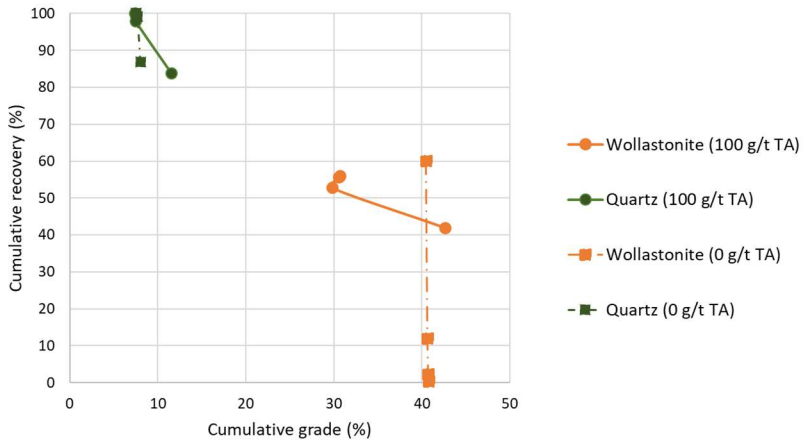

Figure 4.25 Cumulative recovery against cumulative grade for wollastonite and quartz at 35 g/t DDA with 0 g/t TA (squares) and 100 g/t TA (circles).

TA demonstrates some selectivity between diopside and wollastonite since the separation efficiency (SE= $R_{Wollastonite}$- $R_{Diopside}$) increases from ~ 10 % to ~18 % with addition of TA. It must be noted that, the selectivity between wollastonite and diopside remains low in the presence of TA. The grade-recovery curve shows that wollastonite is also depressed in the presence of TA as the concentrate grade decreases below that of the feed with an increase in flotation time to 7 minutes (Figure 4.25). Quartz recovery appears to be unaffected by the addition of TA especially at low TA concentration which resulted in the separation efficiency exceeding 60% between quartz and diopside and 40% between quartz and wollastonite (*Figure 4.24*). Quartz grade improved in the

presence of 100 g/t TA which supports that the separation efficiency increases as diopside and wollastonite are selectively depressed by TA (Figure 4.25). These results imply that TA can be used to selectively float quartz, but it is not a selective depressant for a direct flotation of wollastonite.

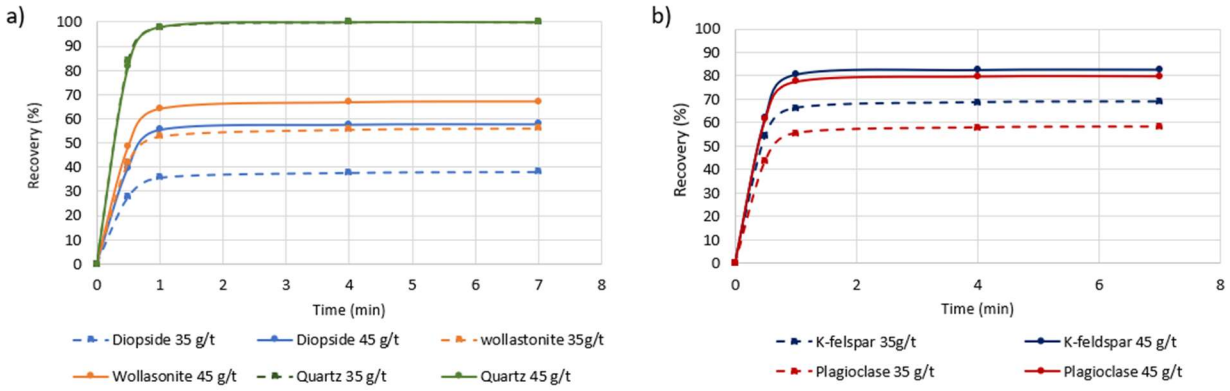

Figure 4.26 a) Recovery vs flotation time for diopside, quartz and wollastonite with 35 g/t DDA(dashed lines) and 45 g/t DDA (solid lines)as collector and 100 g/t TA as a depressant. b) Recovery vs flotation time for plagioclase and K-feldspar with 35 g/t DDA (dashed lines) and 45 g/t DDA (solid lines) as collector and 100 g/t TA as a depressant

Since the separation efficiency between diopside and wollastonite remained low in the presence of TA, the dosage of DDA was increased to 45 g/t in attempt to improve the wollastonite recovery at a 100 g/t TA (*Figure 4.26*). The recovery of all the minerals analysed increased with an increase in the DDA concentration except quartz which reached its maximum recovery at 35 g/t DDA (Figure 4.26 a & Figure 4.26 b). This resulted in a reduction in separation efficiency with an increase in DDA concentration.

Microflotation tests and surface chemistry studies indicated that TA has a higher affinity for diopside than wollastonite, this was not observed in batch flotation tests (*Figure 4.24*). Poor adsorption of TA onto wollastonite was proposed to be a result of dissolution of wollastonite which leaves its surface devoid of calcium ions which are responsible for TA adsorption. The solution chemistry in batch flotation tests is complex compared to the solution chemistry in microflotation tests. Wollastonite might have been accidentally activated for adsorption of TA by solution ions generated from the flotation cell (steel-based equipment), tap water and/or metal ions leached from

other minerals. Adsorption of metal ions onto wollastonite which in turn would result in adsorption of TA might be the reason for lower selectivity of TA in batch flotation tests.

The mechanisms for TA adsorption onto diopside and quartz were suggested in section 4.1.2. Although the surface chemistry of feldspars was not evaluated, since the flotation response of feldspars was affected by TA, it could be suggested that TA is adsorbed onto the K-feldspar and plagioclase surfaces. Plagioclase and K-feldspar share a common metal, aluminium and since TA is proposed to adsorb through a chemisorption with metal ions, aluminium might be responsible for the adsorption of TA. Chemisorption of surfactants through aluminium has been reported for NaOl adsorption onto aluminosilicates [24]. It would be beneficial to conduct some surface chemistry studies on feldspars to gain some insight on TA adsorption mechanisms.

Various challenges would have to be addressed if the batch results presented in this chapter were to be conveyed to the industrial level. A scale up of a laboratory test is often difficult and not yet fully understood [70, 71]. A batch flotation process will differ from a continuous industrial process in terms of that, a batch process will not reach a steady state [71]. In a batch process, water is added throughout the process to maintain a constant water level which changes the solid percentage and dilutes the reagents [71]. In addition, particle size distribution, mineralogy, gas dispersion and more; will not be the same at an industrial scale as in batch flotation tests [70]. For these reasons, researchers have devised various models to scale up both the kinetics and the flotation machine [70, 71]. A use of appropriate scale up factors is necessary to predict both recovery and grade at an industrial level from batch flotation tests [70, 71]. In this study, flotation kinetics were not evaluated and therefore, it will be beneficial to evaluate the flotation kinetics to successfully scale up the process.

Chapter 5. Conclusions

- Microflotation tests demonstrated that wollastonite, quartz and diopside are all floatable using DDA as a collector. Selectivity could be achieved if the DDA concentration is kept low which was supported by both XPS and zeta potential measurements.
- Sodium oleate was not effective in floating all the minerals investigated in this study. Zeta potential measurements indicated that poor floatability of the minerals can be related to the lack of adsorption of NaOl.
- Tannic acid can be used to improve the selectivity between wollastonite and its silicate gangue minerals at a high DDA concentration. Tannic acid was observed to have higher affinity for diopside than wollastonite which was attributed to the high dissolution rates of wollastonite compared to other silicates minerals. The selectivity between wollastonite and diopside was supported by XPS, zeta potential measurements and adsorption density studies. Furthermore, quartz did not appear to be affected by the addition of tannic acid which suggests a possibility for selectivity between quartz and wollastonite. These findings were consistent with zeta potential measurements but not with adsorption density studies.
- For the first time this study briefly investigated the effect of particle shape of wollastonite on floatability. The study demonstrated that the bubble-particle attachment of wollastonite is comparable to that of quartz, and this might support looking into beneficiating wollastonite using a direct flotation.
- Batch flotation tests in the presence of DDA alone were in good agreement with microflotation tests although the recoveries of wollastonite were slightly poor than expected. The recovery of wollastonite is closer to that of diopside than that of quartz. It was concluded that wollastonite is less floatable with DDA in batch flotation tests than it was in microflotation tests which is probably related to the solution chemistry and/or the effect of particle shape in a highly turbulent flotation machine. It was proposed that it will be necessary to either change the flotation cell to a reactor/separator cell or change the cell parameters such as the impeller speed to achieve a direct flotation. If not, a reverse flotation might be a preferable option.

- Batch flotation tests in the presence of TA demonstrated that the selectivity of TA between diopside and wollastonite is low, thus resulting in only a slight increase in separation efficiency. Quartz appears to be unaffected by the addition of TA especially at low TA concentration which implies that quartz can be selectively floated from all the other minerals in the presence of TA and DDA. The batch flotation tests indicated that, selectivity of TA can only be achieved at low concentrations. An increase in the concentration of TA resulted in depression of all the minerals analysed including quartz.

Chapter 6. Future work

- Investigation of mixed collectors to achieve selectivity
- Investigation of other depressants such as carboxymethylcellullose (CMC) and sodium hexametaphosphate (SHMP) and compare their behavior to TA.
- Optimize the batch flotation tests variables (such as reagent concentration, flotation time and impeller speed) using design of experiments (DOE).
- Evaluate the batch flotation tests reagent scheme using a reactor/separator, hydrofloat or a column flotation machine to increase the recovery of wollastonite through increasing the quiescent zone in the flotation machine.

References

[1] P. Ciullo, Industrial Minerals and Their Uses. A handbook and formulary, Westwood, New Jersey, USA: Noyes publications, 1996.

[2] R. Cox, Engineered tribological composites: the art of friction material development, 2011.

[3] S. Bulatovic, Handbook of flotation reagents: chemistry, theory and practice: Flotation of Industrial Minerals. Volume 3, Peterborough: Elsevier, 2015.

[4] T. Grammatikopoulos, A. Clark and B. Vasily, "The St. Lawrence deposit, Seeley's Bay, SE Ontario: A," *CIM bulletin,* vol. 96, no. 1070, pp. 47-54, 2003.

[5] W. Ortega-Lara, D. Cortés-Hernández, S. Best, R. Brooks and A. Hernandez-Ramirez, "Antibacterial properties, in vitro bioactivity and cell proliferation of titania–wollastonite composites," *Ceramics International,* vol. 36, no. 2, pp. 513-519, 2010.

[6] W. Petruk, Applied mineralogy in the mining industry, Ottawa: Elsevier, 2000.

[7] F. Di Lorenzo, C. Ruiz-Agudo, A. Ibañez-Velasco, R. Gil-San Millán, J. Navarro and E. Ruiz-Agudo, "The Carbonation of Wollastonite: A Model Reaction to Test Natural and Biomimetic Catalysts for Enhacenced CO2 Sequestration," *Minerals,* vol. 8, no. 5, p. 209, 2018.

[8] J. Ober, Mineral commodity summaries 2018, US Geological Survey, 2018.

[9] "Canadian Wollastonite," Canadian Wollastonite, 13 February 2015. [Online]. Available: http://www.canadianwollastonite.com/about/history/. [Accessed 01 August 2018].

[10] G. Christidis, Advances in the Characterization of Industrial Minerals. Volume 9, London: European Mineralogical Union and the Mineralogical Society of Great Britain and Ireland, 2011.

[11] M. Ahmed, G. Ibrahim and M. Hassan, "Improvement of Egyptian talc quality for industrial uses by flotation process and leaching," *International Journal of Mineral Processing,* vol. 83, no. 3-4, pp. 132-145, 2007.

[12] G. Bulut and C. Yurtsever, "Flotation behaviour of Bitlis kyanite ore," *International Journal of Mineral Processing,* vol. 73, no. 1, pp. 29-36, 2004.

[13] J. Jin, H. Gao, G. Liu and C. Zhao, "Flotation Separation of Nanyang Kyanite ore," *Applied Mechanics and Materials,* vol. 608, pp. 794-797, 2014.

[14] H. Zhu, H. Deng and C. Chen, "Flotation separation of andalusite from quartz using sodium petroleum sulfonate as collector.," *Transactions of Nonferrous Metals Society of China,* vol. 25, no. 4, pp. 1279-1285., 2015.

[15] B. Wills and J. Finch, Wills' mineral processing technology: an introduction to the practical aspects of ore treatment and mineral recovery, Oxford, UK: Butterworth-Heinemann, 2016.

[16] P. Andrews, "The beneficiation of Canadian garnet ores at CANMET," *CIM bulletin,* vol. 88, no. 995, pp. 55-59, 1995.

[17] L. Zhou and Y. Zhang, "Flotation separation of Xixia andalusite ore," *Transactions of Nonferrous Metals Society of China,* vol. 21, no. 6, pp. 1388-1394, 2011.

[18] L. Wang, W. Sun, Y. Hu and L. Xu, "Adsorption mechanism of mixed anionic/cationic collectors in Muscovite–Quartz flotation system," *Minerals Engineering,* vol. 64, pp. 44-50, 2014.

[19] A. Arguelles-Diaz, J. Taboada-Castro, F. Garcia-Bastante and M. Araujo-Fernandez, "Effects of flotation variables on feldspathic sand concentration," *Dyna,* vol. 81, no. 183, pp. 132-139, 2014.

[20] A. Chaib, "New condition for separation of orthoclase from quartz by flotation; case of Ain Barbar quarry (Algeria)," *Natsional'nyi Hirnychyi Universytet. Naukovyi Visnyk,* vol. 1, no. 6, p. 67, 2016.

[21] S. Rao, Surface Chemistry of Froth Flotation: Volume 1: Fundamentals, New York: Springer Science & Business Media, 2013.

[22] D. Fuerstenau, "Zeta potentials in the flotation of oxide and silicate minerals," *Advances in colloid and,* vol. 114, pp. 9-26, 2005.

[23] L. Filippov, A. Duverger, I. Filippova, H. Kasaini and J. Thiry, "Selective flotation of silicates and Ca bearing minerals: The role of non-ionic reagent on cationic flotation," *Minerals Engineering,* vol. 36, pp. 314-323, 2012.

[24] T. Kumar, S. Prabhakar and G. Raju, "Adsorption of oleic acid at sillimanite/water interface," *Journal of colloid and Interface Science,* vol. 247, no. 2, pp. 275-281, 2002.

[25] H. Wang and M. Linford, "X-ray Photoelectron Spectroscopy and Auger Electron Spectroscopy," *Vacuum Technology & Coating,* pp. 2-7, 2015.

[26] A. Vidyadhar, K. Rao and I. Chernyshova, "Mechanisms of amine–feldspar interaction in the absence and presence of alcohols studied by spectroscopic methods," *Colloids and Surfaces A: Physicochemical and Engineering Aspects,* vol. 214, no. 1-3, pp. 127-142, 2003.

[27] A. Vidyadhar, "Flotation of silicate minerals: physico-chemical studies in the presence of alkylamines and mixed (cationic/anionic/non-ionic) collectors," *Doctoral dissertation, Luleå tekniska universitet,* 2001.

[28] R. Pugh, M. Rutland, E. Manev and P. Claesson, "Dodecylamine collector—pH effect on mica flotation and correlation with thin aqueous foam film and surface force measurements," *International journal of mineral processing,* vol. 46, no. 3-4, pp. 245-262, 1996.

[29] X. Longhua, H. Yuehua, D. Faqin, J. Hao, W. Houqin, W. Zhen and L. Ruohua, "Effects of particle size and chain length on flotation of quaternary ammonium salts onto kaolinite," *Mineralogy and Petrology,* vol. 109, no. 3, pp. 309-316, 2015.

[30] Z. Chen, Z. Ren, H. Gao, J. Lu, J. Jin and F. Min, "The effects of calcium ions on the flotation of sillimanite using dodecylammonium chloride," *Minerals,* vol. 7, no. 2, p. 28, 2017.

[31] C. Demir, I. GüLgonul, I. Bentli and M. Çelik, "Differential separation of albite from microcline by monovalent salts in HF medium," *Minerals & metallurgical processing,* vol. 20, no. 3, pp. 120-124, 2003.

[32] H. Jiang, W. Ji, Q. Yang, L. Xu, C. Zhao and Y. Hu, "Synergistic Adsorption and Flotation of New Mixed Cationic/Nonionic Collectors on Muscovite," *Minerals,* vol. 7, no. 5, p. 74, 2017.

[33] T. Chau, "A review of techniques for measurement of contact angles and their applicability on mineral," *Minerals Engineering,* vol. 22, no. 3, pp. 213-219, 2009.

[34] S. Balachandran, G. Simkovich and F. Aplan, "The influence of point defects on the floatability of cassiterite, II. Electrostatic collector interactions," *International Journal of Mineral Processing,* vol. 21, no. 3-4, pp. 173-184, 1987.

[35] B. Jańczuk, M. Gonzalez-Martin and J. Bruque, "Wettability of cassiterite in presence of sodium dodecyl sulphate," *Materials chemistry and physics,* vol. 38, no. 3, pp. 225-233, 1994.

[36] A. Vidyadhar, K. Rao and K. Forssberg, "Adsorption of n-tallow 1, 3-propanediamine–dioleate collectoron albite and quartz minerals, and selective flotation of albite from greek stefania feldspar ore," *Journal of colloid and interface science,* vol. 248, no. 1, pp. 19-29, 2002.

[37] K. Rao and K. Forssberg, "Mixed collector systems in flotation," *International Journal of Mineral Processing,* vol. 51, no. 1-4, pp. 67-79, 1997.

[38] L. Xu, J. Tian, H. Wu, Z. Lu, W. Sun and Y. Hu, " The flotation and adsorption of mixed collectors on oxide and silicate minerals," *Advances in colloid and interface science,* pp. 1-14, 2017.

[39] L. Wang, Y. Hu, J. Liu, Y. Sun and W. Sun, "Flotation and adsorption of muscovite using mixed cationic–nonionic surfactants as collector," *Powder technology,* vol. 276, pp. 26-33, 2015.

[40] E. Larsen and R. Kleiv, " Flotation of quartz from quartz-feldspar mixtures by the HF method," *Minerals Engineering,* vol. 98, pp. 49-51, 2016.

[41] Y. Han, W. Liu and J. Chen, "DFT simulation of the adsorption of sodium silicate species on kaolinite surfaces.," *Applied Surface Science.,* vol. 370, pp. 403-9, 2016.

[42] C. Veloso, L. Filippov, I. Filippova, S. Ouvrard and A. Araujo, "Investigation of the interaction mechanism of depressants in the reverse cationic flotation of complex iron ores," *Minerals Engineering,* vol. 125, pp. 133-139, 2018.

[43] E. Burdukova, G. Van Leerdam, F. Prins, R. Smeink, D. Bradshaw and J. Laskowski, "Effect of calcium ions on the adsorption of CMC onto the basal planes of New York talc–A ToF-SIMS study," *Minerals Engineering,* vol. 21, no. 12-14, pp. 1020-1025, 2008.

[44] K. Shrimali, V. Atluri, X. Wang and J. Miller, "Adsorption of corn starch molecules at hydrophobic mineral surfaces," *Colloids and Surfaces A: Physicochemical and Engineering Aspects,* vol. 546, pp. 194-202, 2018.

[45] Z. Li, Y. Han, Y. Li and G. Peng, "Effect of serpentine and sodium hexametaphosphate on ascharite flotation," *Transactions of Nonferrous Metals Society of China,* vol. 27, no. 8, pp. 1841-1848, 2017.

[46] Y. Lu, M. Zhang, Q. Feng, L. Tao, L. Ou and G. Zhang, "Effect of sodium hexametaphosphate on separation of serpentine from pyrite," *Transactions of Nonferrous Metals Society of China,* vol. 21, no. 1, pp. 208-213, 2011.

[47] J. Scott and R. Smith, "Calcium ion effects in amine flotation of quartz and magnetite," *Minerals engineering,* vol. 6, no. 12, pp. 1245-1255, 1993.

[48] M. El-Salmawy, Y. Nakahiro and T. Wakamatsu, "The role of alkaline earth cations in flotation separation of quartz from feldspar," *Minerals Engineering,* vol. 6, no. 12, pp. 1231-1243, 1993.

[49] S. Prabhakar, K. Rao and W. Forsling, " Dissolution of wollastonite and its flotation and surface interactions with tallow-1, 3-diaminopropane (duomeen T)," *Minerals engineering,* vol. 18, no. 7, pp. 691-700, 2005.

[50] G. Belardi, E. Spaziani and L. Passeri, "Beneficiation of wollastoite ores from Swedish, Greek and Spanish deposits," in *Minerals to materials conference*, Cairo, Egypt, 2008.

[51] W. Zhang and R. Honaker, "Flotation of monazite in the presence of calcite part II: Enhanced separation performance using sodium silicate and EDTA," *Minerals Engineering,* pp. 318-328, 2018.

[52] R. Rath and S. Subramanian, "Studies on adsorption of guar gum onto biotite mica," *Minerals engineering, 10(12), pp.1405-1420.,* vol. 10, no. 12, pp. 1405-1420, 1997.

[53] D. Lelis, V. Leão and R. Lima, "Effect of EDTA on quartz and hematite flotation with starch/amine in an aqueous solution containing Mn2+ ions," *REM-International Engineering Journal,* vol. 69, no. 4, pp. 479-485., 2016.

[54] E. Oelkers, S. Golubev, C. Chairat, O. Pokrovsky and J. Schott, "The surface chemistry of multi-oxide silicates," *Geochimica et Cosmochimica Acta,* vol. 73, no. 16, pp. 4617-4634, 2009.

[55] Y. Jizu, C. Mingli and Y. Chuxiong, "Flotation separation of wollastonite from diopside," *Journal of Wuhan University of Technology-Materials Science,* vol. 1, pp. 59-64, 1994.

[56] C. Zhang, S. Wei, Y. Hu, H. Tang, J. Gao, Z. Yin and Q. Guan, "Selective adsorption of tannic acid on calcite and implications for separation of fluorite minerals.," *Journal of colloid and interface science,* vol. 512, pp. pp.55-63, 2018.

[57] G. Lecrivain, G. Petrucci, M. H. U. Rudolph and R. Yamamoto, "Attachment of solid elongated particles on the surface of a stationary gas bubble," *International Journal of Multiphase Flow,* vol. 71, pp. 83-93, 2015.

[58] A. Jordens, C. Marion, R. Langlois, T. Grammatikopoulos, R. Sheridan, C. Teng, H. Demers, R. Gauvin, N. Rowson and K. Waters, "Beneficiation of the Nechalacho rare earth deposit. Part 2: Characterisation of products from gravity and magnetic separation," *Minerals Engineering,* vol. 99, pp. 96-110, 2016.

[59] G. Ghigo, S. Berto, M. Minella, D. Vione, E. Alladio, V. Nurchi, J. Lachowicz and P. Daniele, "New insights into the protogenic and spectroscopic properties of commercial tannic acid: the role of gallic acid impurities.," *New Journal of Chemistry,* vol. 42, no. 10, pp. 7703-7712, 2018.

[60] M. Li, Z. Han, W. Bei, X. Rong, J. Guo and X. Hu, "Oleanolic acid attenuates insulin resistance via NF-κB to regulate the IRS1-GLUT4 pathway in HepG2 cells," *Evidence-Based Complementary and Alternative Medicine,* vol. 2015, pp. 1-9, 2015.

[61] G. Da Silva, E. Espiritu, S. Mohammadi-Jam and K. Waters, " Surface characterization of microwave-treated chalcopyrite.," *Colloids and Surfaces A: Physicochemical and Engineering Aspects,* vol. 555, pp. 407-417, 2018.

[62] C. Marion, A. Jordens, S. McCarthy, T. Grammatikopoulos and K. Waters, "An investigation into the flotation of muscovite with an amine collector and calcium lignin sulfonate depressant.," *Separation and Purification Technology,* vol. 149, pp. 216-227, 2015.

[63] S. Uddin, Y. Li, M. Mirnezami and J. Finch, "Effect of particles on the electrical charge of gas bubbles in flotation," *Minerals Engineering,* Vols. 36-38, pp. 160-167, 2012.

[64] E. Espiritu, G. da Silva, D. Azizi, F. Larachi and K. Waters, "Flotation behavior and electronic simulations of rare earth minerals in the presence of dolomite supernatant using sodium oleate collector.," *Journal of Rare Earths,* vol. 37, no. 1, pp. 101-112, 2019.

[65] J. Moulder, W. Stickle, P. Sobol and K. Bomben, Handbook of X-ray photoelectron spectroscopy, Eden prairie: Perkin-Elmer Corporation, 1992.

[66] P. Clarke, D. Fornasiero, J. Ralston and R. Smart, "A study of the removal of oxidation products from sulfide mineral surfaces," *Minerals Engineering,* vol. 8, no. 11, pp. 1347-1357, 1995.

[67] Y. Peng and S. Grano, "Effect of iron contamination from grinding media on the flotation of sulphide minerals of different particle size," *International Journal of Mineral Processing,* vol. 97, no. 1-4, pp. 1-6, 2010.

[68] J. Shibata and D. Fuerstenau, "Flocculation and flotation characteristics of fine hematite with sodium oleate," *International Journal of Mineral Processing,* vol. 72, no. 1-4, pp. 25-32, 2003.

[69] G. Chen and D. Tao, "Effect of solution chemistry on flotability of magnesite and dolomite," *International Journal of Mineral Processing,* vol. 74, no. 1-4, pp. 343-357, 2003.

[70] J. Yianatos, L. Bergh and J. Aguilera, "Flotation scale up: use of separability curves," *Minerals Engineering.,* vol. 16, no. 4, pp. 347-352, 2003.

[71] D. Mesa and P. Brito-Parada, "Scale-up in froth flotation: A state-of-the-art review," *Separation and Purification Technology,* vol. 210, pp. 950-962, 2019.

[72] A. Nicol, Physicochemical methods of mineral analysis, London: A Division of Plenum Publishing Company, 2012.

[73] H. Perkampus, UV-VIS Spectroscopy and Its Application, Berlin, Heidelberg: Springer, 1992.

[74] A. Ismail, F. van de Voort and J. Sedman, "Fourier transform infrared spectroscopy: principles and applications," *InTechniques and instrumentation in analytical chemistry,* vol. 18, pp. 93-139, 1997.

Appendices

Appendix A: X-ray Diffraction (XRD)

X-ray diffraction (XRD) technique is a fast and convenient technique for analysing crystalline material. XRD patterns can be used for determining unit cell parameters, identification of unknown material and more. Powder samples are normally used for XRD analyses but in certain cases, it might be beneficial to analyse single crystals. XRD is governed by the Bragg equation which specifies the conditions for a constructive interference to occur. Bragg considered a three-dimensional crystal as stack of parallel, identical and equidistant plane arrays. When a crystal is irradiated by monochromatic X-rays, a fraction of the X-ray is reflected by the plane array and a fraction passes through to repeat the same process [72]. The Bragg condition for constructive interference of the diffracted X-rays is as follows:

$$n\lambda = 2d \sin\theta$$

Where n is an integer, λ is the wavelength of the incident X-ray, d is the distance between adjacent planes and θ is the angle of incidence of the X-ray beam. A detailed description of XRD can be found from Nicol [72]

Appendix B: Ultraviolet-Visible spectroscopy (UV-vis spectroscopy)

UV-vis spectroscopy is based on the relationship between electromagnetic radiation and atomic or molecular energy states. The energy in the UV-vis range of the electromagnetic spectrum corresponds to the difference in energy between the electronic states of atoms and molecules. Solutions that absorb UV-vis radiation are colored and that includes solutions containing transition metals and organic compounds that contain a chromophoric system. When these solutions are irradiated with UV-vis radiation, they absorb a fraction of the energy of the radiation which results in excitation from ground electronic states. UV-vis spectroscopy is very useful in analytical chemistry for determining concentration for samples of unknown concentration since the absorbance can be related to the concentration of the analyte [73].

Bouguer-Lambert-Beer established a relationship between absorbance and concentration through the following equation:

$$\varepsilon = \frac{A}{cd}$$

Where ε is the molar decadic extinction coefficient, A is the absorbance, c is the concentration of a light absorbing substance and d is the path length of the sample. It should be noted that Bouguer-Lambert-Beer is only limited to dilute solution as the molar decadic extinction coefficient is not constant at high concentrations which results in a nonlinear relationship between absorbance and concentration. In addition, the electronic transitions in UV-vis can be useful in deducing molecular structure [73].

Appendix C: Batch flotation results

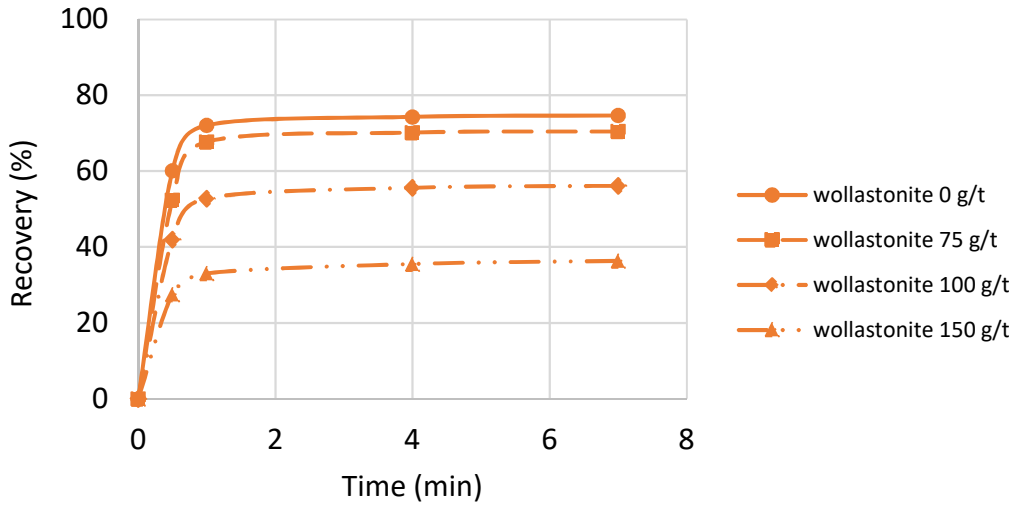

Figure 0.1 Recovery against time for wollastonite at 35 g/t DDA and various TA concentration

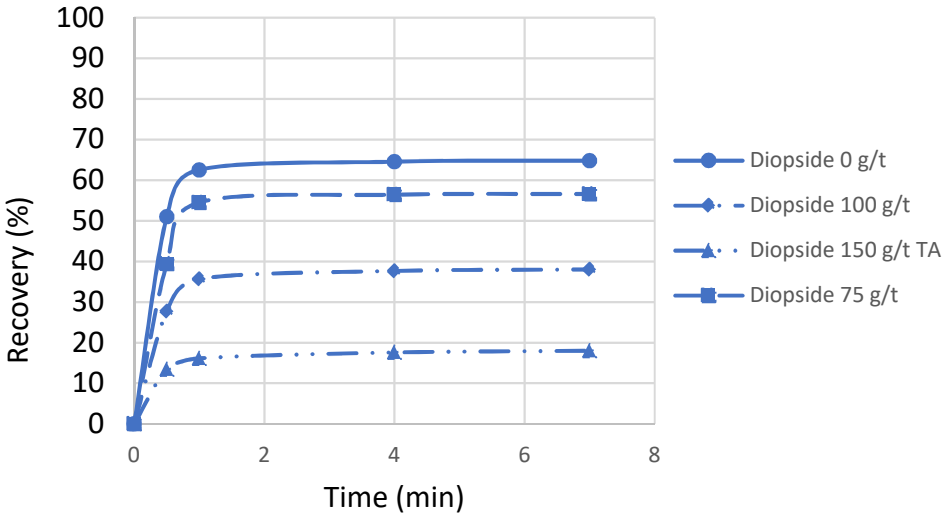

Figure 0.2 Recovery against time for diopside at 35 g/t DDA and various TA concentration

Appendix D: Microflotation

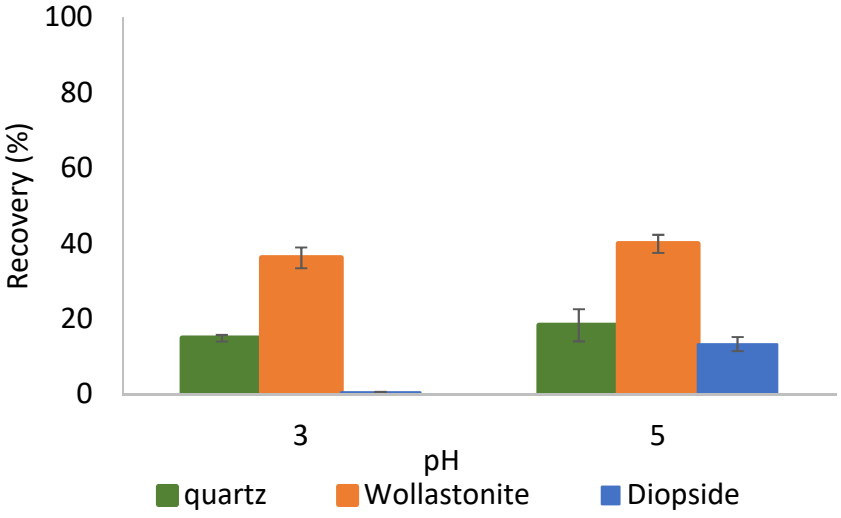

Figure 0.3 Microflotation recoveries of quartz, wollastonite and diopside using 1kg/t sodium dodecylsulfate

Appendix E: Fourier transform Infrared spectroscopy (FTIR)

Infrared spectroscopy relies on absorption of infrared radiation by molecules. The Infrared spectrum peaks represent excitation of the molecule's vibrational modes from the ground level electronic energy state to higher vibrational levels [74]. The peaks on the infrared spectrum can be directly linked to the chemical bonding and functional groups within the molecule and therefore serve as a fingerprint of the molecule [74]. For simple diatomic molecules, the infrared frequency required to excite the vibrational modes of a molecule is simply related to Hooke's law and results in the following equation [74]:

$$\nu = \frac{1}{2\pi}\sqrt{\frac{k}{\mu}} \qquad (2)$$

Where K is related to the bond strength and μ is related to the reduced mass of the atoms involved in the chemical bond [74]. For many atoms' molecules, the frequencies normally do not correlate with frequencies calculated from this equation [74]. The absorption peaks normally reflect a mixture of frequencies resulting from vibrations of various bonds and atoms within the molecule [74]. Additionally, absorption peaks shift due to steric effect; electrical effects; nature, size and electronegativity of neighbouring groups and hydrogen bonding. In many atoms' molecules, group frequencies are normally assigned which are characteristic of specific functional groups present within the compound and allows identification and characterisation of the compound [74].

FTIR is a very useful tool for characterising adsorption of collectors since it identifies additional functional groups on the surface of the mineral [18, 21, 24, 26]. Additionally, FTIR can be used to deduce the mechanism of adsorption [21, 24]. Physically adsorbed collectors will only introduce additional absorption peaks on the IR spectrum of the mineral surface [18, 21, 24, 26]. Chemically adsorbed collectors usually show shifts on the mineral's absorption peaks in addition to the new absorption peaks, the shifts are due to alteration of the bonding structure of the mineral surface elements [18, 21, 24].